



UNIVERSITY OF AEGEAN

DEPARTMENT OF ENVIRONMENT



Ph.D. dissertation

**Determination of the concentrations and the chemical
composition of particulate matter in the North Aegean
region**

ELENI D. TRIANTAFYLLOU

Mytilene 2018



ΠΑΝΕΠΙΣΤΗΜΙΟ ΑΙΓΑΙΟΥ

ΤΜΗΜΑ ΠΕΡΙΒΑΛΛΟΝΤΟΣ



Διδακτορική διατριβή

**Εκτίμηση των συγκεντρώσεων και της χημικής σύστασης
των αιωρούμενων σωματιδίων στην περιοχή του Βορείου
Αιγαίου**

ΕΛΕΝΗ Δ. ΤΡΙΑΝΤΑΦΥΛΛΟΥ

Μυτιλήνη, 2018

This research (Contract Nr. 5928) co-financed by the European Union (European Social Fund – ESF) and Greek national funds (State Scholarships Foundation – IKY) through the Operational Program "Education and Lifelong Learning" of the National Strategic Reference Framework (NSRF) - Scholarship programs for the academic year 2009-2010 for postgraduate studies in Greece, abroad and postdoctoral research.

Η παρούσα έρευνα (Αρ. Σύμβ. 5928) συγχρηματοδοτήθηκε από την Ευρωπαϊκή Ένωση (Ευρωπαϊκό Κοινωνικό Ταμείο - ΕΚΤ) και από εθνικούς πόρους (Ίδρυμα Κρατικών Υποτροφιών ΙΚΥ), μέσω του Επιχειρησιακού Προγράμματος από μέσω του Επιχειρησιακού Προγράμματος «Εκπαίδευση και Δια Βίου Μάθηση» του Εθνικού Στρατηγικού Πλαισίου Αναφοράς (ΕΣΠΑ) – Προγράμματα υποτροφιών ακαδημαϊκού έτους 2009-2010 για μεταπτυχιακές σπουδές στην Ελλάδα, στο εξωτερικό και μεταδιδακτορική έρευνα.



Advisory committee

Biskos George

Associate Professor, Energy Environment and Water Research Centre, The Cyprus Institute, Nicosia, Cyprus (supervisor)

Eleftheriadis Kostas

Researcher A', Environmental Radioactivity Lab, Institute of Nuclear & Radiological Sciences & Technology, Energy & Safety (I.N.Ra.S.T.E.S.), N.C.S.R. "Demokritos", Attiki, Greece

Haralampopoulos Dias

Professor, Department of Environment, University of Aegean, Mytilene, Greece

Examination committee

Biskos George

Associate Professor, Energy Environment and Water Research Centre, The Cyprus Institute, Nicosia, Cyprus

Eleftheriadis Kostas

Researcher A', Environmental Radioactivity Lab, Institute of Nuclear & Radiological Sciences & Technology, Energy & Safety (I.N.Ra.S.T.E.S.), N.C.S.R. "Demokritos", Attiki, Greece

Haralampopoulos Dias

Professor, Department of Environment, University of Aegean, Mytilene, Greece

Kalantzi Olga-Ioanna

Assistant Professor, Department of Environment, University of Aegean, Mytilene, Greece

Matsoukas Christos

Assistant Professor, Department of Environment, University of Aegean, Mytilene, Greece

Pilinis Christodoulos

Professor, Department of Environment, University of Aegean, Mytilene, Greece

Tombrou - Tzella Maria

Associate Professor, Department of Physics, University of Athens, Athens, Greece

Συμβουλευτική επιτροπή

Μπίσκος Γιώργος

Αναπληρωτής Καθηγητής, Κέντρο Ενέργειας, Περιβάλλοντος και Υδάτων, Ινστιτούτο Κύπρου, Λευκωσία, Κύπρος (επιβλέπων)

Ελευθεριάδης Κώστας

Ερευνητής Α', Εργαστήριο Ραδιενέργειας Περιβάλλοντος, Ινστιτούτο Πυρηνικών & Ραδιολογικών Επιστημών & Τεχνολογίας, Ενέργειας & Ασφάλειας (Ι.Π.Ρ.Ε.Τ.Ε.Α.), Ε.Κ.Ε.Φ.Ε. "Δημόκριτος", Αττική, Ελλάδα

Χαραλαμπόπουλος Δίας

Καθηγητής, Τμήμα Περιβάλλοντος, Πανεπιστήμιο Αιγαίου, Μυτιλήνη, Ελλάδα

Εξεταστική επιτροπή

Μπίσκος Γιώργος

Αναπληρωτής Καθηγητής, Κέντρο Ενέργειας, Περιβάλλοντος και Υδάτων, Ινστιτούτο Κύπρου, Λευκωσία, Κύπρος

Ελευθεριάδης Κώστας

Ερευνητής Α', Εργαστήριο Ραδιενέργειας Περιβάλλοντος, Ινστιτούτο Πυρηνικών & Ραδιολογικών Επιστημών & Τεχνολογίας, Ενέργειας & Ασφάλειας (Ι.Π.Ρ.Ε.Τ.Ε.Α.), Ε.Κ.Ε.Φ.Ε. "Δημόκριτος", Αττική, Ελλάδα

Χαραλαμπόπουλος Δίας

Καθηγητής, Τμήμα Περιβάλλοντος, Πανεπιστήμιο Αιγαίου, Μυτιλήνη, Ελλάδα

Καλαντζή Όλγα-Ιωάννα

Επίκουρη Καθηγήτρια, Τμήμα Περιβάλλοντος, Πανεπιστήμιο Αιγαίου, Μυτιλήνη, Ελλάδα

Ματσούκας Χρήστος

Επίκουρος Καθηγητής, Τμήμα Περιβάλλοντος, Πανεπιστήμιο Αιγαίου, Μυτιλήνη, Ελλάδα

Πηλίνης Χριστόδουλος

Καθηγητής, Τμήμα Περιβάλλοντος, Πανεπιστήμιο Αιγαίου, Μυτιλήνη, Ελλάδα

Τόμπρου - Τζέλλα Μαρία

Αναπληρώτρια Καθηγήτρια, Τμήμα Φυσικής, Πανεπιστήμιο Αθηνών, Αθήνα, Ελλάδα



ΠΑΝΕΠΙΣΤΗΜΙΟ ΑΙΓΑΙΟΥ

ΣΧΟΛΗ ΠΕΡΙΒΑΛΛΟΝΤΟΣ
ΤΜΗΜΑ ΠΕΡΙΒΑΛΛΟΝΤΟΣ

ΠΡΑΚΤΙΚΟ ΑΞΙΟΛΟΓΗΣΗΣ ΔΙΔΑΚΤΟΡΙΚΗΣ ΔΙΑΤΡΙΒΗΣ
ΤΗΣ ΥΠΟΨΗΦΙΑΣ ΔΙΔΑΚΤΟΡΟΣ κας ΕΛΕΝΗΣ ΤΡΙΑΝΤΑΦΥΛΛΟΥ

Η Επταμελής Εξεταστική Επιτροπή η οποία ορίστηκε στην υπ' αριθμ. 09/02.05.2018 Συνεδρίαση της Συνέλευσης του Τμήματος Περιβάλλοντος για την τελική αξιολόγηση και κρίση της Διδακτορικής Διατριβής της Υποψήφιας Διδάκτορος κας **Ελένης Τριανταφύλλου** και αποτελείται από τους κ.κ.:

1. Χαραλαμπίδης Δία-Διονύσιος: Καθηγητή Α΄βαθμίδας, Τμήμα Περιβάλλοντος, Πανεπιστήμιο Αιγαίου (επιβλέπων)
2. Μπίσκο Γεώργιο, Αναπληρωτή Καθηγητή, Κέντρο Ενέργειας Περιβάλλοντος και Υδάτων, Ινστιτούτο Κύπρου (μέλος τριμελούς)
3. Ελευθεριάδη Κωνσταντίνο, Ερευνητή Α΄, Εργαστήριο Ραδιενέργειας Περιβάλλοντος, Ινστιτούτο Πυρηνικής Τεχνολογίας και Ακτινοπροστασίας, ΕΚΕΦΕ Δημόκριτος (μέλος τριμελούς)
4. Πηλίνη Χριστόδουλο, Καθηγητή Α΄βαθμίδας, Τμήμα Περιβάλλοντος, Πανεπιστήμιο Αιγαίου
5. Τζέλλα-Τόμπρου Μαρία, Αναπληρώτρια Καθηγήτρια, Τμήμα Φυσικής, Εθνικό και Καποδιστριακό Πανεπιστήμιο Αθηνών
6. Ματσούκα Χρήστο, Επίκουρο Καθηγητή, Τμήμα Περιβάλλοντος, Πανεπιστήμιο Αιγαίου
7. Καλαντζή Όλγα-Ιωάννα, Επίκουρη Καθηγήτρια, Τμήμα Περιβάλλοντος, Πανεπιστήμιο Αιγαίου






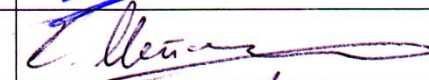
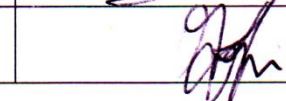
συνήλθε σε συνεδρίαση σήμερα 12/06/2018, ημέρα Τρίτη και ώρα 10:00 π.μ. στην αίθουσα συνεδριάσεων (Γ1) του κτιρίου (Β) του Τμήματος Περιβάλλοντος του Πανεπιστημίου στη Μυτιλήνη, προκειμένου να παρακολουθήσει τη δημόσια υποστήριξη της Διδακτορικής Διατριβής της ανωτέρω υποψήφιας με θέμα «Determination of the concentrations and the chemical composition of particulate matter in the North Aegean region».

Παρόντες ήταν: α) στην αίθουσα τηλεδιάσκεψης οι κ.κ.: Δίας-Διονύσιος Χαραλαμπίδης, Χριστόδουλος Πηλίνης, Χρήστος Ματσούκας, Όλγα-Ιωάννα Καλαντζή β) με e-presence οι κ.κ.: Γεώργιος Μπίσκος, Κων/νος Ελευθεριάδης, Μαρία Τζέλλα-Τόμπρου

Μετά την υποστήριξη της Διατριβής από την κα Ελένη Τριανταφύλλου, σε κλειστή συνεδρίαση την ίδια ημέρα, τα Μέλη της Εξεταστικής Επιτροπής έκριναν ομόφωνα με ~~πλειοψηφία~~ ότι το περιεχόμενο της Διατριβής είναι πρωτότυπο, συμβάλει

ουσιαστικά στην επιστήμη και η παρουσίαση από την Υποψήφια ήταν ~~αξιολογική~~ και απέδωσε ...~~αξιολογικά~~... το χαρακτηρισμό ~~αξιολογική~~.....

Η Επταμελής Εξεταστική Επιτροπή

	Υπογραφή
1. Χαραλαμπίδης Δίας-Διονύσιος Καθηγητής Α΄ βαθμίδας, επιβλέπων	
2. Μπίσκος Γεώργιος, Αναπληρωτής Καθηγητής, μέλος τριμελούς	
3. Ελευθεριάδης Κωνσταντίνος, Ερευνητής Α΄, μέλος τριμελούς	
4. Πηλίνης Χριστόδουλος, Καθηγητής Α΄ βαθμίδας, μέλος τριμελούς	
5. Τζέλλα-Τόμπρου Μαρία, Αναπληρώτρια Καθηγήτρια, μέλος τριμελούς	
6. Ματσούκας Χρήστος, Επίκουρος Καθηγητής, μέλος τριμελούς	
7. Καλαντζή Όλγα-Ιωάννα, Επίκουρη Καθηγήτρια, μέλος τριμελούς	

*Dedicated to A.M.,
my mother Dimitra
and Giannio*

**[.../ the uphill task of self-realization,
to go up and down from the dark hell we have inside
into the mountain of mundane struggle,
and from there to redemption – to wit, the redemption
from every art, act, morality and idea;
from every chimera and every reality.**

(Kazantzakis N., 1934)

*[...] τον ανήφορο της αυτοτελειοποίησης,
ν' ανεβαίνουμε επίπονα από την σκοτεινή Κόλαση
που έχουμε μέσα μας στο βουνό της επίγειας άσκησης,
κι από κει στην λύτρωση - δηλαδή στην απολύτρωση
από κάθε τέχνη, πράξη, ηθική κι ιδέα·
από κάθε χίμαιρα κι από κάθε πραγματικότητα.*

(Καζαντζάκης Ν., 1934)

Acknowledgements

Finding at last 'land' reaching Ithaca after this long scientific journey, I would like to thank God for giving me the strength and persistence to carry on and complete this dissertation. I would also like to express my sincere thanks to all those who have over the years stood by me.

Firstly, I would like to thank my supervisor, Prof. George Biskos, for giving me his advice and the opportunity to experience the PhD process, as well as for his valuable time to proofreading my research texts. Besides my supervisor, I would like to thank my advisory committee, Prof. Dias Haralampopoulos and Prof. Christodoulos Pilinis, for their full understanding and all the support, and Dr. Kostas Eleftheriadis for the crucial help, the fruitful collaboration, and the efficient response to all my scientific queries. I would like to give very special thanks to Prof. Athanasios Triantafyllou for introducing me to the exciting research field of Atmospheric Sciences during my undergraduate years, and for his kindness, irreproachable behavior and his trust to all the years of our collaboration and acquaintance.

I would also like to thank Prof. Christos Matsoukas for the direct help of all my queries, Prof. Maria Tombrou-Tzella for immediate response and intervention, Prof. Nikos Mihalopoulos for his helpful corrections, and Dr. Adamopoulos for providing YPEKA data and for the excellent collaboration. My sincere thanks also go to Dr. Themis Kontos for all our substantive discussions and help in geo-informatics.

In addition, I would like to thank very much Dr. Lila Diapouli for the excellent collaboration and her valuable assistance, as well as Dr. Manos Manousakas, Dr. Pavlos Zampas and Dr. Christina Theodosi for their advices on chemistry and for their contribution to the chemical analysis of the projects. Also, I thank the members of the Water and Air Quality Laboratory, Dr. Maria Giamarellou, Dr. Christos Psanis, Dr. Spyros Bezantakos and Dr. Kostis Barmpounis for the collaboration. Special thanks to my friends and office mates, Dr. Panayiotis Charalambides, Mr. Mario-Bruno Korras-Carraca, Dr. Michael Lasithiotakis and Mr. Panagiotis Polymeneas, as well as to my friends in neighbour offices Dr. Eva Iatrou, Dr. Eirini Zkeri, and Mr. Aggelo Tsaligopoulo for supporting and inspiring each other.

Special thanks to my beloved ones, Giannio and Sofia for their encouragement, their support and for the enlighting discussions in the difficult moments.

I would also like to thank the State Scholarships Foundation of Greece (IKY) for the financial support of my postgraduate studies, and particularly Mrs. Korina Diamantopoulou, for helping me to address various issues related to my scholarship.

Finally I am very grateful to my family for their love, patience, and continued support throughout the years.

Abstract

Particulate matter (PM) pollution is a major environmental problem in urban and remote areas, as it causes adverse effects upon human health and affects directly or indirectly the climate of the Earth. PM can vary considerably in size, chemical composition and origin. Therefore, numerous studies have investigated particle pollution exposure and its effects around the globe, including the region of the Eastern Mediterranean, which is considered a climate change hotspot that is affected by transportation of air pollutants originating from Europe, Africa and Asia. Despite these studies, however, there is still insufficient information on the air quality of insular coastal areas on the northern part of Eastern Mediterranean, i.e., the Northern Aegean Sea (NAS), and on the contribution of the local and the distant sources that influence it.

The objective of this thesis is to estimate the physical-chemical properties of PM in urban and suburban-background sites in the NAS region and to compare them with those of other regions. First, it provides background information for PM_{10} concentration levels in the two major urban centres in Greece, namely Athens and Thessaloniki over the period 2001 to 2010. Results indicate that most of the urban and suburban stations in these two major urban centres exhibit high PM_{10} concentrations and exceed the EU annual and 24-h limits during the entire period. However, PM_{10} levels at urban and suburban stations are lower compared to other European and US cities of the same size. With the exception of the suburban stations in Athens and one station in Thessaloniki, all others had highest and the lowest monthly average PM_{10} concentrations during the autumn/winter and the summer months, respectively. For the suburban stations in Athens, the highest values are observed during the spring and the lowest during the winter, while one station in Thessaloniki did not exhibit any seasonality due to its proximity to an industrial zone.

Second, this thesis reports PM measurements at urban and remote sites in the NAS region. Measurements of atmospheric aerosol particles conducted at a remote site of NAS in summer under representative synoptic meteorological conditions (i.e., Etesian wind conditions) showed that long-range transportation of air pollutants from

industrial and urban environments can significantly affect the quality of the air in remote regions. When strong northeastern winds prevail, the air masses pass over the wider Istanbul region. This results in a shift of the peak particle size from 100 to 20 nm, while an up to a six-fold increase in particle number concentration and high particle values of growth rates (ca. 9.0 nm h^{-1}) are observed. An additional indication that particles observed in the region of NAS are long range transported from urban and/or industrial areas is provided by the increased values of sulfates and nitrates, and the OC/EC ratio during the days of particle transportation compared to the rest of the sampling period.

The characteristics of atmospheric aerosol particles and the potential PM sources in an urban measurement site in the NAS region were investigated during the warm and cold periods. Mean $\text{PM}_{2.0}$ and $\text{PM}_{1.0}$ concentrations at the city centre were lower compared to corresponding values from large cities in the region. Higher average mass and number concentrations were observed in winter compared to summer, due to the additional emissions from domestic heating and the weaker atmospheric dilution. During both seasons, however, PM emissions related to local natural and anthropogenic sources. The elemental composition measurements also showed that natural sources contribute sea-salt and re-suspended soil to the PM load in the city's atmosphere. Non-exhaust traffic emission sources were also found to be important, while a strong contribution from local traffic sources was also identified by the increased number concentrations in the Aitken mode during rush hours. In addition to these sources, long-range transported pollution mainly from Northeastern Turkey enriched the collected particle samples with crustal and anthropogenic elements (i.e., K, Ca, Ti, Mg, Fe, As, S), contributing to the decline of air quality in the region of NAS.

Finally, this thesis evaluates the discrepancy between beta attenuation (BAM) and gravimetric (GM) measurements at a suburban site in the study region, taking into account the effect of factors such as the meteorological conditions and the type of filter material on the PM measurements. An overestimation of the BAM measurements, which was ~30% for the $\text{PM}_{2.5}$ and ~10% for the PM_{10} data, was observed. Discrepancies between BAM and GM $\text{PM}_{2.5}$ measurements increased with: a.) increasing available water vapor, suggesting that the aerosol-bound water has a

strong effect on the measurements, b.) the use of highly hydrophobic Teflon filters to the GM method when the atmospheric water vapor pressure increased, and c.) the potential availability of the volatility or stability in the aerosol phase when species such as ammonium nitrate were present. Better correlation between GM and BAM measurements was observed during the cold rather than the warm period and when GM samples were collected on filters made of glass fiber, which is incidentally the material of the BAM filter tape. The finding from this study can be used for the better interpretation of PM measurements conducted with various BAM monitors.

Περίληψη

Η σωματιδιακή ρύπανση αποτελεί μείζον περιβαλλοντικό πρόβλημα στις αστικές και απομακρυσμένες περιοχές, προκαλώντας δυσμενείς επιπτώσεις στην ανθρώπινη υγεία και επιδρώντας άμεσα ή έμμεσα στην κλιματική αλλαγή. Τα αιωρούμενα σωματίδια (ΑΣ) μπορεί να ποικίλουν σημαντικά στο μέγεθος, στη χημική σύσταση και την προέλευση τους. Ως εκ τούτου, πολυάριθμες επιστημονικές μελέτες έχουν διερευνήσει την έκθεση σε σωματιδιακή ρύπανση και τις επιπτώσεις της παγκόσμια, περιλαμβάνοντας την περιοχή της Ανατολικής Μεσογείου. Η συγκεκριμένη περιοχή θεωρείται μεγάλου ενδιαφέροντος σχετικά με την κλιματική αλλαγή, καθώς επηρεάζεται έντονα από τη μεταφορά ατμοσφαιρικών ρύπων από την Ευρώπη, την Αφρική και την Ασία. Παρά τα ευρήματα αυτά, υπάρχουν ακόμη ελλείψεις πληροφορίες σχετικά με την ποιότητα του αέρα στις νησιωτικές παράκτιες περιοχές στο βόρειο τμήμα της περιοχής της Ανατολικής Μεσογείου, δηλαδή στο Βόρειο Αιγαίο (ΒΑ), και της συμβολής των τοπικών και των μακρινών πηγών που την επηρεάζουν.

Σκοπός της παρούσας διατριβής είναι η εκτίμηση των φυσικοχημικών ιδιοτήτων των ΑΣ σε αστικές και προαστιακές περιοχές του ΒΑ καθώς και η σύγκρισή τους με άλλες περιοχές της Βορειοανατολικής Μεσογείου. Αρχικά η διατριβή παρέχει πληροφορίες για τα επίπεδα συγκέντρωσης των ΑΣ₁₀ στα δύο μεγάλα αστικά κέντρα της Ελλάδας, συγκεκριμένα την Αθήνα και τη Θεσσαλονίκη κατά την περίοδο 2001 έως 2010. Τα αποτελέσματα δείχνουν ότι οι περισσότεροι σταθμοί στα δύο μεγάλα αστικά κέντρα στην Ελλάδα, παρουσιάζουν υψηλές συγκεντρώσεις ΑΣ₁₀ και υπερβαίνουν τα ετήσια και 24ωρα όρια της Ευρωπαϊκής Ένωσης (ΕΕ) κατά τη διάρκεια της ερευνητικής περιόδου, αν και ήταν χαμηλότερες συγκριτικά με άλλες ευρωπαϊκές και αμερικανικές πόλεις του ίδιου μεγέθους. Με εξαίρεση τρεις προαστιακούς σταθμούς στην Αθήνα και έναν σταθμό στη Θεσσαλονίκη, όλοι οι άλλοι παρουσίασαν τις υψηλότερες και τις χαμηλότερες μηνιαίες μέσες συγκεντρώσεις ΑΣ₁₀ κατά τη διάρκεια του φθινοπώρου/χειμώνα και των θερινών μηνών, αντίστοιχα. Για τους προαστιακούς σταθμούς στην Αθήνα, οι υψηλότερες τιμές παρατηρούνται κατά την άνοιξη και οι χαμηλότερες κατά τη διάρκεια του

χειμώνα, ενώ ένας σταθμός στη Θεσσαλονίκη δεν παρουσίασε εποχικότητα λόγω της εγγύτητάς του σε βιομηχανική ζώνη.

Δεύτερον, η διατριβή αναφέρεται σε μετρήσεις ΑΣ σε απομακρυσμένες και αστικές περιοχές στην περιοχή του ΒΑ. Μετρήσεις αιωρούμενων σωματιδίων διενεργήθηκαν στην απομακρυσμένη περιοχή του ΒΑ υπό συνοπτικές μετεωρολογικές συνθήκες την θερινή περίοδο (δηλ. κατά την περίοδο των Ετησίων ανέμων). Οι μετρήσεις έδειξαν ότι η μεταφορά των ατμοσφαιρικών ρύπων σε μεγάλη απόσταση από βιομηχανικές και αστικές περιοχές, μπορεί επίσης να επηρεάσει σημαντικά την ποιότητα του αέρα σε απομακρυσμένες περιοχές. Όταν επικρατούν ισχυροί βορειοανατολικοί άνεμοι, οι αέριες μάζες περνούν πάνω από την ευρύτερη περιοχή της Κωνσταντινούπολης. Αυτό έχει ως αποτέλεσμα την μετατόπιση των υψηλότερων τιμών των σωματιδίων σε μικρότερα μεγέθη (δηλ. από 100 σε 20 nm), ενώ παρατηρείται αύξηση έως έξι φορές της αριθμητικής συγκέντρωσης, καθώς και υψηλοί ρυθμοί αύξησης του μεγέθους των σωματιδίων (περίπου 9.0 nm h^{-1}). Μια επιπλέον ένδειξη ότι τα σωματίδια που παρατηρούνται στην περιοχή του ΒΑ σχετίζονται με μεταφερόμενη ρύπανση σε μεγάλη απόσταση από αστικές ή/και βιομηχανικές περιοχές αποτελούν οι αυξημένες τιμές των θειϊκών και νιτρικών, καθώς και της αναλογίας οργανικού προς στοιχειακό άνθρακα κατά τη διάρκεια των ημερών μεταφοράς των ατμοσφαιρικών ρύπων σε σύγκριση με την υπόλοιπη περίοδο δειγματοληψίας.

Επιπλέον, τα χαρακτηριστικά των αιωρούμενων σωματιδίων και των δυνητικών πηγών τους ερευνήθηκαν σε έναν αστικό σταθμό δειγματοληψίας στην περιοχή του ΒΑ κατά τη θερινή και χειμερινή περίοδο. Οι μέσες συγκεντρώσεις $\text{AS}_{2.0}$ και $\text{AS}_{1.0}$ στο κέντρο της πόλης ήταν χαμηλότερες των αντίστοιχων τιμών που καταγράφηκαν σε μεγάλες πόλεις της περιοχής (δηλ. στην Αθήνα και στη Θεσσαλονίκη). Υψηλότερες μέσες τιμές τόσο για την συγκέντρωση μάζας όσο και για την αριθμητική συγκέντρωση παρατηρήθηκαν το χειμώνα σε σύγκριση με αυτές του καλοκαιριού, λόγω των πρόσθετων εκπομπών οικιακής θέρμανσης και της ασθενέστερης ατμοσφαιρικής αραίωσης. Ωστόσο, και στις δύο εποχές, οι εκπομπές των ΑΣ σχετίζονται με τοπικές φυσικές και ανθρωπογενείς πηγές. Η στοιχειακή ανάλυση σε δείγματα που συλλέχθηκαν κατά την διάρκεια των μετρήσεων έδειξαν επίσης ότι οι φυσικές πηγές όπως το θαλάσσιο αλάτι και η επαναίωρηση της σκόνης

συμβάλλουν στο φορτίο των σωματιδίων στην ατμόσφαιρα της πόλης. Από τις πηγές κυκλοφοριακής κίνησης που δεν σχετίζονται με τα καυσαέρια βρέθηκαν επίσης σημαντικές συνεισφορές, ενώ ισχυρή συμβολή των τοπικών πηγών κίνησης εντοπίστηκε επίσης και από τις αυξημένες αριθμητικές συγκεντρώσεις των σωματιδίων της περιοχής 'Aitken' κατά τις ώρες αιχμής. Εκτός από τις τοπικές πηγές, η μεταφερόμενη ρύπανση σε μεγάλη απόσταση, κυρίως από τη Βορειοανατολική Τουρκία, εμπλούτισε τα συλλεγόμενα δείγματα σωματιδίων με στοιχεία εδαφικής και ανθρωπογενούς προέλευσης (δηλ. K, Ca, Ti, Mg, Fe, As, S), συμβάλλοντας στην υποβάθμιση της ποιότητας του ατμοσφαιρικού αέρα στην περιοχή του ΒΑ.

Τέλος, λαμβάνοντας υπόψη την επίδραση παραγόντων όπως οι μετεωρολογικές συνθήκες και το υλικό του φίλτρου στις μετρήσεις ΑΣ, επιχειρήθηκε να εκτιμηθεί η απόκλιση μεταξύ της μεθόδου απορρόφησης Β-ακτινοβολίας (BAM) και της σταθμικής μεθόδου (gravimetric; GM) μετρήσεων ΑΣ σε ένα προαστιακό-υποβάθρου σταθμό στη περιοχή μελέτης. Παρατηρήθηκε υπερεκτίμηση των μετρήσεων BAM, η οποία ήταν ~ 30% για τα ΑΣ_{2.5} και ~ 10% για τα ΑΣ₁₀. Οι διαφορές μεταξύ των μετρήσεων BAM και GM στα ΑΣ_{2.5} αυξήθηκαν με: α) την αύξηση των πιθανών υδρατμών, γεγονός που υποδηλώνει ότι το δεσμευμένο νερό στα αεροζόλ έχει ισχυρή επίδραση στις μετρήσεις, β) την χρήση εξαιρετικά υδρόφοβων φίλτρων Teflon για την μέθοδο GM όταν η ατμοσφαιρική πίεση υδρατμών αυξάνεται, και γ) την πιθανή πτητικότητα ή σταθερότητα στη σωματιδιακή φάση ειδών όπως το νιτρικό αμμώνιο. Καλύτερη συσχέτιση μεταξύ των μετρήσεων με τις μεθόδους GM και BAM παρατηρήθηκε κατά τη διάρκεια της χειμερινής αντί της θερινής περιόδου και όταν τα δείγματα της GM μεθόδου συλλέχθηκαν σε φίλτρα κατασκευασμένα από ίνες υάλου, δηλαδή το ίδιο υλικό με αυτό της ταινίας διηθήσεως στην μέθοδο BAM. Αυτή η μελέτη στοχεύει στην καλύτερη ερμηνεία των μετρήσεων των ΑΣ που διεξάγονται με διάφορους ελεγκτές εκπομπών μεθόδου απορρόφησης Β-ακτινοβολίας.

List of publications

List of scientific papers

Triantafyllou, E., Diapouli, E., Korras-Carraca, M.B., Manousakas, M., Psanis, C., Floutsi, A.A., Spyrou, C., Eleftheriadis, K., Biskos, G. ‘*Characterisation of the atmospheric urban aerosol in a background marine region*’. Atmospheric Environment (submitted 23 May 2018).

Triantafyllou, E., Diapouli, E., Tsilibari, E.M., Adamopoulos, A.D., Biskos, G., Eleftheriadis, K., 2016. ‘*Comparisons between gravimetric & b-attenuation methods at the suburban station of Agia Paraskevi in Athens, Greece*’. Atmospheric Environment, 131, 409 – 417.

Triantafyllou, E., Giamarelou, M., Bossioli, E., Zarnpas, P., Theodosi, C., Matsoukas, C., Tombrou, M., Mihalopoulos, N., Biskos, G., 2016. ‘*Particulate pollution transport episodes from Eurasia to a remote region of northeast Mediterranean*’. Atmospheric Environment, 128, 45 – 52.

Triantafyllou, E., Biskos, G., 2012. *Overview of the Temporal Variation of PM₁₀ Mass Concentrations in the two Major Cities in Greece: Athens and Thessaloniki*. Global-NEST, 4, 431-441

List of scientific conferences

Triantafyllou, E., Psanis, C., Floutsi, A.A., Diapouli, E., Eleftheriadis, K., Biskos, G. *Air Pollution at a coastal city of the Northern Aegean Sea*. European Aerosol Conference (EAC), Milan, Italy, 6 - 11 September 2015.

Triantafyllou, E., Giamarelou, M., Bossioli, E., Zarnpas, P., Theodosi, C., Matsoukas, C., Tombrou, M., Mihalopoulos, N., Biskos, G. *Long-range transported air pollutants from continental areas to the remote region of the North Aegean Sea*. 14th International Conference on Environmental Science and Technology (CEST), Rhodes, Greece, 3 - 5 September 2015.

Triantafyllou, E., M. Giamarelou, M., Bezantakos, S., Barmounis, K., Bossioli, E., Theodosi, Ch., Tombrou, M., Mihalopoulos, N., Eleftheriadis, K., Biskos, G. *Physicochemical Properties of Ultrafine Aerosol Particles in the North Aegean during the AEGEAN-GAME Field Campaign*. European Aerosol Conference (EAC), Granada, Spain, 2 - 7 September 2012.

Triantafyllou, E., Biskos, G. *Overview of PM₁₀ concentrations in Athens and Thessaloniki, Greece*, International Aerosol Conference (IAC), Helsinki, Finland, 29 August - 3 September 2010.

Table of Contents

Chapter 1

Introduction	1
1.1 Atmospheric pollution	1
1.2 Atmospheric particles and their characteristics	1
1.3 Effects of particulate matter in air pollution.....	4
1.3.1 Visibility degradation	4
1.3.2 Effects on climate change.....	5
1.3.3 Health effects of particulate matter	6
1.4 Air quality legislation and standards for particulate matter	8
1.5 Methods of particulate matter measurements.....	10
1.6 Chemical analysis methods for particulate matter.....	13
1.7 Urban particulate matter observations.....	15
1.8 Scope and structure of the Thesis	16

Chapter 2

Overview of the temporal variation of PM₁₀ mass concentrations in the two major cities in Greece: Athens and Thessaloniki	17
2.1 Abstract.....	17
2.2 Introduction	17
2.3 Methods and techniques	19
2.3.1 Study areas and sampling stations	19
2.3.2 Data Analysis.....	21
2.4 Results and discussion	21
2.4.1 Annual variation	21
2.4.2 Seasonal and monthly variation.....	27
2.5 Conclusions	31

Chapter 3

Particulate pollution transport episodes from Eurasia to a remote region of northeast Mediterranean	33
3.1 Abstract.....	33
3.2 Introduction	34
3.3 Experimental.....	35

3.4 Results and discussion	37
3.4.1 Chemical composition of aerosols.....	41
3.4.2 Transportation pathways of the sampled air masses	43
3.5 Conclusions	46

Chapter 4

Characterisation of the atmospheric urban aerosol in a background marine region

4.1 Abstract.....	47
4.2 Introduction	48
4.3. Methods	49
4.3.1. Study areas and meteorology.....	49
4.3.2. Measurements and analytical methods	51
4.4 Results and discussion.....	52
4.4.1 Particle mass concentrations.....	52
4.4.2 PM chemical composition	56
4.4.3 Particle number size distributions and concentrations	65
4.5 Conclusions	66

Chapter 5

Assessment of factors influencing PM mass concentration measured by gravimetric & beta attenuation techniques at a suburban site.....

5.1 Abstract.....	68
5.2 Introduction	69
5.3 Methodology.....	71
5.3.1 The study area.....	71
5.3.2 Measurements and Methods	73
5.4 Results and discussion.....	74
5.4.1 PM _{2.5} measurements	74
5.4.1.1 Concentration levels	74
5.4.1.2 Correlation between BA and GM measurements	75
5.4.1.3 Effect of meteorological and sampling conditions	77
5.5 PM ₁₀ measurements.....	83
5.6 Conclusions	85

Chapter 6	
Summary and future research	89
6.1 Summary and conclusions	87
6.2 Future research	91
References	93
Appendix A	127
Appendix B	141
PART A - Additional Data	141
PART B - Calculation of [H ₂ SO ₄].....	141
Appendix C	143
Additional Data.....	143

List of Figures

Figure 1.1: The principal modes, particle formation and removal mechanisms of particles in the atmospheric environment.	3
Figure 1.2: Three effects of particle light interactions including reflection, diffraction and refraction.	5
Figure 1.3: The changes of greenhouse gases, aerosols and solar activity and their effect in globally averaged radiative forcing from year 1750 to 2011.	6
Figure 1.4: The human respiratory system and the three groups of particles according to their health risks.	7
Figure 1.5: A typical arrangement of “hi-volume” sampler for the particle mass concentration measurements. (1) is the hood, (2) is the air inlet, (3) is the flow control, (4) is the fan, while (5) and (6) is electronics and the motor control. Finally, (7) is the air exhaust.	11
Figure 1.6: A typical arrangement of β -ray attenuation sensor for the particle mass concentration measurements. (1) and (2) are the booths of ionization, (3) is the radioactive source (Krypton-85), (4) is the booth of particle matter collection, (5) is the filter tape, and (6) is the recorder.	12
Figure 1.7: A typical arrangement of electrical mobility spectrometer for the particle number concentration and size distribution measurements. The main parts are (1) the aerosol charger, (2) a Differential Mobility Analyser (DMA), (3) a condensation particle counter (CPC), and (4) the data recorder (PC).	13
Figure 1.8: A typical arrangement of energy dispersive x-ray fluorescence spectroscopy (EDXRF) for the elemental analysis of particulate matter measurements. The main parts are a x-ray source, a sample cassette, an energy dispersion detector, a multi-channel analyzer and a data recorder (PC).	14
Figure 1.9: A typical arrangement of ion chromatography system for chemical analysis of anions and cations of particulate matter. The main parts are a pump, a sample loop; where is injected the sample solution, a column in which the separation of solutions molecules occurs, a detector and a data recorder (PC).	15
Figure 2.1: Map of Greece showing the cities of Athens (ATH) and Thessaloniki (THS) and the locations of the stations from which we obtained PM daily average PM_{10} concentrations.	20
Figure 2.2: Annual average PM_{10} concentrations ($\mu g m^{-3}$) at three urban (PIR, MAR, ARI) and three suburban (LYK, THR, AGP) monitoring stations in Athens. Each box plot shows the median (middle line of the box), upper (25%) and lower (75%) quartile (top and bottom lines of the box, respectively) as well as the minimum and maximum values (upper and lower end of the whisker lines).	23

Figure 2.3: Time series of annual average PM ₁₀ concentrations ($\mu\text{g m}^{-3}$) at two urban (KOD, AGS) and three suburban (PAO, SIN, KAL) monitoring stations in Thessaloniki. Each box plot shows the median (middle line of the box), upper (25%) and lower (75%) quartile (top and bottom lines of the box, respectively) as well as the minimum and maximum values (upper and lower end of the whisker lines).	25
Figure 2.4: Monthly average PM ₁₀ concentrations ($\mu\text{g m}^{-3}$) at three urban (PIR, MAR, ARI) and three suburban (LYK, THR, AGP) monitoring stations in Athens. Each box plot shows the median (middle line of the box), upper 25% and lower 75% quartile (top and bottom lines of the box, respectively) and the minimum and maximum values (upper and lower end of the whisker lines).....	29
Figure 2.5: Monthly average PM ₁₀ concentrations ($\mu\text{g m}^{-3}$) at two urban (KOD, AGS) and three suburban (PAO, SIN, KAL) monitoring stations in Thessaloniki. Each box plot shows the median (middle line of the box), upper 25% and lower 75% quartile (top and bottom lines of the box, respectively) and the minimum and maximum values (upper and lower end of the whisker lines).	30
Figure 3.1: Map showing the island of Lemnos (39° 58' N, 25° 04' E) and the location of the station at Vigla (420 m a.s.l.). The most important industrial sites and the largest cities close to the monitoring station are also shown.	36
Figure 3.2: Wind rose for Lemnos during the sampling period. Calm conditions are identified when the wind speeds are $< 1 \text{ m s}^{-1}$	37
Figure 3.3: Particle size distributions measured from 27 August to 10 September 2011 at the Vigla station. Normalized particle number size distributions (a), time series of particle number concentrations having sizes in the range 10-500 nm (black line), 10-25 nm (blue line), 26-90 nm (red line), 91-500 nm (green line) (b), and of the wind speed (solid black line) and direction (dashed black line) during the entire sampling period (c). The days of Etesians (ED) are indicated at the top of the figure. The black dashed line shown in 3b indicates the $N_{d<25\text{nm}}$ above which we have PT episodes. Light shaded areas in 3b and 3c indicate the periods with PT episodes that are characterized as moderate (i.e., on 27 (239 DOY), 28 (240 DOY), and 29 (241 DOY) August, as well as on 5 (248 DOY), 6 (249 DOY), 7 (250 DOY)), while the dark shaded area indicates the period with the strong PT episode (on 10 (253 DOY) September). The red rectangle in 3.3b and 3.3c corresponds to the period when the prevailing wind conditions were similar to those during the PT episodes but $N_{d<25\text{nm}}$ was below the threshold value.....	38
Figure 3.4: Particle number size distribution measurements before (a), during (b and c) and after (d) the PT episode on 241 DOY. The square symbols represent the measurements, whereas the solid and the dashed lines are the overall and the individual-mode lognormal fits, respectively.....	40

Figure 3.5: Ion mass fractions of PM _{1.0} samples collected on filters during ordinary days (a), PT episodes (b), and transition periods (c).....	42
Figure 3.6: Horizontal (a) and vertical (b) paths of 5-day back-trajectory calculations during the PT episodes and on 8 (251 DOY) September. All the trajectories on 27 (239 DOY), 28 (240 DOY), and 29 (241 DOY) August as well as on 5 (248 DOY), 6 (249 DOY), 7 (250 DOY), 8 (251 DOY) and 10 (253 DOY) September (magenta, red, blue, orange, cyan, yellow, dark green and green lines, respectively) start at 12:00 UTC. The dots on each trajectory indicate the position of the air parcels at the end of each 6-h interval before reaching the monitoring station.....	44
Figure 3.7: Vertical wind motion (omega fields) at 500 hPa during the PT episode on 27 (239 DOY) August (a) and during the non episode day on 30 (242 DOY) August (b) based on daily reanalysis data from the National Centers for Environmental Prediction (NCEP).The color bar shows the changes of the vertical velocity (Pa min ⁻¹).	45
Figure 4.1: Map of Greece showing the islands of Lesvos (39° 10' N, 26° 20' E) and the cities of high population density (up to 1 million inhabitants) in the Eastern Mediterranean area (black solid circles). The detailed map on the right, show the city of Mytilene, the airport, the power plant and the monitoring stations, at the centre (Sapfous Square, SSM) and at the port (Port Authorities, PAM) of the city.....	50
Figure 4.2: Mass concentrations of TSP, PM _{2.0} and PM _{1.0} measured at SSM during winter and summer.....	52
Figure 4.3: Mass concentrations of TSP, PM _{2.0} and PM _{1.0} during the days with or without desert dust sources measured at SSM of Mytilene during winter.....	54
Figure 4.4: Mass size distributions of particles having diameters in the size range 0.1-3.2 μm measured at SSM during (a) winter and (b) summer.	56
Figure 4.5: Enrichment factors for the major elements in TSP mass at SSM and PAM and in PM _{2.0} and PM _{1.0} at SSM in winter (a) and summer (b) period.	62
Figure 4.6: Elemental size distributions of S, Ti and K measured at the monitoring site SSM during winter (a, c and e, respectively) and summer (b, d and f, respectively).	64
Figure 4.7: Diurnal evolution of the normalized particle number size distributions and of the average number concentrations of particles having sizes in the range 10-500 nm (black line), 10-25 nm (blue line), 26-90 nm (red line) and 97-500 nm (green line), measured at SSM during winter (a, and c, respectively) and summer (b, and d, respectively).	65
Figure 5.1: Map showing the location of the monitoring stations operated by NCSR “Demokritos” (DEM Station) and the National Monitoring Network (NMN Station) at the suburban area of Agia Paraskevi in Athens, Greece.	72

Figure 5.2: Time series of PM_{2.5} mass concentrations measured by gravimetric (blue circles) and beta attenuation (red diamonds) methods at Agia Paraskevi from 2009 to 2012.74

Figure 5.3: Linear correlation between BAM PM_{2.5} and GM PM_{2.5} measurements for (a) all the data, and when (b) Teflon, (c) Glass fiber and (d) Quartz were used in the GM measurements. Red and blue circles correspond to measurements during the warm and the cold period, respectively. Outliers are depicted by diamond-shaped data points. The black line represents the linear fit for all data, while red and blue dashed lines are the fitted equations to the warm and cold season data, respectively.76

Figure 5.4: Variation of the monthly averaged BAM PM_{2.5} to GM PM_{2.5} concentration ratio (bars and blue line) and of the corresponding temperature (red line), relative humidity (green line) and the water vapor pressure normalized by PM_{2.5} concentrations (orange line).78

Figure 5.5: Correlation between the BAM PM_{2.5}/GM PM_{2.5} ratio and the normalized water vapor pressure, for (a) the entire data set and separately when (b) Teflon, (c) glass fiber, and (d) quartz filters were used in the GM measurements. The dashed line show best fit regression models.....79

Figure 5.6: Correlation between the BAM PM_{2.5}/GM PM_{2.5} ratio and the relative humidity when Teflon filters were used in the GM measurements and the ambient temperature was (a) less than 10°C, (b) between 11 and 22°C, and (c) higher than 22°C. The dashed line show best-fit regression models.....81

Figure 5.7: Correlation between the normalized water vapor pressure and the BAM PM_{2.5}/GM PM_{2.5} ratio (blue solid circles), or the relative humidity (blue open circles), when the ambient temperature was (a) less than 10 °C, (b) between 11 and 22°C, and (c) higher than 22°C. The black solid line and the blue dashed line represent best linear fit for the correlations between the normalized water vapor pressure and the BAM PM_{2.5}/GM PM_{2.5} ratio and the relative humidity, respectively. These correlations include the PM_{2.5} samples collected on Teflon filters.....82

Figure B1: Time series of hourly-averaged ambient temperature (black line), relative humidity (blue line), and ultraviolet radiation (red line) (a), hourly-averaged sulfur dioxide concentration (b), condensation sink (c), sulfuric acid concentration (black line) and nucleation-mode particle number concentration (green line) (d) observed on Lemnos from 27 August to 10 September 2011. The red dashed line shown in subplot c and d indicates the threshold values of condensation sink and sulfuric acid for PT episodes. Light shaded areas indicate transportation episodes that are characterized as moderate (239, 240, 241, 248, 249, and 250 DOY), while the dark shaded indicates the day with a strong PT episode (253 DOY).....141

Figure C1: The time series of concentrations of TSP on an 8h basis (a), PM_{2.0} and PM_{1.0} on a 48h basis (b), as well as average 1h values of wind direction and wind speed (c) in Mytilene during summer period. The dashed lines in 3a and 3b show the average TSP concentrations at SSM and PAM (black and red lines, respectively) and the average PM_{2.0} and PM_{1.0} concentrations at SSM (black and green lines, respectively). The light and dark grey shaded areas refer to the days when pollution was transported to Mytilene from distant and desert dust sources, respectively. 143

Figure C2: The time series of concentrations of TSP on an 8h basis (a), PM_{2.0} and PM_{1.0} on a 48h basis (b), as well as average 1h values of wind direction and wind speed (c) in Mytilene during winter period. The dashed lines in 1a and 1b show the average TSP concentrations at SSM and PAM (black and red lines, respectively) and the average PM_{2.0} and PM_{1.0} concentrations at SSM (black and green lines, respectively). The light and dark grey shaded areas refer to the days when pollution was transported to Mytilene from distant and desert dust sources, respectively. Light blue shaded areas show the days with precipitation. 144

Figure C3: Map and the figure show the horizontal (top) and vertical (bottom) motion of the 5-day back-trajectory calculations arriving at SSM in Mytilene during the winter (a) and summer (b). All the trajectories on 29 (29 DOY) January, and on 4 (35 DOY), 8 (39 DOY), 15 (46 DOY), 19 (50 DOY), 20 (51 DOY) and 21 (52 DOY) February (orange, blue, magenta, green, red, turquoise and yellow lines, respectively), as well as on 28 (179 DOY) June and on 4 (185 DOY), 8 (189 DOY), 9 (190 DOY) and 13 (194 DOY) July (magenta, pink, green, red and turquoise lines, respectively) start at 12 UTC. The dots on each trajectory indicate the position of air parcels at the end of each 6-h interval before reaching the monitoring station. The main origin sectors of air masses during the sampling periods were: OS1-western air masses transported from the region of Crete, OS2-northeastern and southeastern air masses coming from the Turkey and OS3-northwestern and southwestern from the region of Thessaloniki and Athens, respectively. 144

Figure C4: Map and the figure show the horizontal (top) and vertical (bottom) motion of the 5-day back-trajectory calculations arriving at the monitoring site in Mytilene when air masses transported from North Africa (OS4) during winter and summer period. All the trajectories on 11 (42 DOY), 22 (53 DOY) and 23 (54 DOY) February, and on 26 (177 DOY) and 27 (178 DOY) June (red, orange, yellow, green and blue lines, respectively) start at 12 UTC. The dots on each trajectory indicate the position of air parcels at the end of each 6-h interval before reaching the monitoring station. 145

Figure C5: Maps of dust aerosol concentrations ($\mu\text{g m}^{-3}$) by SKIRON model and the motion of wind speed (m s^{-1}) at 12 UTC when air masses transported from North Africa on 23 (53 DOY) February (a and b, respectively) and on 26 (177 DOY) June (c and d, respectively). 146

Figure C6: Average number concentrations having sizes in the range 10-500 nm during the days without transported air pollution, with transport of anthropogenic air pollution and with desert dust sources measured at SSM of Mytilene during winter and summer. 146

List of Tables

Table 1.1: Effects of short-term and long-term exposure to particulate matter on human health.....	8
Table 1.2: Comparison of the Unites States and European Union current air quality guidelines.....	9
Table 4.1: Statistics of average hourly wind speed and boundary layer height during the winter and summer sampling periods.....	53
Table 4.2: Concentration ratios of the different PM fractions measured at Mytilene during winter and summer period.	55
Table 4.3: Average and the standard deviation of elemental concentrations (in ng m ⁻³) in TSP mass at the monitoring sites SSM and PAM in winter and summer.....	57
Table 4.4: Average and standard deviation of elemental concentrations (in ng m ⁻³) of the PM _{2.0} and PM _{1.0} samples collected at the monitoring site SSM in winter and summer.	58
Table 4.5: Correlation coefficients (R ²) among the TSP elemental concentrations at SSM and PAM during winter (a and b, respectively) and summer (c and d, respectively). Only R ² equal or higher than 0.40 (p-value of 0.05) are shown. ...	60
Table 4.6: Correlation coefficients (R ²) between the elemental concentrations of the PM _{2.0} and PM _{1.0} mass at SSM, that were equal or higher than 0.40 (p-value of 0.05) in winter (a and b, respectively) and summer (c and d, respectively).....	61
Table 5.1: Descriptive statistics for the GM PM _{2.5} and BAM PM _{2.5} concentrations measured at Agia Paraskevi from 2009 to 2012.	75
Table 5.2: Descriptive statistics of PM ₁₀ concentrations measured at Agia Paraskevi by beta-attenuation (BAM) and gravimetric method (GM) for the years 2011 and 2012.	84
Table A1: Information of the sampling stations at the two largest cities in Greece. The last column indicates the operator of each air quality network.....	127
Table A2: Descriptive statistics (Mean, Standard Deviation, N total values, Min and Max) for average PM ₁₀ concentrations (µg m ⁻³) and the exceedances (Ex.D.; more than 35 days) of the EU 24-h limit value (50 µg m ⁻³) at the monitoring stations in Athens.....	128
Table A3: The results of Kolmogorov - Smirnov test for PM ₁₀ concentrations and log transformed averaged PM ₁₀ concentrations in Athens from 2001 to 2010	129
Table A4: The results of Levene's test of log-transformed annual-averaged PM ₁₀ concentrations in Athens from 2001 to 2010.....	129
Table A5: The results of One-way ANOVA procedure for log-transformed (LN) annual averaged PM ₁₀ concentrations in Athens from 2001 to 2010.	130

Table A6: The Tukey HSD test log-transformed annual-averaged PM ₁₀ concentrations at ARI station from 2001 to 2010. The critical level of confidence was 0.05.....	130
Table A7: The Tukey HSD test log-transformed annual-averaged PM ₁₀ concentrations at THR station from 2001 to 2010. The critical level of confidence was 0.05.	130
Table A8: The Tukey HSD test of log-transformed annual-averaged PM ₁₀ concentrations at LYK station from 2001 to 2010. The critical level of confidence was 0.05.	131
Table A9: The results of Welch ANOVA procedure of log-transformed (LN) annual-averaged PM ₁₀ concentrations at PIR, MAR and AGP stations in Athens from 2001 to 2010.	131
Table A10: The Games-Howell post hoc test of log-transformed annual-averaged PM ₁₀ concentrations at PIR station in Athens from 2001 to 2010.....	132
Table A11: The Games-Howell post hoc test of log-transformed annual-averaged PM ₁₀ concentrations at MAR station in Athens from 2004 to 2010...	132
Table A12: The Games-Howell post hoc test of log-transformed annual-averaged PM ₁₀ concentrations at AGP station from 2001 to 2010.....	132
Table A13: Descriptive statistics (Mean, Standard Deviation, N total values, Min and Max) for average PM ₁₀ concentrations ($\mu\text{g m}^{-3}$) and the exceedances (Exc.D.; more than 35 days) of the EU 24-h limit value ($50 \mu\text{g m}^{-3}$) at all stations in Thessaloniki from 2001 to 2010.....	133
Table A14: The results of Kolmogorov-Smirnov test for PM ₁₀ concentrations and log transformed (LN) averaged PM ₁₀ concentrations in Thessaloniki from 2001 to 2010.	134
Table A15: The results of Levene's test of log-transformed (LN) annual-averaged PM ₁₀ concentrations in Thessaloniki from 2001 to 2010.....	134
Table A16: The results of One-way ANOVA procedure for log-transformed (LN) annual-averaged PM ₁₀ concentrations at SIN and PAO stations in Thessaloniki from 2001 to 2008.....	135
Table A17: The Tukey HSD test of log-transformed (LN) annual-averaged PM ₁₀ concentrations at SIN station from 2001 to 2010. The critical level of confidence was 0.05.....	135
Table A18: The Tukey HSD test of log-transformed annual-averaged PM ₁₀ concentrations at PAO station from 2001 to 2010. The critical level of confidence was 0.05.	135
Table A19: The results of Welch ANOVA procedure of log-transformed (LN) annual-averaged PM ₁₀ concentrations at KOD, AGS and KAL stations in Thessaloniki from 2001 to 2010.....	136

Table A20: The Games-Howell post hoc test of log-transformed (LN) annual-averaged PM ₁₀ concentrations at KOD station in Thessaloniki from 2001 to 2010.	136
Table A21: The Games-Howell post hoc test of log-transformed (LN) annual-averaged PM ₁₀ concentrations at AGS station in Thessaloniki from 2001 to 2010	136
Table A22: The Games-Howell post hoc test of log-transformed (LN) annual-averaged PM ₁₀ concentrations at KAL station in Thessaloniki from 2001 to 2010.	137
Table A23: The results of Levene's test of log-transformed (LN) seasonal-averaged PM ₁₀ concentrations in Athens from 2001 to 2010.....	137
Table A24: The results of Welch ANOVA procedure of log-transformed (LN) seasonal-averaged PM ₁₀ concentrations in Athens stations from 2001 to 2010.	137
Table A25: The Games-Howell post hoc test of log-transformed (LN) seasonal-averaged PM ₁₀ concentrations at PIR, MAR, ARI, THR, LYK and AGP stations in Athens from 2001 to 2010.....	138
Table A26: The results of Levene's test of log-transformed (LN) seasonal-averaged PM ₁₀ concentrations in Thessaloniki from 2001 to 2010.....	139
Table A27: The results of Welch ANOVA procedure of log-transformed (LN) seasonal-averaged PM ₁₀ concentrations at all the stations in Thessaloniki from 2001 to 2010.	139
Table A28: The Games-Howell post hoc test of log-transformed (LN) seasonal-averaged PM ₁₀ concentrations at all the stations in Thessaloniki from 2001 to 2010.	139

List of Notation

%	Per cent
°C	Celsius or centigrade
As	Arsenic
Ba	Barium
Br	Bromine
Ca ²⁺	Calcium
Cd	Cadmium
Cl	Chlorine
cm ²	Centimeter of square meter
cm ³	Centimeter of cubic meter
Co	Cobalt
Cr	Chromium
Cu	Copper
dN/dlogDp	Normalized particle number concentration
EFs	Enrichment factors
Fe	Iron
H	Hour or hours
H ₂ SO ₄ or ([H ₂ SO ₄])	Sulphuric acid
(HNH ₄) ₂ SO ₄	Ammonium sulphate
HNO ₃	Nitric acid
hPa	Hectopascal
K ⁺	Potassium
Km	Kilometers
log	Logarithm
m	Meter
m asl or m a.s.l.	Meter above sea level
m s ⁻¹	Meters per second
m ³ h ⁻¹	Cubic meter per hour
Mg	Magnesium
Min	Minute or minutes
Mn	Manganese
molecules cm ⁻³	Molecules per centimeter of cubic meter
Na ⁺	Sodium
NH ₃	Ammonia
NH ₄ ⁺	Ammonium
NH ₄ HSO ₄	Ammonium bisulphate
NH ₄ NO ₃	Ammonium nitrate
Ni	Nickel
Nm	Nanometers
nm h ⁻¹	Nanometers per hour
NO	Nitrogen monoxide
NO ₂	Nitrogen dioxide
NO ₃ ⁻	Nitrate
NO _x	Nitrogen oxides
O ₃	Ozone
P	Phosphorus
Pa min ⁻¹	Pascal per minute
particles cm ⁻³	Particles per centimeter of cubic meter
Pb	Lead
people/km ²	People per square kilometer
PM	Particulate matter
PM ₁₀	Particulate matter with a diameter of 10 micrometers

PM _{2.5}	Particulate matter with a diameter of 2.5 micrometers
R ²	Coefficient of determination
S	Sulfur
SO ₂	Sulphur dioxide
SO ₄ ²⁻	Sulfate
SO _x	Sulphur oxides
Sr	Strontium
Ti	Titanium
TSP	Total suspended particles
V	Vanadium
VOC	Volatile organic compounds
Wm ⁻²	Watt per square meter
Zn	Zinc
µg m ⁻³	Micrograms per cubic meter
µm	Micrometers

List of abbreviations

ACTRIS networks	Aerosol, Clouds, and Trace gases Research InfraStructure Networks
AGP	Agia Paraskevi
AGS	Agia Sofia square
ANOVA	Analysis Of Variance
ARI	Aristotelous
ATH	Athens
BAM	Beta attenuation method
ca.	Approximately
cf.	See also or compare (conferre)
CS	Condensation sink
DOY	Day Of Year
E	East
e.g.	For example (exempli gratia)
EC	European Commission
ENE	East - northeast
EPA	Environmental Pollution Agency
<i>e_s</i>	Maximum water vapor pressure
ESE	East - southeast
EU	European Union
Fig.	Figure
GAW	Global Atmosphere Watch
GM	Gravimetric method
HMEECC	Hellenic Ministry of Environment Energy & Climate Change
i.e.	In essence, that means or it is (id est)
IPCC	Integrated Pollution Prevention and Control
KAL	Kalamaria
KOD	Kordelio
KR	Kountouriotou
LYK	Lykovrissi
MAR	Maroussi
MEPPPW	Ministry of Environmental Physical Planning and Public Works
N	North
NAS	North Aegean Sea

NE	Northeast
NMMB/BSC-dust transport	Non-hydrostatic Multiscale Model/Barcelona Supercomputing Center – dust transport
NMN	National Monitoring Network
NNE	North - northeast
NNW	North – northwest
NOAA HYSPLIT model	National Oceanic and Atmospheric Administration Hybrid Single Particle Lagrangian Integrated Trajectory Model
NSCR	National Center for Scientific Research
NW	Northwest
OC/EC	Organic carbon / Elemental carbon
OD	Ordinary days
PAM	Port Authorities of Mytilene
PAO	Panorama
PIR	Piraeus
PT	Particulate transport
RCM	Region of Central Macedonia
RH	Relative humidity
S	South
SE	Southeast
SIN	Sindos
SSE	South - southeast
SSQ	Sapfous square
SSW	South - southwest
SW	Southwest
T	Temperature
TEOM	Tapered-Element Oscillating Microbalance
THR	Thrakomacedones
THS	Thessaloniki
TP	Transition periods
Tukey HSD tests	Tukey Honestly Significant Difference tests
US	United States
US-EPA	US Environmental Protection Agency
UTC	Coordinated Universal Time
UV	Ultraviolet radiation
W	West
WNW	West - northwest
WSW	West - southwest

Greek abbreviations

ΑΓΠΑΡ	Αγία Παρασκευή
ΑΣ ₁₀	Αιωρούμενα σωματίδια με διάμετρο μικρότερη από 10 μm
ΑΣ _{2.5}	Αιωρούμενα σωματίδια με διάμετρο μικρότερη από 2.5 μm
ΑΣ _{2.0}	Αιωρούμενα σωματίδια με διάμετρο μικρότερη από 2.0 μm
ΑΣ _{1.0}	Αιωρούμενα σωματίδια με διάμετρο μικρότερη από 1.0 μm
ΒΑ	Βόρειο Αιγαίο
ΘΡΑ	Θρακομακεδόνες
ΚΑΛ	Καλαμαριά
ΛΥΚ	Λυκόβρυση
ΠΕΙ	Πειραιά
ΣΙΝ	Σίνδος

Chapter 1

Introduction

1.1 Atmospheric pollution

Deterioration of air quality is an important environmental issue in urban and remote areas, which occurs as a result of local and regional emissions as well as transportation of air pollutants. Air pollutants are considered to be all compounds that deliberately, or through a natural process, enter the atmosphere that are not part of the original, normal composition. They can be classified as primary and secondary. Primary pollutants are those emitted directly into the atmosphere (e.g., SO₂, NO, CO, hydrocarbons, most suspended particles), while secondary pollutants are those formed in the atmosphere through chemical transformation of primary pollutants or products of different complicated reactions (e.g., O₃, H₂SO₄, HNO₃). In the atmosphere, pollutants can be in the form of gases or liquid droplets and solid particles, usually referred to as particulate matter (PM). Particle pollutants are of particular interest because of their impact on public health (Pope III et al., 1995; Pope III, 2000; Dockery, 2001) and their contribution to climate change (Penner et al., 1998; Jacobson, 2001; Kanakidou et al., 2005; Seinfeld and Pandis, 2006) as discussed below.

1.2 Atmospheric particles and their characteristics

Atmospheric particles are microscopic liquid and solid particles such as dust, carbon particles, pollen, sea salts and microorganisms suspended in the air, that range in size from a few nanometers (nm) to tens of micrometers (µm) (Seinfeld and Pandis, 2006). They mostly contain inorganic ions, metal compounds, elemental carbon, organic compounds and crustal compounds (EPA, 2004). The term of

atmospheric aerosol is used to describe both the particulate and the gaseous phase (Hinds, 1999).

Emissions of atmospheric particles are from natural and anthropogenic sources. Major natural sources of particles include desert and soil dust, sea salt, volcanic eruptions, and forest fires (Boubel et al., 1994), while the major anthropogenic sources of particle emissions related to the transportation (i.e., diesel vehicles, aircrafts), industrial processes and other miscellaneous sources including household and commercial sources (Wark et al., 1997).

Particles enter and exit the atmospheric environment by various processes (Colls, 2002). They may be emitted directly (primary) or formed in the atmosphere (secondary) by transformations of gaseous emissions such as sulphur oxides (SO_x), nitrogen oxides (NO_x), and volatile organic compounds (VOC) (Seinfeld and Pandis, 2006). Examples of secondary particle formation include: (1) the conversion of sulphur dioxide (SO_2) to sulphuric acid (H_2SO_4) droplets that further react with gaseous ammonia (NH_3) to form various sulphate particles (e.g., ammonium sulphate, $(\text{NH}_4)_2\text{SO}_4$, ammonium bisulphate, NH_4HSO_4 , etc.), (2) the conversion of nitrogen dioxide (NO_2) to nitric acid (HNO_3) vapour that reacts further with ammonia to form ammonium nitrate (NH_4NO_3) particles, and (3) reactions involving gaseous VOCs yielding organic compounds with low vapour pressures that nucleate or condense on existing particles to form secondary organic aerosol particles (EPA, 2004).

The chemical composition of PM consists of inorganic and organic species such as sulfates, nitrates, ammonium, crustal species, sea salt, hydrogen ions and water. The contribution of organic and inorganic compounds to their total mass depends on various factors such as their sources, the atmospheric conditions, and their size. Nitrates can be found in both the fine and coarse particles, while sulfates, ammonium, organic and elemental carbon and some transition metals mainly originate from combustion sources (i.e., in fine fraction).

Particles can participate in physical and chemical processes in the atmosphere; thereby significantly affecting its properties. They can change their size and concentration by nucleation, condensation, evaporation, aggregation, precipitation and

participation in chemical reactions (cf. Figure 1.1; Colbeck and Lazaridis, 2014). Because particle size plays an important role on their potential impacts (e.g., environment, human health), it is important to know the distribution of their size.

Particles having diameters greater than ca. 2.5 μm are characterized as coarse, while those with diameter less than ca. 2.5 μm are referred to as fine. The fine mode fraction typically includes most of the total number of particles and a large part of the mass. Fine particles can also be divided into two sub-modes. The accumulation mode includes particles having a diameter between about ca. 0.08 and 2.1 μm , and the nucleation together with Aitken mode includes particles with diameter less than 0.08 μm (Finlayson-Pitts and Pitts, 1986). Nucleation mode particles can grow both through coagulation and by condensation of low volatility compounds into accumulation mode particles (Jacobson, 2002).

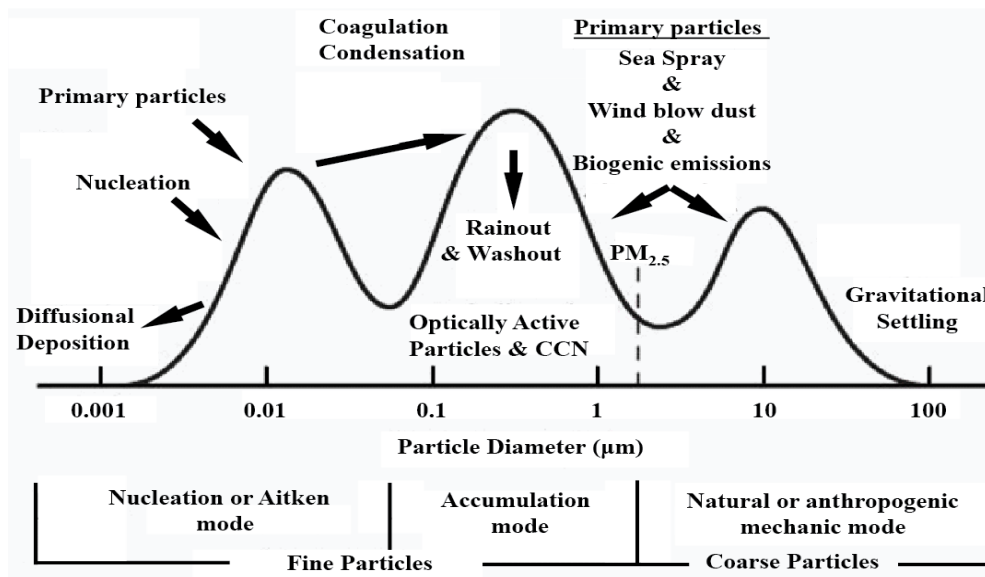


Figure 1.1: The principal modes, particle formation and removal mechanisms of particles in the atmospheric environment.

The coarse mode consists of coarse particles with diameters from 2.5 to 10 μm that are usually formed by mechanical processes such as attrition and suspension of dust. Because of their natural mechanical formation, they have relatively large size and can be removed from the atmosphere by deposition (Finlayson-Pitts and Pitts, 1986).

The accumulation mode is important because particles in this mode are more likely to cause adverse health effects by penetrating deep into the lungs, and also reduce visibility as they have sizes close to the peak wavelengths of visible light. Generally, nucleation mode particles have the highest surface area concentrations and the coarse mode particles have the highest volume and mass concentrations (Jacobson, 2002). The residence time of the particles in the atmosphere varies from a few days, when the particle size is greater than 1 micron and a few weeks for the particles smaller than 1 micron (Colbeck and Lazaridis, 2014).

1.3 Effects of particulate matter in air pollution

Atmospheric particulate matter has been demonstrated to have a significant number of effects in the environment. PM can impair atmospheric visibility by scattering and absorption of solar radiation, affect directly (by both scattering and absorption of solar radiation) and indirectly (by acting as cloud condensation nuclei) the Earth's climate, and cause serious health problems (IPCC, 2013).

1.3.1 Visibility degradation

Several factors determine how far one can see through the atmosphere, including the gas phase composition of the atmosphere and the concentration and chemical composition of the suspended atmospheric particles (Seinfeld, 1986). Although most suspended particles in the atmosphere reflect light, some can also absorb it. The strongest aerosol particle absorbing material in the visible spectrum is black carbon, while sulfates and nitrates as well as other translucent particles scatter light. Also, particles like those of mineral dust can either scatter or absorb both incoming and outgoing radiation (Jacobson, 2002).

Particles having diameters within the range of the wavelength of light reduce the atmospheric visibility through absorption and light scattering (Malm, 1999). Absorption takes place when electromagnetic radiation interacts with the particles, transferring energy to them. Light scattering by particles change the direction and/or the frequency of the light (Boubel et al., 1994). More precisely, particle scattering is

the combination of reflection, refraction, and diffraction (Figure 1.2). When a wave approaches a particle it can be absorbed, transmitted through the particle and refracted out, or reflected internally one or more times and then refracted out (Jacobson, 2002). Scattering of solar radiation by aerosol particles is the main process limiting visibility in the troposphere. Anthropogenic aerosols in urban environments typically reduce visibility by one order of magnitude relative to unpolluted conditions. The atmospheric haze is a case of reduced visibility, caused by the presence of fine particles (typically ammonium sulphate) and NO_2 in the atmosphere. The reduction in visibility is greatest at high relative humidities when the aerosol particles swell due to water uptake, increasing the cross-sectional area and therefore their ability to scatter and absorb light (Jacob, 1999).

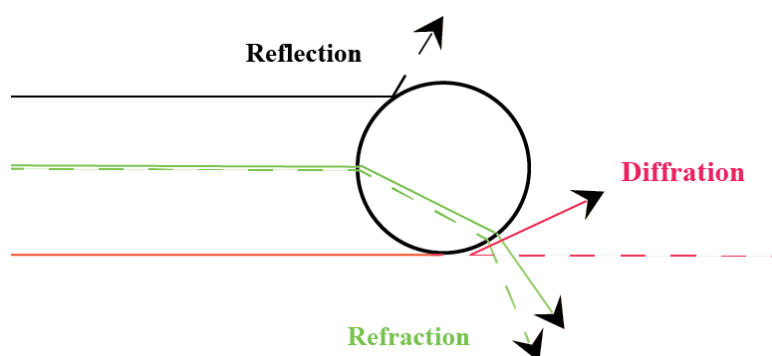


Figure 1.2: Three effects of particle light interactions including reflection, diffraction and refraction.

1.3.2 Effects on climate change

Changes of the concentrations of greenhouse gases and aerosols in the atmosphere of solar radiation, and of the properties of the Earth's surface contribute to the climate by causing changes to the Earth's energy balance. These changes are expressed in correspondence of the radiation intensity, which is used to compare how a range of human and natural factors can cause heating or cooling of the planet (IPCC, 2013).

Aerosols perturb the climate directly through scattering and absorption of solar radiation and indirectly through their ability to act as cloud condensation nuclei (Seinfeld and Pandis, 2006). Scattering and absorbing properties of aerosols depend primarily on their composition. Compared to the greenhouse gases, which have a

warming effect and act only on the outgoing infrared radiation, aerosol particles act on both sides of the energy balance (Seinfeld and Pandis, 2006). Consequently, anthropogenic aerosols may partly explain why the Earth's surface is not getting as warm as one would have expected when the concentrations of greenhouse gases continue to increase (Figure 1.3). Although it is difficult to access the impact of aerosols on climate, they are believed to have an overall negative contribution to the radiative balance of the planet.

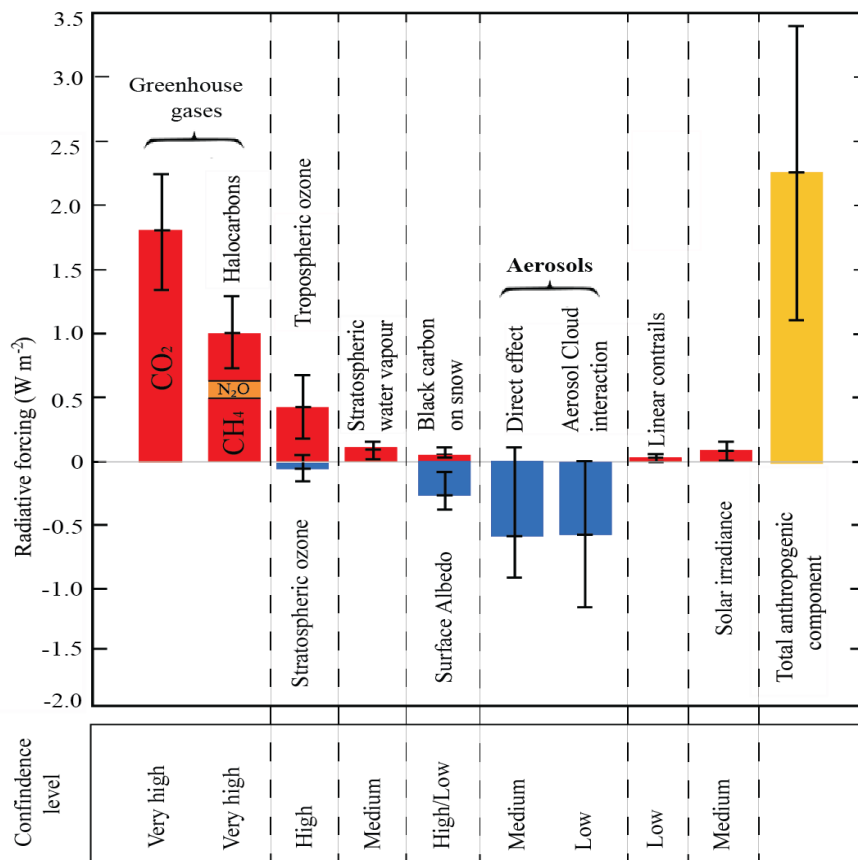


Figure 1.3: The changes of greenhouse gases, aerosols and solar activity and their effect in globally averaged radiative forcing from year 1750 to 2011.

1.3.3 Health effects of particulate matter

Particulate matter pollution is serious health threat. PM enters the human body mainly through the respiratory system, and causing a number of harms (Baron and Willeke, 2001). Deposition of particles in different parts of the human respiratory system depends on the size, shape and density (ICPR, 1994; Löndahl et al., 2007). It has been estimated that 20-60% of the inhalable particles having sizes between 0.01

and 2.5 μm , penetrate and deposit in the lungs (Wark et al., 1997) or onto the skin surface, depending on their size and surface properties (Hoet et al., 2004). According to their health risks, inhalable particles are categorized into three groups: i) the extrathoracic fraction that does not penetrate beyond the larynx; ii) the thoracic fraction that enters the throat and is deposited beyond the larynx, within the lung's airways, and iii) the respirable fraction which is deposited in the gas exchange regions of our respiratory system, i.e., the alveoli (Fig.1.4; ISO, 1995; ACGIH, 1998).

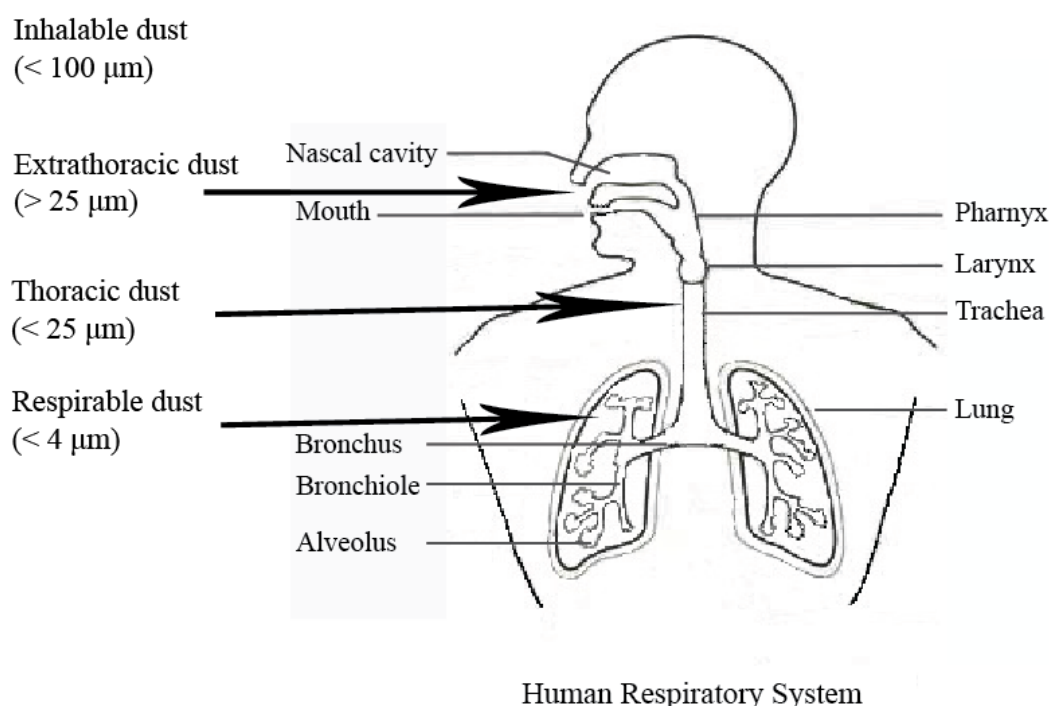


Figure 1.4: The human respiratory system and the three groups of particles according to their health risks.

The extent of the negative effect that inhaled particles have on the human body is also affected by the chemical composition of the particles, the length of exposure and individual's sensitivity (Jimoda, 2012). Epidemiological studies showed that morbidity and mortality are strongly associated with particle concentrations in the ambient air (e.g., Dockery et al., 1993; Ostro et al., 2006; Goldberg et al., 2006; Theophanides et al., 2007) and in particular the fine and ultrafine fraction (Englert, 2004; Hoek et al., 2010). According to the World Health Organization (WHO, 2013) there are several important short-term and long-term effects of exposure to particulate matter (Table.1.1).

Table 1.1: Effects of short-term and long-term exposure to particulate matter on human health.

Short-term effects	Long-term effects
Lung inflammation	Increased in lower respiratory symptoms
Respiratory problems	Reduction of lung function in children
Adverse effects on the cardiovascular system	Increased of chronic obstructive pulmonary disease
Increased use of drugs	Reduction of pulmonary function in adults
Increase in hospital admissions	Reduction in life expectancy, mainly due to cardiopulmonary mortality and probably to lung cancer
Increased mortality	

1.4 Air quality legislation and standards for particulate matter

Evidence on the health effects of air pollution from air pollutants and specifically from particulate matter and their implications has forced policy-makers to promote the development of more effective strategies to reduce air pollution. National air quality standards for particulate matter (i.e., total suspended particulate matter; TSP) were first established in 1971 in the USA by the Environmental Protection Agency (EPA). Since then, the indicators for PM have been further modified to enforce size-specific standards (PM₁₀ in 1987 and PM_{2.5} in 1997). The last revision of the air quality standards for particle pollution was in 2013 (Esworthy, 2013). The 2013 standards tighten the 24-hour fine (i.e., PM_{2.5}) particle standard from 65 to 35 $\mu\text{g m}^{-3}$, and the annual fine particle standard from 15 $\mu\text{g m}^{-3}$ to 12 $\mu\text{g m}^{-3}$. EPA decided to retain the existing 24-hour PM₁₀ standard of 150 $\mu\text{g m}^{-3}$ for no more than one exceedance per year on average over three years. Also, EPA revoked the annual PM₁₀ standard because available evidence does not suggest a link between long-term exposure to PM₁₀ and health problems (Esworthy, 2013; Kuklinska et al., 2015).

In the European Union (EU), some initial air quality directives were adopted during the Union's pollution policy developments in the first part of the 1980s. However, the significant development of EU policy in the field of air quality started at

Table 1.2: Comparison of the Unites States and European Union current air quality guidelines.

Pollutant	Unites States		European Union	
	Limit value	Margin of tolerance/ Date by which limit value is to be met	Limit value	Margin of tolerance/ Date by which limit value is to be met
PM _{2.5}	Annual limit value of 12 $\mu\text{g m}^{-3}$	The 3-year average of the weighted annual mean PM _{2.5} concentrations from single or multiple community-oriented monitors must not exceed 12 $\mu\text{g m}^{-3}$	Annual limit value of 25 $\mu\text{g m}^{-3}$	20% on 11 June 2008, reducing on 1 January 2009 and every 12 months thereafter by equal annual percentages to reach 0% by 1 January 2015
	24-hour limit value of 35 $\mu\text{g m}^{-3}$	The 3-year average of the 98th percentile of 24-hour concentrations at each population-oriented monitor within an area must not exceed 35 $\mu\text{g m}^{-3}$ (effective March 18, 2013).	-	-
PM ₁₀	Annual limit value was revoked	Due to a lack of evidence linking health problems to long-term exposure to coarse particle pollution, the agency revoked the annual PM ₁₀ standard in 2006 (effective December 17, 2006).	Annual limit value of 40 $\mu\text{g m}^{-3}$	20% on 11 June 2008, reducing on 1 January 2009 and every 12 months thereafter by equal annual percentages to reach 0% by 1 January 2015
	24-hour limit value of 150 $\mu\text{g m}^{-3}$	The 3-year average of the weighted annual mean PM ₁₀ concentrations from single or multiple community-oriented monitors must not exceed 150 $\mu\text{g m}^{-3}$	24-hour limit value of 50 $\mu\text{g m}^{-3}$	Not to be exceeded more than 35 times a calendar year. / Already in force since 1 January 2005

the beginning of the 1990s. EU then formally put forward a proposal for an air quality framework directive in the beginning of July of 1994. According to the

developing legislation, the Member States were in pressure to achieve continuous improvements in air quality and to move closer towards harmonisation of national air quality measurement programmes until today. In order to improve air quality, the European Conciliation Committee published the new air quality directive 2008/50/EC on 21 May 2008. This directive sets new strict air quality objectives for PM_{2.5} including the limit value and exposure reduction targets and merges the existing legislations in a single directive, leaving the existing objectives of air pollutants unchanged. For the case of particulate matter, the annual limit value is 25 $\mu\text{g m}^{-3}$ and 40 $\mu\text{g m}^{-3}$ for PM_{2.5} and PM₁₀, respectively, while a daily value of 50 $\mu\text{g m}^{-3}$ only exists for PM₁₀ that should not be exceeded more than 35 times per year. Stricter PM₁₀ and PM_{2.5} annual limit values proposed by WHO (i.e. limit values of 10 $\mu\text{g m}^{-3}$ and 20 $\mu\text{g m}^{-3}$; WHO, 2006) compared to those of the EC directive (2008/50/EC; EU-Commission, 2008), which WHO target values must be reached gradually in forthcoming years to prevent or reduce harmful effects on human health and the environment.

1.5 Methods of particulate matter measurements

The measuring processes of particulate matter provide important information of air quality. The most common parameters for characterizing particulate pollution are the mass and number concentration and the particle size (particle size distribution). The mechanisms for capturing particles for further analysis, including measurements of their mass may be classified in six categories as gravitational settling, centrifugal impaction, inertial impaction, direct interception, diffusion and electrical attraction (Wark et al., 1997). The capturing efficiency of these mechanisms of particle sampling depend on the flow rate, the composition and nature of the particles, particle size, and the type of filter media (Hinds, 1999). To measure the concentration and size distribution of the particles, one can probe their optical properties, the diffusion, the aerodynamic resistance, the mass and the electrical mobility (Baron and Willeke, 2001). Measurements of the particle mass (i.e., gravimetric and Beta-ray absorption) and number (i.e., electrical mobility) concentration were used in this study as discussed below.

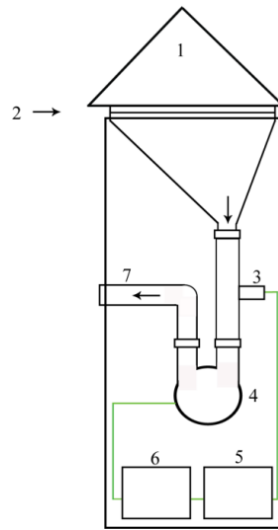


Figure 1.5: A typical arrangement of “hi-volume” sampler for the particle mass concentration measurements. (1) is the hood, (2) is the air inlet, (3) is the flow control, (4) is the fan, while (5) and (6) is electronics and the motor control. Finally, (7) is the air exhaust.

The **gravimetric method** is the most straightforward method for determining the mass concentrations of particles in the atmosphere. In this method, the sample air is pumped continuously through a specifically designed inlet for keeping particles with diameter larger than the threshold value (10, 2.5, or 1 μm) out of the flow through impaction deposition. Then the sample air is passed through a specific filter on which the total particle mass is collected. The mass of the particles is then estimated by the difference on the filter’s weight before and after the sampling. The concentration of the particle mass is then calculated as the particulate matter mass collected on the filter divided by the total volume of the air sampled through the system (Figure 1.5, showing the schematic of a high-volume sampler).

The method of Beta-ray absorption is based on the measurement of the intensity of β radiation passing through a filter on which particulate matter is being collected. The advantage of this method is that PM mass concentrations can be measured in nearly real-time. Typically, a glass fiber filter in the form of a film is moved over the radioactive source automatically in given time intervals (typically ranging from 1 to 24 h). The radioactive source (Krypton-85) is placed opposite two booths (the sample and the reference booths) of ionization where the radiation is measured as current. The absorption in the sample booth is larger because of the dust that is collected on

the filter. Differences in the current measured between the two booths is proportional to the total particle mass collected (Figure 1.6; Baron and Willeke, 2001).

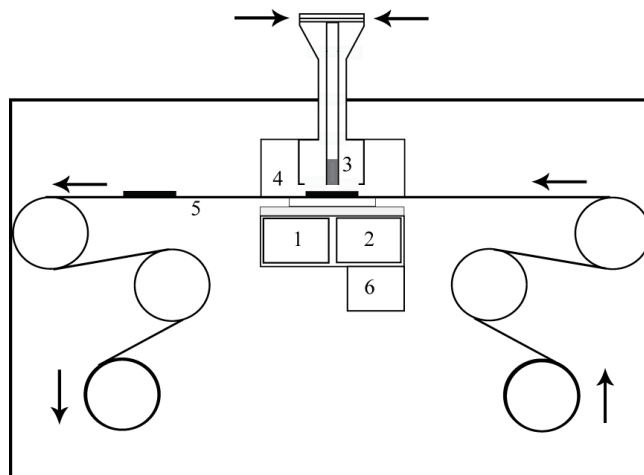


Figure 1.6: A typical arrangement of β -ray attenuation sensor for particle mass concentration measurements. (1) and (2) are the booths of ionization, (3) is the radioactive source (Krypton-85), (4) is the booth of particle matter collection, (5) is the filter tape, and (6) is the recorder.

The size distribution of atmospheric particle can be measured by **electrical mobility techniques** with optical particle detection. As shown in Figure 1.7, particles are passed through the sampling tube and neutralized (using a radioactive source) due to have a Fuchs equilibrium charge distribution to the sampled particles. Then they are classified according to their electrical mobility by a Differential Mobility Analyser (DMA). A DMA consists of a cylinder, with a charged rod at the center. Particles with a positive charge move across a sheath flow towards the central high voltage rod, at a rate determined by their electrical mobility, and only particles of a narrow selective range of mobility exit (i.e., monodisperse aerosol), while all other particles exit with the exhaust air flow. The monodisperse particles are then passed through a light scattering counter (i.e., a condensation particle counter; CPC) after their size has been increased by condensation of a known produced vapor. The magnitude of supersaturation determines the minimum detectable particle of the CPC. In the counter used in this thesis individual drops go through the focal point of a laser beam, with a flash of light and are counted. Finally, the data are stored on a PC (McMurry, 2000).

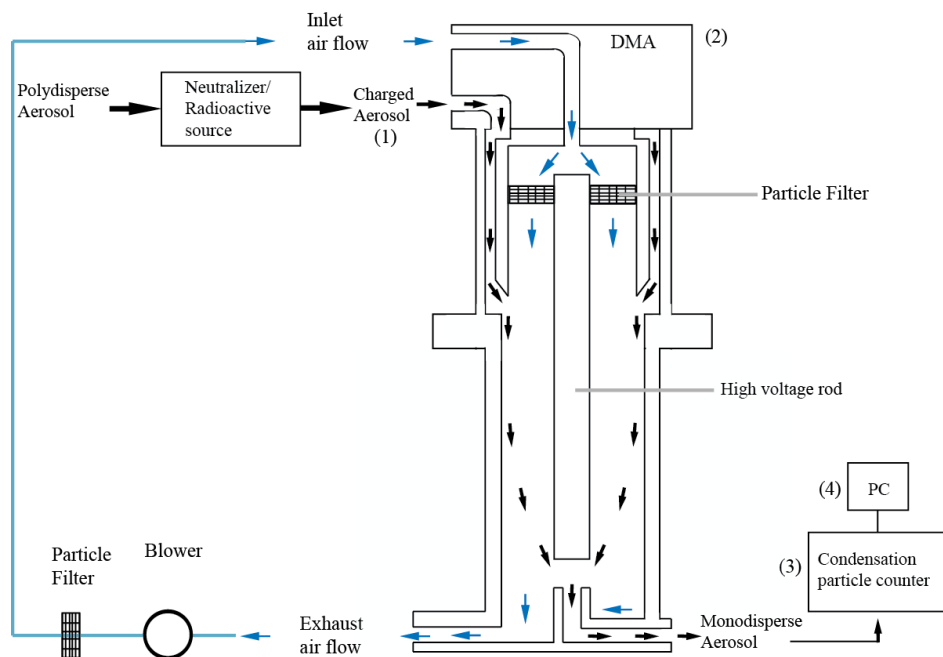


Figure 1.7: A typical arrangement of electrical mobility spectrometer for the particle number concentration and size distribution measurements. The main parts are (1) the aerosol charger, (2) a Differential Mobility Analyser (DMA), (3) a condensation particle counter (CPC), and (4) the data recorder (PC).

1.6 Chemical analysis methods for particulate matter

There are various techniques for analyzing the chemical composition of particulate matter and to identify important categories of chemical species such as heavy metals and inorganic and organic anions and cations. Numerous macroscopic methods for the chemical determination of the total particulate matter are based on X-Ray Diffraction (XRD), including: Particle Induced X-ray Emission spectroscopy (PIXE), Graphite Furnace Atomic Absorption Spectrometry (FAAS), X-Ray Fluorescence spectroscopy (XRF). The main advantage of these methods is that they do not require any pretreatment of the sample before analysis, and that they are not destructive thus preserving the samples for additional chemical analysis. Another macroscopic method is ion chromatography (IC) for the separation and simultaneous detection of anions and cations in pre-prepared liquid samples. This high sensitivity method is a powerful tool for rapid multi-element analyses and enables simultaneous detection of many elements in a solid or liquid sample.

Energy dispersive x-Ray Fluorescence spectroscopy (EDXRF) is a method for non destructive elemental analysis in different types of samples (i.e., solids, filters),

even in those cases where only small sample amounts are available. This method is applied to elements with atomic numbers ranging from 11 (Na) to 92 (U). A typical set-up of an EDXRF instrument is shown in Figure 1.8. The sample is irradiated with high-energy x-rays by a power x-ray source (i.e., x-ray tube) or a radioisotope. Then a fluorescence radiation emitted from the sample is collected by an energy dispersive detector, which determines the energy of the x-ray photons and accumulates the data in a multi-channel analyzer. The multi-channel analyzer separates the different energies of the characteristic radiation from each of the different sample elements into a complete fluorescence energy spectrum. This spectrum which is then processed for qualitative or quantitative analysis (Verma, 2007).

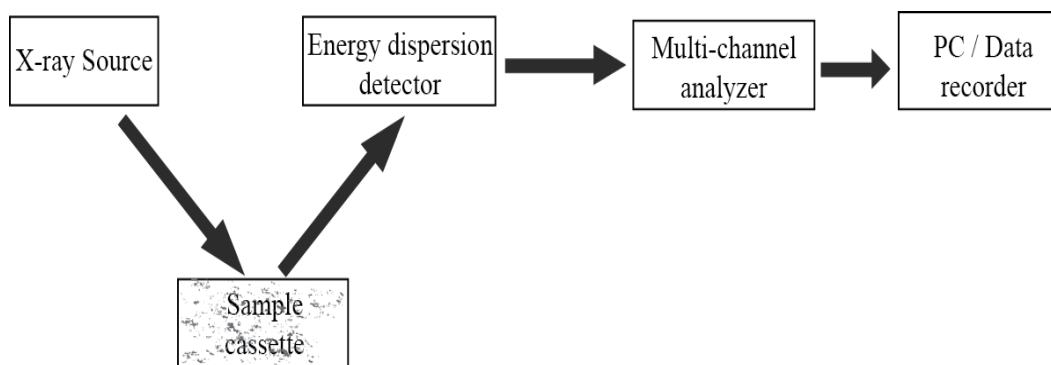


Figure 1.8: A typical arrangement of energy dispersive x-ray fluorescence spectroscopy (EDXRF) for the elemental analysis of particulate matter measurements. The main parts are a x-ray source, a sample cassette, an energy dispersion detector, a multi-channel analyzer and a data recorder (PC).

Ion chromatography (IC) is an analytical technique that separates ionic species by combining chromatographic and ion equilibrium theory into one application. This technique has the capability to analyze simultaneously a large range of anions (e.g., F^- , Cl^- , Br^- , I^- , ClO_4^- , NO_3^- and SO_4^{2-}) and cations (e.g. NH_4^+ , Na^+ , K^+ , Ca^{2+} , Sr^{2+} , Li^+). First, the PM samples are prepared as aqueous solution. For solid phase extraction of particulate matter samples, ions are extracted into the aqueous phase by sonication in water. In some cases a small amount (<1%) of wetting substance, such as propan-2-ol, is used to improve the extraction of the ions. The method starts with the introduction of this solution into a sample loop of known volume, which carries the sample (the mobile phase) from the loop onto a column filled with an appropriate material (i.e., typically a resin or gel matrix that contains charged groups – the stationary phase). Then the separation of solutions molecules occurs due to their relative interaction

(e.g., differences in the speed of motion) with the mobile and stationary phases. Ions in the sample are detected by a conductance detector after they pass through the column, and are separated according to their retention times that are known for the ions to be detected (Dodds and Whiles, 2010).

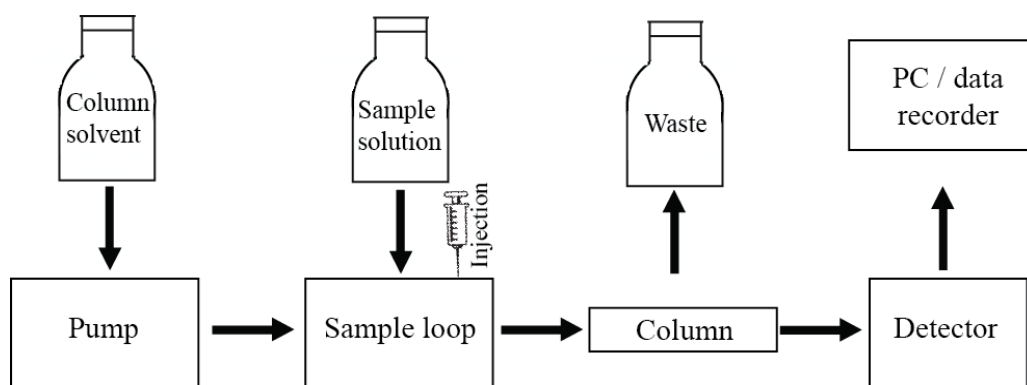


Figure 1.9: A typical arrangement of ion chromatography system for chemical analysis of anions and cations of particulate matter. The main parts are a pump, a sample loop; where is injected the sample solution, a column in which the separation of solutions molecules occurs, a detector and a data recorder (PC).

1.7 Urban particulate matter observations

Particulate matter concentration measurements in big cities of Europe and the United States are conducted since the early 1970's (Houthuijs et al., 2001; Aarnio et al., 2008; Bardouki et al., 2003; Querol et al., 2004; Ketzel et al., 2007; Calvo et al., 2008). In Greece, total suspended particles and black smoke (soot) measurements have been performed since the early 1980s, with airborne particles having diameters smaller than 10 μm (coarse particle measurements, PM_{10}) being systematically measured since 1990 (Triantafyllou, 2001; Chaloulakou et al., 2005; Samara, 2005; Vassilakos et al., 2005). Today, the average daily PM_{10} concentrations are measured by organized networks of air pollution monitoring stations in major cities of Greece, namely Athens and Thessaloniki. Smaller cities such as Volos, Kavala and Heraklion have a limited number of stations, while many cities, including Mytilene, lack of air pollution monitoring stations. In the recent past, a number of studies have been conducted to estimate the concentration and the chemical composition of particulate matter in different sites in Greece. Most of the studies have taken place in the cities of Athens (Manalis et al., 2005; Pateraki et al., 2008; Theodosi et al., 2011;

Paraskevopoulou et al., 2015; Diapouli et al., 2017b), Thessaloniki (Tsitouridou et al., 2003; Samara and Voutsas, 2005; Voutsas et al., 2014; Argyropoulos et al., 2016; Yotova et al., 2016; Sarigiannis et al., 2017), Heraklion and Akrotiri in Crete (Mihalopoulos et al., 1997; Lazaridis et al., 2008; Kopanakis et al., 2012; Bougiatioti et al., 2016), Patras in Western Greece (Koliadima et al., 1998; Pikridas et al., 2013; Kostenidou et al., 2015; Manousakas et al., 2017b), Kozani in Western Macedonia (Petaloti et al., 2006a; Terzi et al., 2008; Tolis et al., 2014; Matthaïos et al., 2017), and the city of Volos in central Greece (Papanastasiou and Melas, 2008; Proias et al., 2012; Emmanouil et al., 2017; Manoli et al., 2017).

1.8 Scope and structure of the Thesis

This thesis investigates the quantitative (concentration and size) and qualitative (chemical composition) characteristics of aerosols in urban and suburban-background sites in the North Aegean Sea region, which have been largely ignored. In addition, PM levels in the region of NAS compared to those in different sites in Greece and internationally.

Chapter 2 provides an overview of the temporal variation of PM₁₀ mass concentrations at urban and suburban areas in the two major cities in Greece, namely Athens and Thessaloniki. More specifically, the chapter presents the annual, seasonal and monthly variation of PM₁₀ concentration levels and provides a statistical analysis of the data. The purpose of chapter 3 is to assess and identify the main particulate pollution sources, based on the gravimetric method and chemical analysis of particulate matter, in a remote environment (Lemnos Island) during the summer period. In chapter 4, the characterisation of air particulate matter as well as their potential sources in the capital city of the North Aegean Sea (NAS) region in Greece, namely Mytilene, during winter and summer are investigated. Chapter 5 provides information of the differences in sampling/measurement conditions between reference gravimetric and continuous monitoring methods of particulate matter. For this purpose, systematic PM_{2.5} measurements performed at a suburban site in Athens, Greece, are presented and analysed. Finally, chapter 6 summarizes the most important conclusions of this research and recommends future work.

Chapter 2

Overview of the temporal variation of PM₁₀ mass concentrations in the two major cities in Greece: Athens and Thessaloniki

2.1 Abstract

Literature reports have indicated that Particulate Matter (PM) concentrations in the atmosphere over the major urban centres of Greece are high compared to other European cities of the same size. The great majority of these reports are based on measurements that have been conducted over a limited amount of time. This study provides an overview of the temporal variation that shows the trends of PM₁₀ concentrations in the two major urban centres of Greece (Athens and Thessaloniki) during the last decade (i.e., from 2001 to 2010). Annual average PM₁₀ concentrations at the urban monitoring stations in Athens range from 32.3 to 62.5 $\mu\text{g m}^{-3}$, and at the suburban stations from 21.5 to 62.9 $\mu\text{g m}^{-3}$. In Thessaloniki the respective values range from 41.7 to 70.8 $\mu\text{g m}^{-3}$ for the urban stations, and from 23.4 to 51.5 $\mu\text{g m}^{-3}$ for the suburban. The highest and the lowest monthly average PM₁₀ concentrations at the urban stations in Athens are observed during the autumn/winter and the summer months, respectively. For the suburban stations the highest values are observed during the spring and the lowest during the winter. In Thessaloniki, autumn exhibits the highest and summer the lowest PM₁₀ values both for the urban and the suburban stations.

2.2 Introduction

Particulate matter (PM) pollution is of great concern due to its association with adverse effects upon human health (e.g., Pope III, 2000; Dockery, 2001). These effects are more pronounced in densely populated cities where PM concentrations are high as a result of intensive human activity (e.g., Harrison et al., 2001; Querol et al.,

2008). Indeed, as health impact assessment studies show, a reduction of the ambient concentration of PM₁₀ by 5 µg m⁻³ in European cities can prevent between 3 to 8 thousand early deaths annually (Medina et al., 2004). A growing number of such studies underline the importance for systematic monitoring of PM concentration levels for facilitating control of particle-pollution sources.

Apart from local sources, PM concentrations in the atmosphere over urban and suburban areas can be affected by regional and long-range transport of natural and human-made particles. In Greece for instance, the dominance of northern winds during the summer transport polluted air masses from continental Europe to the East Mediterranean (e.g., Lelieveld et al., 2002), thereby having a significant contribution of PM concentrations in the region (Bougiatioti et al., 2009). Moreover, due to the proximity to North Africa, Saharan dust is frequently observed during spring and autumn in the region (Kaskaoutis et al., 2008). These phenomena make PM pollution in the region of particular complexity, thereby posing great challenges in the design and implementation of pollution control strategies.

Several studies have reported PM concentration measurements conducted at the two major urban centres in Greece. Kambezidis et al. (1986) were among the first ones to report PM concentration measurements at the city of Athens. Almost two decades later, Chaloulakou et al. (2003) reported a comprehensive yearlong (1999-2000) record of simultaneous PM₁₀ and PM_{2.5} measurements conducted at a single station in the centre of Athens. In an attempt to identify the spatial variation of PM pollution in the city of Athens, Mantis et al. (2005) have reported PM₁₀ concentration performed at four monitoring stations from 2001 to 2002. Most recently, Vardoulakis and Kassomenos (2008) and Grivas et al. (2008) have correlated three-year (2001-2003) and four-year-long (2001-2004) PM concentration measurements, respectively, with gaseous species concentration measurements to identify the sources and to assess the temporal variation of PM pollution in the city of Athens.

PM pollution at the city of Thessaloniki has been the subject of many studies since the early 90's (e.g., Samara et al., 1990; Tsitouridou and Samara, 1993). In a more recent study, Manoli et al. (2002) have reported a yearlong record (1994-1995) of PM

concentration and composition measurements from a single traffic-impacted urban site in an attempt to identify the main sources of particulate pollution in the city. To investigate the spatial and temporal variation of PM pollution, Voutsas et al. (2002) have reported similar measurements conducted at three urban sites in Thessaloniki for the period 1997-1998. Samara and Voutsas, (2005) and more recently Chrysikou and Samara (2009), have provided size-segregated PM concentration and composition measurements in order to identify the potential risks associated to the inhalable fractions.

The objective of this paper is to provide an overview of the temporal variation of PM₁₀ concentration levels in the two major urban centres in Greece over the period 2001 to 2010. Using daily average PM₁₀ concentration measurements provided by the standardized air pollution monitoring networks, we estimate the annual and the seasonal variation of PM concentrations for that period. Employing one-way ANOVA and Tukey's multiple comparison tests, or Welch ANOVA and Games-Howell tests depending on the homogeneity and the normality of the data, we estimate the statistically significant differences among the annual and monthly average PM₁₀ concentrations (cf. Appendix A). This analysis allows us to draw conclusions on the trends of PM pollution in the two cities and to assess the significance of human contribution.

2.3 Methods and techniques

2.3.1 Study areas and sampling stations

Athens is the largest urban centre in Greece having a population of 3.8 million inhabitants (Hellenic Statistical Authority, 2011). The city is surrounded by Parnitha mountain (1413 m asl) in the North, by Penteli mountain (1109 m asl) in the North-East, by Hymettus mountain (1026 m asl) in the East, and by open sea (the Saronic Gulf) in the South-West. Systematic PM₁₀ measurements in Athens are performed since 2001 by an authority of the Ministry of Environmental Physical Planning and Public Works. The measurements used in our study were collected from 2001 to 2010

from six stations in Athens, including the urban stations at Aristotelous (ARI), Maroussi (MAR), and Piraeus (PIR), and the suburban stations at Agia Paraskevi (AGP), Thracomacedones (THR) and Lykovrissi (LYK) (cf. Figure 2.1).

Thessaloniki is the second largest city in Greece having a population of 1.1 million inhabitants (Hellenic Statistical Authority, 2011). The city is situated in the northern part of Greece and is surrounded in the North-Northeast by Hortiatis Mountain (1200 m asl) and in the South by Thermaikos Gulf. Daily PM_{10} concentration measurements in Thessaloniki are conducted by the Department of Environment and Public Works of the District of Central Macedonia since 2001. The measurements used in our study have been collected during the period 2001–2010 from five stations in the city, including the urban stations at Kordelio (KOD) and Agia Sofia square (AGS), and the suburban stations at Kalamaria (KAL), Panorama (PAO), and Sindos (SIN), as shown in Figure 2.1. More details about the stations are available in the HMECC (2010) report for Athens and in the RCM (2007) report for Thessaloniki. The instruments used for measuring PM_{10} mass concentrations at all stations in both cities are beta radiation attenuation monitors (ESM-Andersen, Model FH 62 I-R).

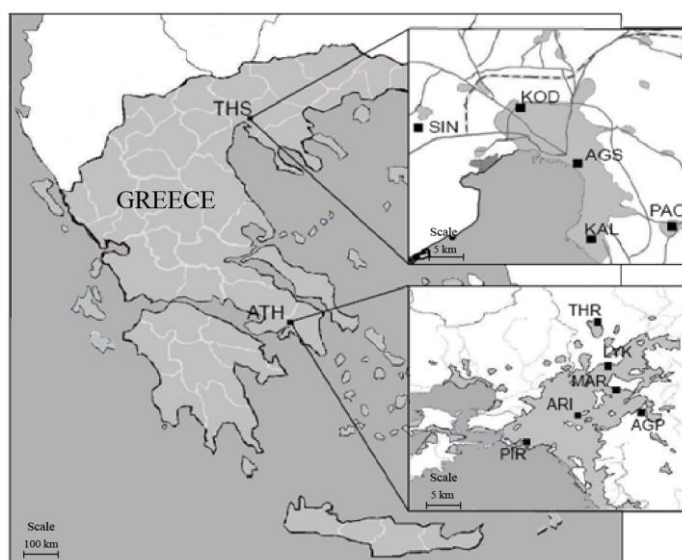


Figure 2.1: Map of Greece showing the cities of Athens (ATH) and Thessaloniki (THS) and the locations of the stations from which we obtained PM daily average PM_{10} concentrations.

2.3.2 Data Analysis

The daily average PM₁₀ concentration measurements from each monitoring station were grouped on an annual basis, and for each year the data were further separated in sub-groups on a monthly basis. To identify whether normal or log-normal probability density functions best fit the measurements for each group we used one-sample Kolmogorov-Smirnov (K-S) tests at a 0.05 significance level before continuing with the rest of the analysis. Normal probability density functions can be indicative of natural sources, whereas the lognormal of human sources (Zikovsky et al., 1987).

Analysis of the annual and seasonal variation for each station was conducted by one-way analysis of variance (ANOVA) to identify whether the average values for each group are significantly different among each other. The homogeneity of variance between the different groups was also investigated using Levene's test (p-value of 0.05). For the groups that failed the Levene tests (i.e., the grouped measurements that did not show similar variances) we performed Welch ANOVA to identify potential differences among the average values for each sub-group. In both cases, the analysis was completed with *post hoc* tests to determine similarities and differences among the various groups. Depending on whether the variances among the groups were equal or not we employed Tukey Honestly Significant Difference (HSD) or the Games-Howell tests, respectively (cf. Lomax, 2007).

2.4 Results and discussion

2.4.1 Annual variation

Figure 2.2 shows the temporal variation of the annual average PM₁₀ concentrations for all the monitoring stations in Athens. The stations that exhibit the highest and the lowest concentrations during the entire period we investigated are LYK and THR having average values 54.6 and 30.3 $\mu\text{g m}^{-3}$, respectively. Interestingly, both the highest and the lowest concentrations are observed at suburban stations. The high values at LYK can be explained by the fact that the station is located in an area that is characterized by high agricultural activity and is also close (at a distance of ca. 100 m)

to a highway. For the urban stations, the highest and the lowest values are observed at ARI and MAR with average values 54.0 and 47.2 $\mu\text{g m}^{-3}$, respectively. The EU annual PM_{10} concentration limit of 40 $\mu\text{g m}^{-3}$ (European Council Directive 1999/30/EC, 1999) was exceeded at all urban stations and at the suburban station of LYK for almost the entire period that we investigated. The EU 24-h PM_{10} limit (i.e., concentrations higher than 50 $\mu\text{g m}^{-3}$ for more than 35 days per year) was exceeded for all the urban stations in Athens during the period we investigated. For the suburban stations, LYK exceeded the EU 24-h PM_{10} for the entire period from 2001 to 2010, whereas THR only for 2010 and AGP only from 2001 to 2005.

In general, the annual average PM_{10} concentrations in Athens are higher at the urban than at the suburban stations. The average PM_{10} concentration at the urban stations (PIR, ARI and MAR) is 50.1 $\mu\text{g m}^{-3}$, while the respective value for the suburban stations (LYK, THR and AGP) is 39.8 $\mu\text{g m}^{-3}$ for the entire period that we investigated (2001 to 2010). Excluding the measurements at LYK, which are affected by high traffic and agricultural activity as mentioned above, the average PM_{10} concentrations for the suburban stations in Athens is 32.5 $\mu\text{g m}^{-3}$. An overall decrease in PM_{10} concentrations is observed at PIR (by 29.2 $\mu\text{g m}^{-3}$), in MAR (by 14.9 $\mu\text{g m}^{-3}$), in AGP (by 18.3 $\mu\text{g m}^{-3}$) and in LYK (by 21.1 $\mu\text{g m}^{-3}$) during the entire period. ARI shows fairly constant concentration levels with values ranging from 51.7 to 57.9 $\mu\text{g m}^{-3}$ throughout the period from 2001 to 2008, and a decrease (by 7.9 $\mu\text{g m}^{-3}$) from 2008 to 2010. The only station that shows an increase of the annual average concentration is THR (by 15.2 $\mu\text{g m}^{-3}$) from 2008 to 2010.

K-S tests revealed that the probability density functions of the measurements for each year and each station can be represented in almost all the cases by lognormal distributions. Investigation of the homogeneity of annual variances (Levene's test) shows that there are no significant deviations among the annual average PM_{10} concentrations in ARI, LYK and THR (p-value of 0.05). Using one-way ANOVA for those stations, the PM_{10} annual average concentrations were found to vary significantly (p-value of 0.05) from one another. Tukey HSD tests showed that four groups of PM_{10} annual average concentrations having annual average PM_{10} values of 27.9 $\mu\text{g m}^{-3}$ for the years 2001-2005 and 2009 (p-value of 0.444), 23.1 $\mu\text{g m}^{-3}$ for the

years 2006 and 2008 (p-value of 1.000), $31.1 \mu\text{g m}^{-3}$ for the years 2002 and 2010 (p-value of 0.056), and $18.8 \mu\text{g m}^{-3}$ for the year 2007 (p-value of 1.000) can be identified for THR. This grouping indicates that the variability in the annual PM_{10} concentration for this station is random. In a similar manner, three groups can be distinguished for LYK, having a PM_{10} annual average values of $55.6 \mu\text{g m}^{-3}$ for the years 2001-2004 (p-value 0.152), $50.3 \mu\text{g m}^{-3}$ for the years 2005-2008 (p-value 0.142) and $36.1 \mu\text{g m}^{-3}$ for the years 2009-2010 (p-value 0.116), showing a clear decreasing trend. Two main groups can be distinguished for ARI having mean values of $51.3 \mu\text{g m}^{-3}$ for the years 2001 to 2008 (p-value of 0.106) and $44.7 \mu\text{g m}^{-3}$ for the years 2009 and 2010 (p-value 0.142).

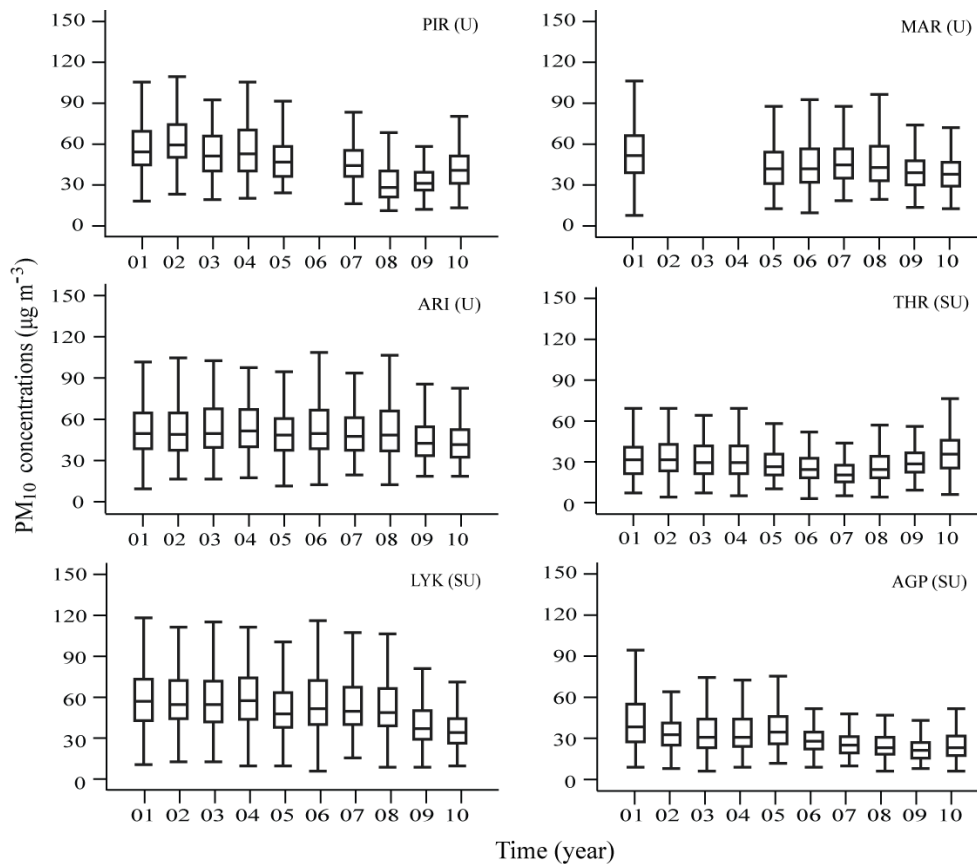


Figure 2.2: Annual average PM_{10} concentrations ($\mu\text{g m}^{-3}$) at three urban (PIR, MAR, ARI) and three suburban (LYK, THR, AGP) monitoring stations in Athens. Each box plot shows the median (middle line of the box), upper (25%) and lower (75%) quartile (top and bottom lines of the box, respectively) as well as the minimum and maximum values (upper and lower end of the whisker lines).

For the stations PIR, MAR and AGP that exhibit data in homogeneity we used the

Welch ANOVA and the Games-Howell *post hoc* test. In all these stations, the Welch ANOVA showed significant differences among the PM₁₀ annual average concentrations from one year to another (p-value of 0.05). The Games-Howell *post hoc* tests showed that three groups can be distinguished for PIR. The first includes the years 2001-2005 having an annual average PM₁₀ concentration of 53.1 µg m⁻³ (p-value of 0.599), the second includes the years 2005, 2007 and 2010 and has an average value of 44.2 µg m⁻³ (p-value 0.351), and the third the years 2008 and 2009 with an average value of 29.6 µg m⁻³ (p-value 0.357). This classification indicates that although a statistically significant decrease is observed at PIR after 2005, the variation in PM₁₀ concentrations from 2007 to 2010 is random. In a similar manner, two groups can be distinguished for MAR: one including the years 2005-2008 having an average value of 43.6 µg m⁻³ (p-value of 0.991), and one including the years 2009 and 2010 with an average value of 38.4 µg m⁻³ (p-value of 0.774), indicating that there is a systematic decreasing trend. Finally, the annual average concentrations observed in AGP can be divided in four groups that are significantly different from one another: the first group includes the years 2002-2004 and has an annual average PM₁₀ concentration of 33.7 µg m⁻³ (p-value of 0.939), the second group includes the years 2002, 2004 and 2005 and has an average value of 35.0 µg m⁻³ (p-value of 0.517), the third includes the years 2003 and 2006 and has an average value of 31.3 µg m⁻³ (p-value of 0.462), and the fourth group includes the years 2007, 2008 and 2010 of 25.4 µg m⁻³ (p-value of 0.990). This classification suggests that there is a statistically significant decreasing trend of PM₁₀ concentrations at AGP over the years that are investigated in this paper.

Figure 2.3 shows the temporal variation of the annual average PM₁₀ concentrations for all monitoring stations in Thessaloniki. The stations that exhibit the highest and the lowest values are the urban station KOD (having an average value of 59.2 µg m⁻³) and the suburban station PAO (having an average value of 30.3 µg m⁻³), respectively. The annual average PM₁₀ concentrations at the two urban stations KOD and AGS, as well as the suburban station SIN are considerably higher than the annual EU limit value. The PM₁₀ concentrations at the suburban station KAL also exceed the annual limit for the year 2008, while the measurements at PAO are below the limit for the entire ten-year period that we investigated. The 24-h limit is exceeded in both the

urban and the suburban stations in Thessaloniki during the entire period we investigated. The only exceptions are the urban station AGS in 2004 (only 28 days exhibited 24-h PM_{10} concentrations higher than $50 \mu g m^{-3}$), the suburban station of SIN in 2009 (21 days having PM_{10} concentrations higher than $50 \mu g m^{-3}$) and the suburban station PAO for the periods 2003-2004, and 2006-2009 (26 and 12 days with concentrations higher than $50 \mu g m^{-3}$, respectively). The station with the most days above the 24-h limit was AGS (with 149 days per year in average), which is located in the center of the city.

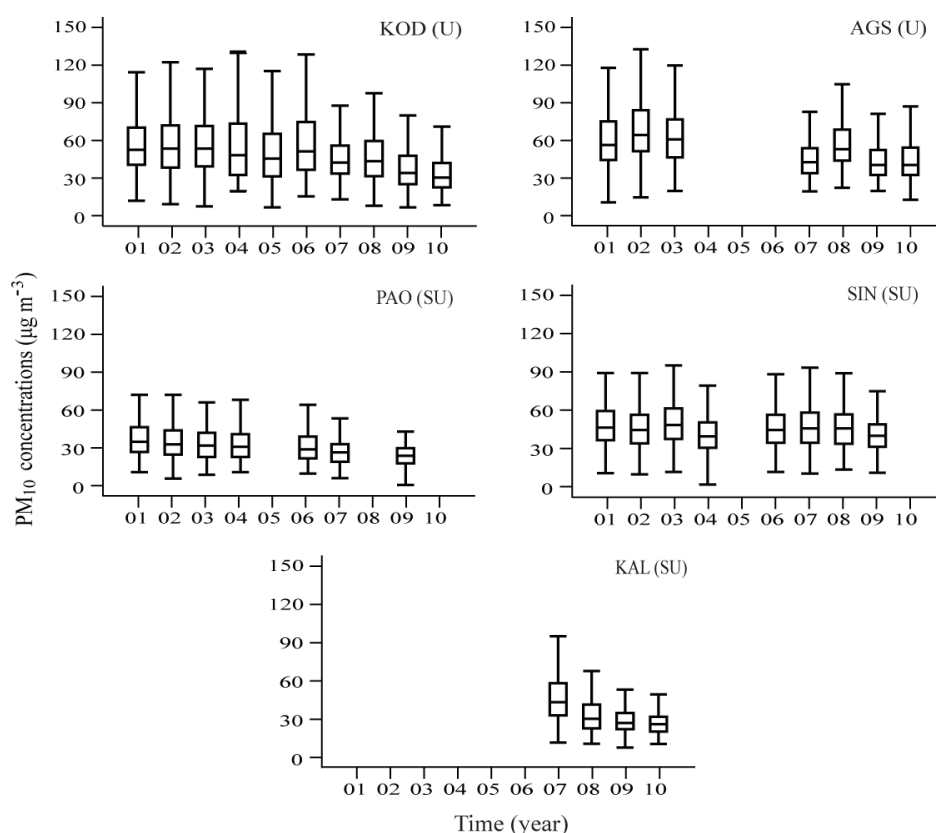


Figure 2.3: Time series of annual average PM_{10} concentrations ($\mu g m^{-3}$) at two urban (KOD, AGS) and three suburban (PAO, SIN, KAL) monitoring stations in Thessaloniki. Each box plot shows the median (middle line of the box), upper (25%) and lower (75%) quartile (top and bottom lines of the box, respectively) as well as the minimum and maximum values (upper and lower end of the whisker lines).

In general, the annual average PM_{10} concentrations in Thessaloniki are higher at the urban stations than the suburban stations. The average PM_{10} concentrations at the urban stations (KOD and AGS) are $57.7 \mu g m^{-3}$, whereas for the suburban stations

(SIN, KAL, and PAO) the respective value is $37.7 \mu\text{g m}^{-3}$ for the period 2001-2010. Interestingly, the PM_{10} concentrations at the urban stations of Thessaloniki are much higher compared to those at the urban stations in Athens. An explanation that has been offered for this observation is that apart from heavy traffic there is intensive industrial activity in the city of Thessaloniki (Samara et al., 2003; Moussiopoulos et al., 2009). It is worth noting that 20% of the industrial activity of the country is located in this area.

Despite the high values, an overall decrease of the PM_{10} annual average concentrations is observed at almost all the monitoring stations in Thessaloniki from 2001 to 2010. More specifically, a decrease is observed for the urban stations of KOD (by $27.3 \mu\text{g m}^{-3}$) and of AGS (by $17.3 \mu\text{g m}^{-3}$), as well as for the suburban stations of PAO (by $13.5 \mu\text{g m}^{-3}$) for the entire period we investigated, of SIN (by $6.3 \mu\text{g m}^{-3}$) from 2008-2009, and of KAL (by $20 \mu\text{g m}^{-3}$) from 2007 to 2010 (measurements are not available for previous years for this station). SIN is the only station that does not show any increasing or decreasing trend, having PM_{10} concentrations that vary randomly between 44.9 and $51.5 \mu\text{g m}^{-3}$ from 2001 to 2008. This observation can be explained by the fact that the station is located close to the industrial zone of the city, which is a continuous and constant source of PM pollution.

The K-S tests revealed that the measurements for each year at each station can be well represented in almost all the cases by lognormal distributions. The only exceptions are the measurements from PAO during 2007 and SIN during 2009, which follow a normal distribution. The Levene's test showed that the variances do not differ significantly among the different years in SIN and PAO (p-value of 0.05), indicating that either the sources or the conditions affecting the PM_{10} concentrations are similar for all the years. One-way ANOVA for these two stations showed that the PM_{10} annual average concentrations vary significantly from one another (p-value of 0.05). The Tukey HSD tests showed that annual average PM_{10} concentrations at SIN can be classified in three groups having significantly different values: the first having an average value of $45.5 \mu\text{g m}^{-3}$ for the years 2001-2003, and 2006-2008 (p-value of 0.443), the second of $38.7 \mu\text{g m}^{-3}$ for 2004 and 2009 (p-value of 0.726), and the third group with $42.7 \mu\text{g m}^{-3}$ for 2002, 2004 and 2008 (p-value of 0.063). The annual

average PM₁₀ values at PAO can be classified in three groups: the first one having average value of 32.4 µg m⁻³ for the years 2001 and 2002 (p-value of 0.143), the second 29.4 µg m⁻³ for the years 2002-2004 and 2006 (p-value of 0.076), and the third 22.7 µg m⁻³ for 2007 and 2009 (p-value of 0.252). Despite the lack of data for the years 2008 and 2010, an overall decreasing trend is observed at this station.

Because of the significantly different variances for the annual average PM₁₀ measurements at the stations KOD, AGS, and KAL (as indicated by the Levene's tests), we proceed with the Welch ANOVA and Games-Howell *post hoc* tests. The analysis showed that the annual average PM₁₀ concentrations vary significantly from one another (p-value of 0.05) at all these stations. The Games-Howell *post hoc* tests revealed that three groups of PM₁₀ annual average concentrations can be distinguished for KOD: the first one having mean value of 59.1 µg m⁻³ for the years 2001-2006 (p-value of 0.926), the second 51.0 µg m⁻³ for the years 2005, 2007, and 2008 (p-value 0.938), and the third 38.3 µg m⁻³ for the years 2009-2010 (p-value of 0.830). This classification indicates a clear decreasing trend over the years that were investigated. At AGS the annual average PM₁₀ concentrations can be categorized in two groups that differ significantly from one another: the first includes the years 2001, 2003 and 2008 and has a mean value of 56.4 µg m⁻³ (p-value of 0.700), whereas the second includes the years 2007, 2009 and 2010 and has a mean value of 45.7 µg m⁻³ (p-value of 0.790). Finally, at KAL the annual average concentrations are significantly different among each other for the entire period that data were available (i.e., from 2007 to 2010), showing a systematic decreasing trend over the years.

2.4.2 Seasonal and monthly variation

As shown in Figure 2.4, the highest monthly average PM₁₀ values at the urban stations in Athens are observed during the autumn/winter seasons and the lowest during the summer. For the suburban stations the respective values are observed during the spring and during the winter. This systematic difference between the urban and the suburban stations in Athens indicates that the former are influenced to a greater extent by sources that exhibit seasonality (e.g., domestic heating systems)

compared to other PM sources (e.g., traffic).

The urban stations MAR and ARI exhibit higher monthly-average concentrations in November (56.2 and 65.8 $\mu\text{g m}^{-3}$, respectively) and lower in June (39.7 $\mu\text{g m}^{-3}$) and August (47.5 $\mu\text{g m}^{-3}$), respectively. The PM₁₀ concentrations measured at the urban station PIR ranged between 40.6 and 53.7 $\mu\text{g m}^{-3}$ without showing any significant monthly variations. This can be explained by the fact that the station of PIR is located close to the main port of Athens, and as a result is influenced by its intensive activity. Monthly average PM₁₀ concentrations measured at the suburban stations of THR and AGP (cf. Figure 2.4) were found to be higher in April and in September (having average values of 41.3 and 40.0 $\mu\text{g m}^{-3}$, respectively) and lower in December (having average values of 22.5 and 24.3 $\mu\text{g m}^{-3}$, respectively). At AGP and THR, the measurements showed systematically higher concentrations during April for all the years. This observation suggests that both these stations, which are situated close to pine and conifer forests, are significantly influenced by the spring flowering period (Apostolou and Yannitsaros, 1977; Vassilakos et al., 2005). Measurements at the other suburban station (i.e., LYK) showed higher PM₁₀ concentrations in November and lower in August (60.7 and 49.5 $\mu\text{g m}^{-3}$, respectively). This observation suggests that PM₁₀ concentrations at LYK are predominantly determined by sources (e.g., the high traffic on the highway located < 100 m away) other than flowering.

The variance of the monthly average PM₁₀ measurements at all stations was found to be inhomogeneous as indicated by the Levene's tests (p-value of 0.05). With the exception of PIR, Welch ANOVA and Games-Howell *post hoc* tests showed that the seasonal average concentrations were significantly different from one another (p-value of 0.05) for all the stations in Athens. The Games-Howell test at PIR showed that although the average PM₁₀ concentrations in spring (44.6 $\mu\text{g m}^{-3}$) and winter (42.9 $\mu\text{g m}^{-3}$) are higher compared to those in autumn (42.4 $\mu\text{g m}^{-3}$) and summer (41.0 $\mu\text{g m}^{-3}$), they do not differ significantly from each other (p-value of 0.508). At MAR the respective concentrations for winter (45.3 $\mu\text{g m}^{-3}$) and autumn (43.4 $\mu\text{g m}^{-3}$) do not differ significantly from each other (p-value of 0.478), but are significantly higher compared to those in spring (43.1 $\mu\text{g m}^{-3}$) and summer (40.6 $\mu\text{g m}^{-3}$). In a similar manner, the PM₁₀ concentrations in spring (29.4 $\mu\text{g m}^{-3}$) and summer (29.1 $\mu\text{g m}^{-3}$) are

similar (p-value of 0.947) at THR, and significantly higher compared to autumn (24.9 $\mu\text{g m}^{-3}$) and winter (19.5 $\mu\text{g m}^{-3}$). At ARI the average PM_{10} values in autumn, winter and spring do not differ significantly (p-value of 0.355) from each other (having average values 52.7 $\mu\text{g m}^{-3}$, 49.9 $\mu\text{g m}^{-3}$ and 49.4 $\mu\text{g m}^{-3}$, respectively), but are significantly higher compared to those for the summer (46.7 $\mu\text{g m}^{-3}$). At LYK the PM_{10} concentrations for spring, summer and autumn, do not vary significantly (p-value of 0.543) from each other (having average values 50.9, 48.9 and 48.0 $\mu\text{g m}^{-3}$), but are significantly higher compared to the measured values in winter (46.8 $\mu\text{g m}^{-3}$). Finally, at AGP the respective PM_{10} values for summer and spring do not differ significantly (p-value of 0.059) from each other (having average values 34.9 $\mu\text{g m}^{-3}$ and 32.9 $\mu\text{g m}^{-3}$), but are much higher compared to those in autumn (30.4 $\mu\text{g m}^{-3}$) and in winter (23.2 $\mu\text{g m}^{-3}$).

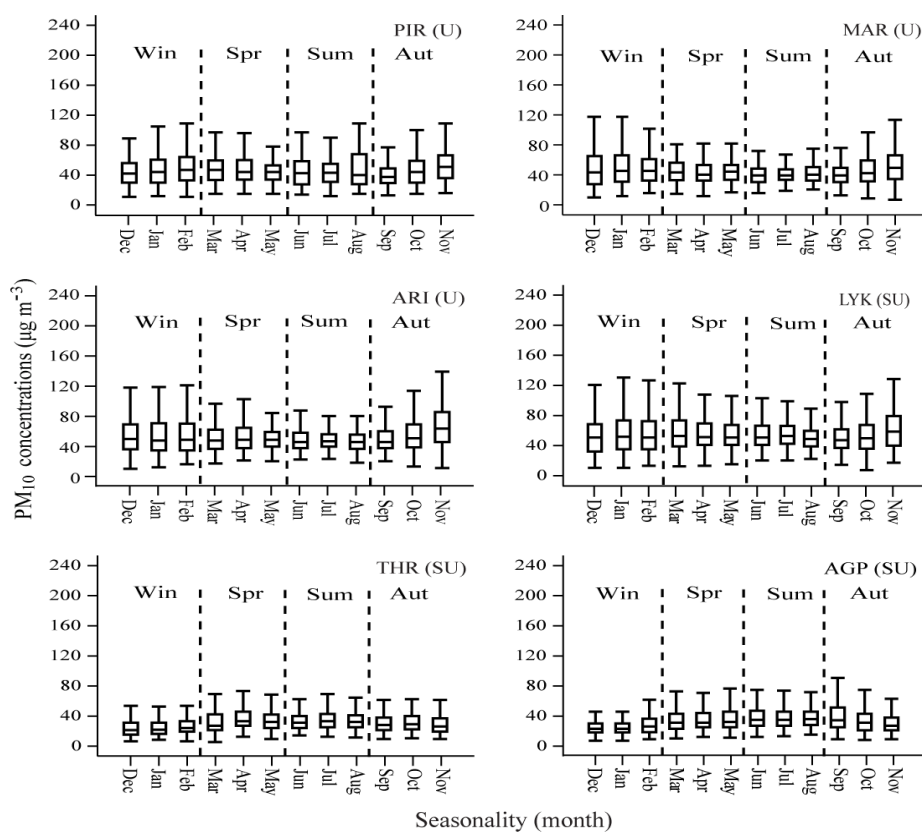


Figure 2.4: Monthly average PM_{10} concentrations ($\mu\text{g m}^{-3}$) at three urban (PIR, MAR, ARI) and three suburban (LYK, THR, AGP) monitoring stations in Athens. Each box plot shows the median (middle line of the box), upper 25% and lower 75% quartile (top and bottom lines of the box, respectively) and the minimum and maximum values (upper and lower end of the whisker lines).

Both urban and suburban stations in Thessaloniki exhibit the highest monthly average PM₁₀ values during the “cold” seasons (autumn and winter) and the lowest during the summer. The only exception is PAO station that exhibits highest seasonal average PM₁₀ values during spring and the lowest during the winter. This seasonal difference could be attributed to the fact that the station is located close to a forest, which can be an important source of airborne particles (i.e., pollen) during the flowering period (April to July). As shown in Figure 2.5, the stations KOD, AGS, and SIN exhibit the highest PM₁₀ concentrations in November (with average values 78.4 and 75.9 and 64.1 $\mu\text{g m}^{-3}$, respectively) and the lowest in July (50.1 $\mu\text{g m}^{-3}$), July (48.6 $\mu\text{g m}^{-3}$) and March (43.6 $\mu\text{g m}^{-3}$), respectively. The suburban stations KAL and PAO exhibit the highest monthly average PM₁₀ concentrations in November (48.0 $\mu\text{g m}^{-3}$) and in April (34.4 $\mu\text{g m}^{-3}$), and the lowest in September (30.6 $\mu\text{g m}^{-3}$) and in December (29.0 $\mu\text{g m}^{-3}$), respectively.

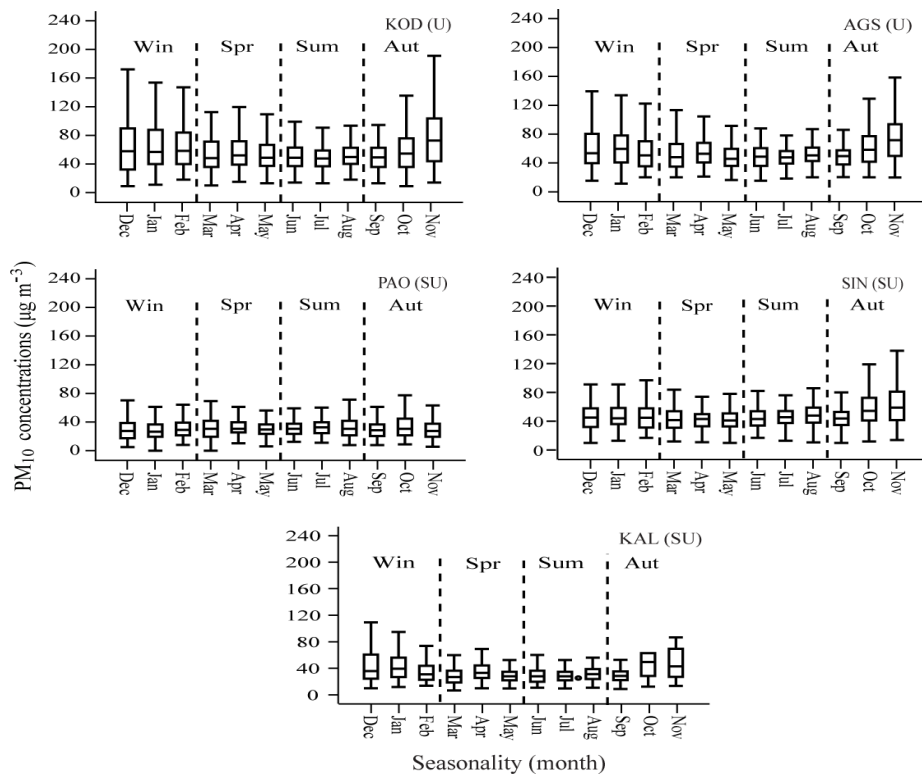


Figure 2.5: Monthly average PM₁₀ concentrations ($\mu\text{g m}^{-3}$) at two urban (KOD, AGS) and three suburban (PAO, SIN, KAL) monitoring stations in Thessaloniki. Each box plot shows the median (middle line of the box), upper 25% and lower 75% quartile (top and bottom lines of the box, respectively) and the minimum and maximum values (upper and lower end of the whisker lines).

The seasonal variations of the log-transformed PM₁₀ concentrations differ significantly among the different seasons in all the monitoring stations (Levene's test, p-value 0.05). The Welch ANOVA and the Games-Howell *post hoc* tests showed that the seasonal average PM₁₀ concentrations also vary significantly from one another for all the monitoring stations. The seasonal average PM₁₀ values at KOD for autumn and winter (average values of 55.2 and 56.5 $\mu\text{g m}^{-3}$, respectively) do not differ significantly from each other (p-value of 0.892), but are higher compared to those in spring (49.8 $\mu\text{g m}^{-3}$) and summer (47.9 $\mu\text{g m}^{-3}$). In a similar manner, the respective concentrations for autumn (55.9 $\mu\text{g m}^{-3}$) and winter (53.5 $\mu\text{g m}^{-3}$) at AGS do not differ significantly from each other (p-value of 0.429), but are higher compared to those in spring and summer (48.7 $\mu\text{g m}^{-3}$ and 47.4 $\mu\text{g m}^{-3}$, respectively). The average PM₁₀ values at PAO do not differ significantly (p-value of 0.865) between summer and spring (having average values of 29.5 $\mu\text{g m}^{-3}$ and 29.0 $\mu\text{g m}^{-3}$, respectively), but are higher compared to winter (27.0 $\mu\text{g m}^{-3}$). For SIN, the seasonal average PM₁₀ values do not differ significantly (p-value of 0.997) for winter and summer (43.7 $\mu\text{g m}^{-3}$ and 43.9 $\mu\text{g m}^{-3}$, respectively), but are significantly higher compared to spring (40.7 $\mu\text{g m}^{-3}$). Finally the concentrations at KAL do not differ significantly (p-value of 0.518) for winter and autumn (37.0 $\mu\text{g m}^{-3}$ and 34.5 $\mu\text{g m}^{-3}$, respectively), but are significantly higher compared to spring and summer (30.5 $\mu\text{g m}^{-3}$ and 30.1 $\mu\text{g m}^{-3}$, respectively).

2.5 Conclusions

The two major urban centres in Greece, Athens and Thessaloniki, exhibit high PM₁₀ concentrations compared to other European and US cities of the same size. In both cities, all urban stations exceeded the EU annual and 24-h limits during the entire period that we investigated. With the exception of LYK and AGP in Athens, and of SIN and KAL in Thessaloniki, all suburban stations showed lower than the EU limit PM₁₀ concentration levels. The urban stations in Thessaloniki exhibited higher PM₁₀ concentrations, compared to those in Athens, which can be attributed to the more intensive industrial activity in the city.

The annual average PM₁₀ concentrations exhibited an overall decreasing trend in

both cities during the entire period we investigated. Exception to this observation was observed for the suburban station of THR in Athens, that showed an increasing trend from 2007 to 2010, as well as for the stations PIR in Athens and SIN in Thessaloniki that did not exhibit any trend, most likely due to their proximity to constant PM sources (the station at PIR is close to the main port of the country, whereas the station at SIN is close to an industrial zone). The seasonal variation was shown to be different between urban and suburban station in Athens and Thessaloniki. The highest PM₁₀ concentrations at the urban stations in Athens were higher during the autumn and winter and lower during the summer, while the highest values at the suburban stations were observed during the spring and the lowest during the winter. A possible explanation for this difference is that the former are influenced to a greater extent by domestic heating systems compared to other sources of PM₁₀. In Thessaloniki, with the exception of one station (SIN) that does not exhibit any seasonality; seasonal variations were found to be similar both at the urban and the suburban stations, exhibiting highest and lowest concentrations during autumn and summer, respectively.

Chapter 3

Particulate pollution transport episodes from Eurasia to a remote region of northeast Mediterranean

3.1 Abstract

Long-range transportation of air pollutants from industrial and urban environments can significantly affect the quality of the air in remote regions. In this study, we investigate episodes of particulate transport (PT) from Eurasia to the remote environment of Northeastern Mediterranean, i.e., the region of the North Aegean Sea (NAS), during the summer when the synoptic Etesian wind conditions prevail. A temporary monitoring station was set up at a remote region on the island of Lemnos, which is located at the center of the NAS at a distance of ca. 250 km from the continent. Measurements of the aerosol particle size distributions, the total number and mass concentrations, as well as the chemical composition of the particles were conducted from 27 August to 10 September 2011. During this period, the wind speeds were high (typically higher than 5.5 m s^{-1}) with a direction that mostly ranged from north to northeast (68% frequency). Winds having direction ranging from northwest to south were less frequent (7% frequency), while the rest of the cases were characterized as calm (i.e., wind speeds less than 1 m s^{-1} ; 25% frequency). Seven PT episodes were observed during the sampling period. When the wind direction was northeastern we observed up to a six-fold increase in particle number concentration of nucleation mode, while the peak size of the particles decreased from 100 to 20 nm. Interestingly, the nucleation-mode particles grew from ca. 15 to 25 nm with rates of ca. 9.0 nm h^{-1} , which are representative of polluted areas. Analysis of the chemical composition of particle samples collected on filters during the PT episodes shows that the concentration of sulfates and nitrates increased by ca. 60%, while the OC/EC ratio increased by ca. 22% compared to the rest of the sampling period. Back-trajectory analysis for the period during the episodes shows that the air masses arriving at the station passed over the greater Istanbul area and the Black Sea 9 to 12 hours before

reaching our station. These observations provide strong evidence that the air quality in the remote region of the NAS can be significantly affected by the transportation of particulate pollution during the summer period, having potentially important effects upon human health and climate in the region.

3.2 Introduction

Long range air pollution transport can significantly affect air quality and therefore human health and climate in both urban (Kubilay et al., 2000; Karaca et al., 2009) and remote (Masplet et al., 1988; Kato et al., 2001) regions. For instance, the region of the Eastern Mediterranean, which is considered a climate hotspot, is strongly affected by transportation of air pollutants originating from Europe, Africa and Asia. While, numerous studies have focused on the southern part of the Eastern Mediterranean (Kouvarakis et al., 2002; Smolík et al., 2003), its northern part, i.e., the Northern Aegean Sea (NAS), has largely been ignored.

The NAS is an important part of the Mediterranean region, located very close to big cities of Greece (Athens and Thessaloniki), Turkey (Istanbul, Izmir, and Bursa) and Bulgaria (Burgas and Plovdiv) that have organized industrial zones, including large factories, power plants, and mines (Thöni et al., 2011; Civan et al., 2011). The area is of particular interest since on the one hand the economic crisis in Greece has affected everyday human practices, which in turn have led to an increase in anthropogenic emissions of particles (Saffari et al., 2013; Paraskevopoulou et al., 2014) and a decrease of gaseous pollutants such as NO₂ and SO₂ (Vrekoussis et al., 2013), while on the other the expanding economy of Turkey has strongly affected regional air quality (Alyuz and Alp, 2014).

The seasonal pattern of air pollution transport is strongly affected by the annual variability of the wind patterns in NAS (Kallos et al., 2007). During summer and early autumn, the prevailing winds (i.e., the Etesians) have a northeasterly direction. (Kallos et al., 1998; Poupkou et al., 2011). The Etesian winds are associated with horizontal and vertical transport of air masses to the region of the Aegean Sea and the Eastern Mediterranean (Tyrlis et al., 2013; Anagnostopoulou et al., 2014). This in turn

perplexes the air pollution pathways between southern Balkans, Turkey and the NAS (Kotroni et al., 2001) and influences the quality of the air and the climate of the entire region (Bezantakos et al., 2013; Tombrou et al., 2013, 2015).

In this study, we investigate the properties of atmospheric particles observed in the remote environment of the NAS during the summer period when Etesian winds prevail, in order to understand how cross-border air pollution transport affects local air quality. Measurements of the size distributions, the number and mass concentrations, as well as the chemical composition of the atmospheric particles were conducted on Lemnos, a remote island located at the center of the NAS.

3.3 Experimental

Measurements were conducted from 27 August to 10 September 2011 (239 –253 Day of Year; DOY) at a temporary monitoring station at Vigla; a remote region on the island of Lemnos (39° 58' N, 25° 04' E; 420 m a.s.l.), which is located at a distance of ca. 250 km from mainland Greece and Turkey at the center of the NAS (cf. Fig. 3.1). A Scanning Mobility Particle Sizer (SMPS; TSI Model 3034) was used to measure the size distribution of aerosol particles having diameters in the range from ca. 10 to 500 nm with a 3-min time resolution. In addition, a micro-orifice uniform deposit cascade impactor (MOUDI; MSP Model 110) was used to collect PM₁ samples on Teflon filters (Pall Life Sciences Zefluor Supported PTFE filter, 47mm in diameter; Part No. P5PL047) at a flow rate of 30 lpm. A separate sampler operated at 20 lpm was used to collect samples on pre-treated quartz filters (Pall Life Sciences Pall flex Tissuquartz, 47mm in diameter; Part No.7202) for determining the mass of the total suspended particles (TSP). After gravitational analysis, the filter samples were analyzed for inorganic ions (i.e., NH₄⁺, Na⁺, K⁺, Ca²⁺, Cl⁻, NO₃⁻ and SO₄²⁻) using an ion chromatograph (Dionex Model DX-500) equipped with a conductivity detector (Dionex Model CD20) and a gradient pump (Dionex Model GP50). Organic and elemental carbon (OC and EC) were analyzed with the Thermal Optical Transmission (TOT) technique (Birch and Cary, 1996), using a Sunset Laboratory OC/EC Analyzer (Sunset Laboratory Inc. Model 4L ECOC Lab Instrument). In particular, a punch of

1.5 cm² from each sample was analyzed using the EUSAAR-2 protocol (cf. Paraskevopoulou et al., 2014).

Meteorological data including wind speed, wind direction, mean hourly temperature and relative humidity were provided by the meteorological station located at the airport of the island. Ultraviolet radiation (UV) radiation data were obtained by the Greek UV monitoring network operated by the Laboratory of Atmospheric Physics of the Aristotle University of Thessaloniki. Back-trajectories (5-days long) of the air masses arriving at Vigla station were determined by the NOAA HYSPLIT model (Draxler and Hess, 1998; Draxler and Rolph, 2003). The trajectories were calculated at 12:00 UTC, which is around the starting time of the episodes. In addition, we investigated the vertical wind velocity motion (omega fields) using the NCEP/NCAR Reanalysis 1 by NOAA (Kalnay et al., 1996) on a daily basis during the entire campaign.



Figure 3.1: Map showing the island of Lemnos (39° 58' N, 25° 04' E) and the location of the station at Vigla (420 m a.s.l.). The most important industrial sites and the largest cities close to the monitoring station are also shown.

3.4 Results and discussion

The prevailing winds had north to northeast direction (68% frequency) with wind speeds ranging up to 11.3 m s⁻¹ (cf. Fig. 3.2). Calm conditions (i.e., average wind speed < 1 m s⁻¹) were observed ca. 25% of the entire sampling period with the majority (73%) being observed during nighttime (from 8:00 in the morning to 18:00 in the evening). In eight out of the fifteen days of the campaign (i.e., 239, 240, 241, 246, 247, 248, 249 and 250 DOY), the meteorological conditions were representative of the Etesian conditions as identified by Tyrllis and Lelieveld (2013).

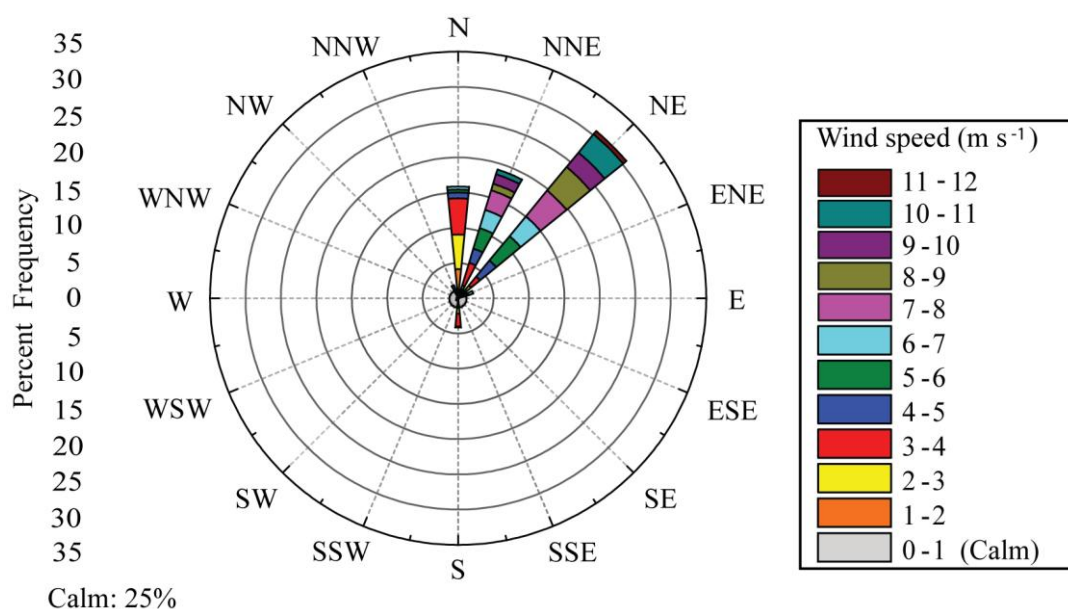


Figure 3.2: Wind rose for Lemnos during the sampling period. Calm conditions are identified when the wind speeds are < 1 m s⁻¹.

Figure 3.3a shows the evolution of the normalized particle number size distributions throughout the campaign. The mean particle size during the entire period was ca. 100 nm, with 47% of the size distributions exhibiting a single mode, 40% two modes and 13% more than two modes. The total particle number concentration ranged from 1×10^3 to 7×10^3 particles cm⁻³, having a mean value of 2×10^3 particles cm⁻³, which is in agreement with measurements conducted in the Eastern Mediterranean (Kalivitis et al., 2008; Pikridas et al., 2010) and other coastal areas in Europe (Weijers et al., 2004). As shown in Fig. 3.3b, the mean number concentration of nucleation-mode particles (i.e., particles having diameters smaller than 25 nm; $N_{d < 25 \text{ nm}}$) was ca.

20 particles cm^{-3} (average value for most of the sampling period), but increased to values higher than 1×10^2 particles cm^{-3} during almost all the Etesian days (referred as particle transportation PT episode days hereinafter): i.e., on 27 (239 DOY), 28 (240 DOY), and 29 (241 DOY) August as well as on 5 (248 DOY), 6 (249 DOY), and 7 (250 DOY) September. The same pattern was observed for 10 September (253 DOY), which is not identified as an Etesian day.

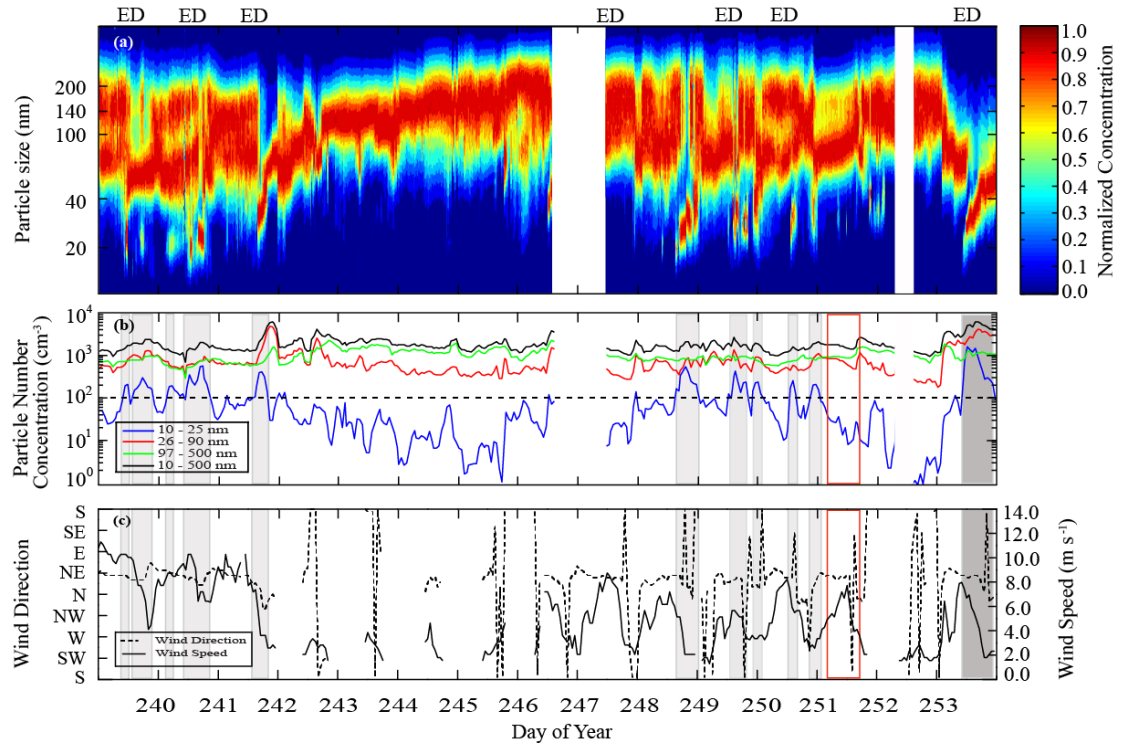


Figure 3.3: Particle size distributions measured from 27 August to 10 September 2011 at the Vigla station. Normalized particle number size distributions (a), time series of particle number concentrations having sizes in the range 10-500 nm (black line), 10-25 nm (blue line), 26-90 nm (red line), 91-500 nm (green line) (b), and of the wind speed (solid black line) and direction (dashed black line) during the entire sampling period (c). The days of Etesians (ED) are indicated at the top of the figure. The black dashed line shown in 3b indicates the $N_{d<25\text{nm}}$ above which we have PT episodes. Light shaded areas in 3b and 3c indicate the periods with PT episodes that are characterized as moderate (i.e., on 27 (239 DOY), 28 (240 DOY), and 29 (241 DOY) August, as well as on 5 (248 DOY), 6 (249 DOY), 7 (250 DOY)), while the dark shaded area indicates the period with the strong PT episode (on 10 (253 DOY) September). The red rectangle in 3.3b and 3.3c corresponds to the period when the prevailing wind conditions were similar to those during the PT episodes but $N_{d<25\text{nm}}$ was below the threshold value.

All the PT episodes started around midday and lasted for ca. six hours, coinciding with the period of the day that the lower troposphere influences most the boundary layer. During this period, the vertical distributions and the transport of air masses is

enhanced (Tyrlis and Lelieveld, 2013). Almost all the episodes exhibited $N_{d<25\text{nm}}$ values that reached up to ca. 5×10^2 particles cm^{-3} and can therefore be characterized as moderate events (light shaded areas in Fig. 3.3b). The PT episode on 253 DOY was characterized as strong (dark shaded area in Fig. 3.3b) with $N_{d<25\text{nm}}$ reaching values of ca. 1.2×10^3 particles cm^{-3} . The particle number concentration of the Aitken mode during all the PT episodes exhibited a 100% increase (i.e., from 0.7×10^3 to 1.4×10^3 particles cm^{-3}), while that of the accumulation mode ca. 30% decrease (i.e., from 1.2×10^3 to 0.8×10^3 particles cm^{-3}) compared to the rest of the sampling period.

Generally, $N_{d<25\text{nm}}$ increased up to 1.2×10^3 particles cm^{-3} (strong episodes) when strong north-northeastern winds (average speed 7.5 ± 1.9 m s^{-1}) prevailed during the PT episode days, while $N_{d<25\text{nm}}$ increased up to 5×10^2 particles cm^{-3} (weak episodes) under weaker north-northeastern winds (average speed 4 m s^{-1}). Some episodes (e.g., on 249 and 250 DOY) were interrupted for several hours as indicated by the decreases of $N_{d<25\text{nm}}$ below 100 particles cm^{-3} (Fig. 3.3b), coinciding with short and sudden changes in wind speed and direction, as well as with the presence of clouds. It should be noted here that although the prevailing wind conditions on 251 DOY (indicated by the red rectangle in Fig. 3.3b and 3.3c) were similar to those during the PT episodes, the observed $N_{d<25\text{nm}}$ was less than 100 particles cm^{-3} . This can be attributed to the different paths of the air masses (cf. dark green back-trajectory that does not pass over Istanbul in Fig. 3.6), and/or the moderate or weak nucleation events occurring upwind.

Characteristic particle size distributions before the beginning and until the end of a PT episode on 241 DOY are shown in Fig. 3.4. Size distributions before the episode (i.e., at 8:00; Fig. 3.4a) showed a single peak at ca. 100 nm. Immediately after the episode started (i.e., at 12:00; Fig. 3.4b), the measured particle size distributions were best fitted by a trimodal distribution, indicating that polluted air masses from different sources are transported to the region and blend with local emissions. Three hours later (i.e., at 15:00; Fig. 3.4c), the size distribution showed a sharp peak at ca. 30 nm having a maximum concentration of 4.5×10^3 particles cm^{-3} . Four hours after the end of the episode (i.e., at 21:00; Fig. 3.4d) the particle number concentration (for particles having diameters from ca. 10 to 500 nm) increased almost by a factor of five,

while the size distribution also exhibited a peak shift towards larger diameters (ca. 60 nm). After 3 h (i.e., at 24:00) the size distributions returned to the normal mode, showing a peak at 70 nm (maximum value of 2.5×10^3 particles cm^{-3}).

Interestingly, during all the episodes, the nucleation mode particles appear at relatively large sizes (ca. 15-17 nm) and grow to ca. 25 nm over a period of an hour (i.e., having a growth rate of ca. 9.0 nm h^{-1}). The fact that they are relatively large when they first appear in our measurements indicates that they are formed in a region further upwind and that they grow during their transportation to our site. Typical particle growth rate values in clean coastal areas are $< 4 \text{ nm h}^{-1}$ (Ehn et al., 2010; Peng et al., 2014), while higher values are observed at highly polluted urban and industrial areas (Birmili et al., 2003; Kulmala et al., 2005; Hamed et al., 2007). This provides an additional indication that the nucleation-mode particles observed in our station during the PT events have been formed at the urban and/or the industrial region of Istanbul further upwind.

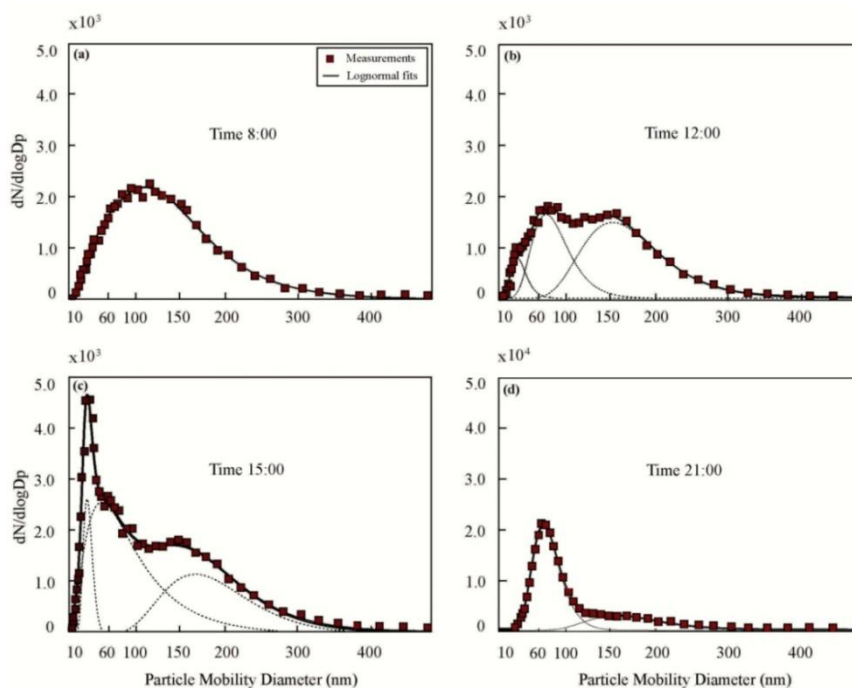


Figure 3.4: Particle number size distribution measurements before (a), during (b and c) and after (d) the PT episode on 241 DOY. The square symbols represent the measurements, whereas the solid and the dashed lines are the overall and the individual-mode lognormal fits, respectively.

To further investigate the assumption that these particles are produced by nucleation events that take place upwind, we correlate their concentration with that of sulfuric acid (H_2SO_4) determined by the empirical model described by Mikkonen et al. (2011a) (cf. Appendix B-Part A and B). In brief, the concentration of H_2SO_4 was estimated using measurements of the UV, relative humidity, as well as predictions of the concentration of SO_2 by the WRF-Chem model (sulfur WRF-chemsimulation; Grell et al., 2005), whereas the condensation sink (CS) was determined using the size distribution measurements (cf. Appendix B-Part B). The estimated $[\text{H}_2\text{SO}_4]$ had an average value of 1.6×10^5 molecules cm^{-3} during the PT episodes, with maximum values reaching up to 5.7×10^5 molecules cm^{-3} . Considering that H_2SO_4 is believed to induce new particle formation at concentrations higher than 10^5 molecules cm^{-3} (Curtius, 2006), our estimations indicate that it plays an important role in the formation (upwind of the station) and growth of the nucleation-mode particles observed over Lemnos. The correlation between the estimated gaseous $[\text{H}_2\text{SO}_4]$ and $N_{d<25\text{nm}}$ was moderate ($R^2 = 0.50$), but increased ($R^2 = 0.71$) when a time lag of ca. 7 h was used between the data sets (i.e., the concentrations of $N_{d<25\text{nm}}$ were time shifted from 6 to 8 h backwards to achieve the highest correlation with $[\text{H}_2\text{SO}_4]$). This increase in correlation provides additional evidence that the nucleation-mode particles did not form in the region of NAS, but further upwind.

3.4.1 Chemical composition of aerosols

Figure 3.5 shows the composition of the inorganic fraction of $\text{PM}_{1.0}$ filter samples (38 in total) collected during the entire sampling period. These samples were further classified to those corresponding to the period during the PT episodes (8 samples), before (6 samples) or after (6 samples) the PT episodes (referred as transition periods; TP), and to the periods when the atmosphere over Lemnos was not affected by PT (referred as ordinary days; OD).

Figure 3.5 a indicates that sodium and chloride were the dominant ionic constituents of the $\text{PM}_{1.0}$ mass concentration (51% of the total $\text{PM}_{1.0}$ mass) during the OD, which is expected for a coastal site. During those days, sulfates nitrates and ammonium accounted for 17% of the total $\text{PM}_{1.0}$ mass. In contrast, during the PT

episodes or the TP, the $PM_{1.0}$ mass fraction in sulfates, nitrates and ammonium increased respectively to 70% and 83% (cf. Fig. 3.5b and 3.5c). Given that these ions are associated with secondary inorganic aerosols (e.g., Deshmukh et al., 2011; Talwar and Bharati, 2012), the measurements shown in Fig. 3.5 provide an additional indication that the particles observed on Lemnos during the PT episodes have an urban and/or industrial origin.

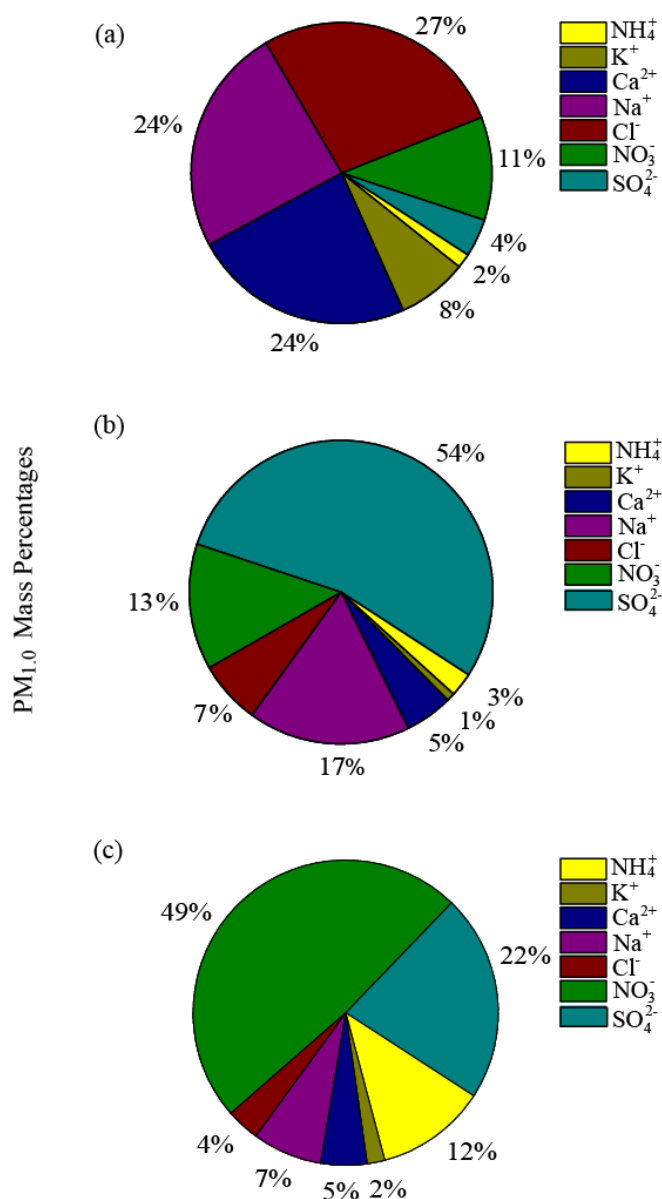


Figure 3.5: Ion mass fractions of $PM_{1.0}$ samples collected on filters during ordinary days (a), PT episodes (b), and transition periods (c).

Organic carbon (OC) was the most abundant component and accounted for 91% of the total carbon during the entire sampling period, which is indicative of urban/industrial emissions. Mean concentrations of organic and elemental carbon (OC and EC) in TSP were 2.2 ± 1.1 and $0.2 \pm 0.2 \mu\text{g m}^{-3}$, respectively. Similar levels of carbonaceous particles have been reported in the Eastern Mediterranean region (Sciare et al., 2003; Koulouri et al., 2008). The relationship between OC and EC levels was significantly high ($R^2 = 0.67$), which suggests common dominant combustion sources (Sillanpää et al., 2005; Cao et al., 2007; Xu et al., 2012). With the exception of 28 August (240 DOY) during which the aerosol was affected by a fire event in Northern Greece, the OC/EC ratio ranged from 4 to 46 (median = 10), with those observed during the PT episodes or the TP being higher compared to those measured during the OD (10.0 and 9.0, respectively).

3.4.2 Transportation pathways of the sampled air masses

Figure 3.6a shows five-day back-trajectories of air masses reaching the measuring site during the PT episodes. With the exception of 10 September (253 DOY), all the transported air masses originated from northeastern regions, when strong winds prevailed (mean wind speed of $6.3 \pm 2.7 \text{ m s}^{-1}$). More precisely air masses passed over Black Sea (12h before reaching the monitoring station), the Greater Istanbul Area (9h) and the Northern Greece (6h). Until the end of the transportation episode, the winds had a northwestern direction with local wind speeds of 1.9 m s^{-1} . Of particular interest is the back-trajectory on 8 September (251 DOY), which has a northeastern origin but by –passes the wider Istanbul region. It should be noted that this is the day that no PT was observed although the favoring prevailing winds. On 10 September (253 DOY), the air masses passed over the industrial areas of Bulgaria (18h before reaching the station) and the regions of Evros in Northern Greece (7h).

Overall, these observations show air masses coming from industrial areas that travel and transport pollutants to the remote region. For the rest of the sampling days, the back-trajectory calculations show that the air passed over Northern Greece and the Balkan under weak northern and southern winds before reaching the monitoring

station. The vertical component of the 5-day back trajectories is shown in Fig. 3.6b. During the PT episodes, all the trajectories were below ca. 2000 m for at least 24 hours before reaching the station, but approached the ground level halfway when reaching the Greater Istanbul Area. For the rest of the days, the trajectories indicate vertical mixing and influences of the air masses received at our station from different sources (data not shown).

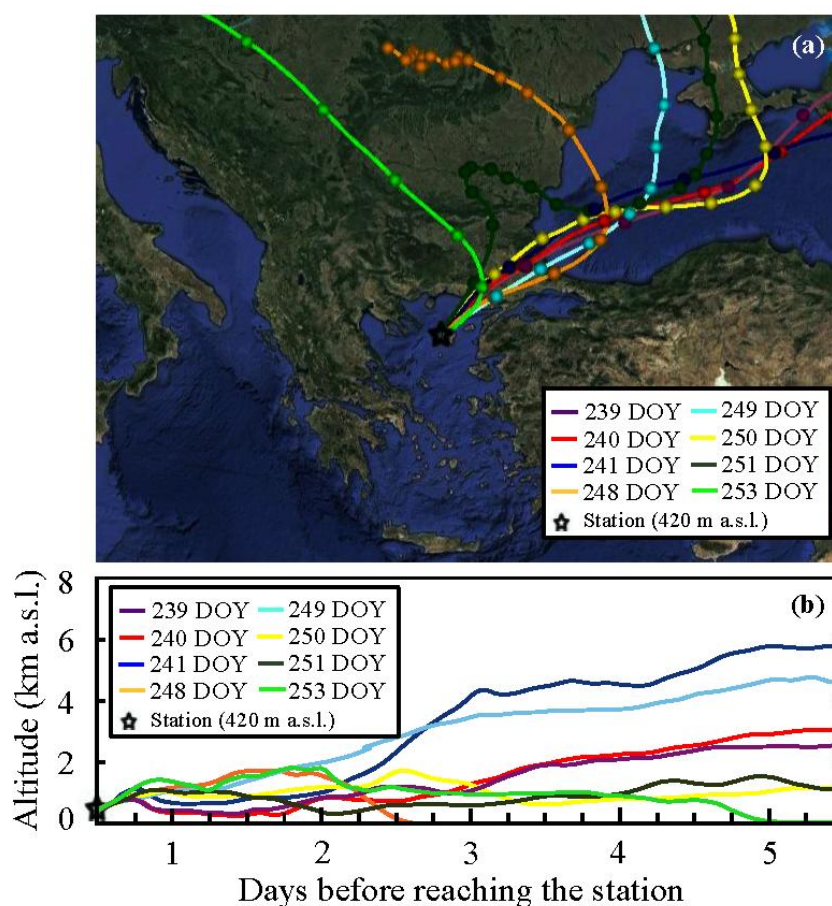


Figure 3.6: Horizontal (a) and vertical (b) paths of 5-day back-trajectory calculations during the PT episodes and on 8 (251 DOY) September. All the trajectories on 27 (239 DOY), 28 (240 DOY), and 29 (241 DOY) August as well as on 5 (248 DOY), 6 (249 DOY), 7 (250 DOY), 8 (251 DOY) and 10 (253 DOY) September (magenta, red, blue, orange, cyan, yellow, dark green and green lines, respectively) start at 12:00 UTC. The dots on each trajectory indicate the position of the air parcels at the end of each 6-h interval before reaching the monitoring station.

In addition, the vertical component of the wind from the analysis of the omega fields (at a pressure level of 500 hPa) during the PT episodes shows downward movement of air masses (up to 7.5 Pa min^{-1}) over the NAS. For example, the vertical

omega profile on 239 DOY shows subsidence conditions over the region of north and central Aegean Sea and strong wind fields (up to 15 Pa min^{-1}) over the Black Sea and the Greater Istanbul Areas (cf. Fig. 3.7a). Considering also that the height of the back trajectories does not fluctuate substantially once they reach the lower levels over the Black Sea and the Greater Istanbul Areas (cf. Fig. 3.6b), this analysis supports the hypothesis that the increased particle number concentrations in the remote region of the NAS are due to transportation of polluted air masses from anthropogenic sources.

For the rest of the sampling days (e.g., 242 DOY; cf. Fig. 3.7b showing the associated omega field), the profiles show a high-pressure over the NAS, which prevents any air mass transport to the region.

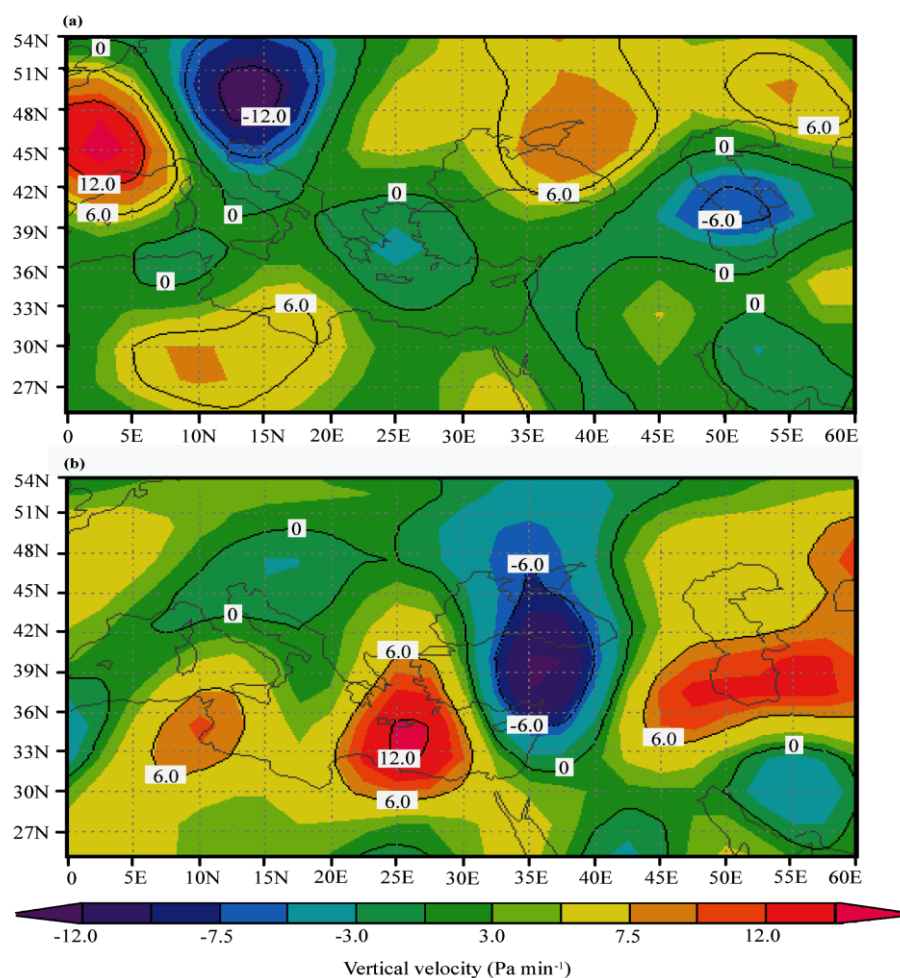


Figure 3.7: Vertical wind motion (omega fields) at 500 hPa during the PT episode on 27 (239 DOY) August (a) and during the non episode day on 30 (242 DOY) August (b) based on daily reanalysis data from the National Centers for Environmental Prediction (NCEP). The color bar shows the changes of the vertical velocity (Pa min^{-1}).

3.5 Conclusions

Elevated aerosol number concentrations (with a mean value of 2.2×10^3 particles cm^{-3}) were observed during particle transportation (PT) episodes in the NAS when the meteorological conditions were representative of the Etesian conditions. During these episodes, the particle size distributions exhibited a peak shift towards lower diameters (i.e., from 100 to ca. 20 nm), while the number concentration increased substantially. The nucleation-mode particles observed during all the PT episodes had sizes from ca. 15 to 17 nm and grew with a rate of ca. 9.0 nm h^{-1} , providing a first indication that they have been formed in highly polluted areas and their size was increased during transportation to the NAS. The estimated concentrations of sulfuric acid during the episodes were in the order of 10^5 molecules cm^{-3} , suggesting that it plays an important role in the formation and growth of the observed nanoparticles. The correlation between $N_{d < 25 \text{ nm}}$ and $[\text{H}_2\text{SO}_4]$ was moderate but became strong ($R^2 = 0.71$) when a time lag of 7 ± 1 h was used between the two data sets. The fraction of sulfates, nitrates, and ammonium on $\text{PM}_{1.0}$ samples exhibited an increase of ca. 60%, whereas the OC/EC ratio was systematically higher during the PT days compared to the rest of the days. In addition, a strong correlation ($R^2 = 0.67$) was observed between OC and EC, suggesting that they have common combustion sources. These observations provide an additional indication that the particles observed in the region of NAS have an urban and/or industrial origin, as also confirmed by the analysis of back-trajectories and the omega fields. Considering that the aerosol is not influenced by many other sources during their transport over the sea, air quality measurements at this site provide a great opportunity to study the ageing of anthropogenic particles.

Chapter 4

Characterisation of the atmospheric urban aerosol in a background marine region

4.1 Abstract

The concentrations, size distributions, and elemental compositions of the atmospheric aerosol over a small but representative insular coastal city in the North Aegean Sea were measured during the warm and cold periods. Mean $PM_{2.0}$ and $PM_{1.0}$ concentrations at the city centre were respectively 26 and 21 $\mu\text{g m}^{-3}$ during winter and 21 and 15 $\mu\text{g m}^{-3}$ during summer. Although these concentrations are considerably lower compared to corresponding values recorded in large cities in the region, they are still very close to the mean annual standards set by the EU for $PM_{2.5}$. Higher average mass (by ca. 26%-36% for TSP, $PM_{2.0}$ and $PM_{1.0}$) and number (ca. 44%) concentrations were observed in winter compared to those in summer, due to the additional emissions from domestic heating and the weaker atmospheric dilution. The elemental composition measurements showed that crustal and anthropogenic elements (i.e., K, Ca, Ti, Mg, Fe, As, S) in the collected particle samples were also enriched when polluted air masses were transported from Northeastern Turkey. These measurements also showed that natural sources contribute sea-salt and re-suspended soil to the particulate matter load in the city's atmosphere. Non-exhaust traffic emission sources were also found to be an important contributor, as indicated by the good correlations ($R^2 = 0.40 - 0.91$) between crustal and traffic-related elements (i.e., Zn, Cr, Cu, and Mn). The strong contribution of local traffic sources was also identified by the increased number concentrations in the Aitken mode during rush hours. Overall, PM measurements in the urban environment in the region are relatively high, being influenced by both local sources and long transported air masses.

4.2 Introduction

Urban air quality is affected by natural and anthropogenic sources of particulate matter (PM) and gaseous species (Fenger, 2009) that can cause adverse effects upon human health (e.g., Kampa and Castanas, 2008; D'Amato et al., 2013; Lelieveld et al., 2015; Stafoggia et al., 2017). Although the concentrations of main air pollutants has been decreasing in large European cities during the last decade (Klimont et al., 2013; Guerreiro et al., 2014), airborne particles having sizes smaller than ca. 2.5 μm (i.e., $\text{PM}_{2.5}$) often exhibit values above or close to the EU annual standard (25 $\mu\text{g m}^{-3}$) mainly due to the numerous and intense anthropogenic sources, including transportation, domestic combustion processes and industrial activities (Szigeti et al., 2013; Eleftheriadis et al., 2014; Manousakas et al., 2015; Diapouli et al., 2017a; Mamali et al., 2018).

The air quality in small cities (i.e., cities with less than 100000 inhabitants) is believed to be better than that in large urban agglomerations due to the smaller number of emission sources and high natural ventilation with clean marine ambient air. Previous studies, however, have shown that small cities can be influenced by major particle sources under certain meteorological conditions. In the small agricultural city of Ciudad Real (75000 inhabitants) in Spain, for instance, high $\text{PM}_{2.5}$ concentrations are mostly influenced by crustal sources and transported air masses from the Sahara desert, while vehicular traffic accounts for only 14% of those concentrations (Aranda et al., 2015). Also, in Lycksele and Gundsømagle, two small Scandinavian cities, the high concentrations of coarse and fine particles (PM_{10} , $\text{PM}_{2.5}$ and $\text{PM}_{1.0}$) typically observed in winter are the result of local traffic and wood combustion emissions in combination with low air temperatures and stable weather conditions (Glasius et al., 2006; Krecl et al., 2008).

Apart from local/regional sources, air quality in small cities may be significantly affected by transported air pollution from distant sources under specific meteorological conditions (i.e., wind direction and speed). A number of studies at coastal cities in the region of Eastern Mediterranean have shown that high PM concentrations are in many cases linked to air masses transported from Africa and the

Middle East (Kubilay et al., 2000; Lazaridis et al., 2005; Sciare et al., 2008; Floutsi et al., 2016). Especially for the region of the Northern Aegean Sea (NAS), air quality can be significantly affected by polluted air masses transported from Eastern Europe and the Black Sea (Bezantakos et al., 2013; Tombrou et al., 2013, 2015; Triantafyllou et al., 2016). Despite this evidence, however, there is still insufficient information on the quality of the air in coastal urban areas in this region and on the contribution of the local and distant sources that influences it.

The aim of this work is to characterize, for the first time, the atmospheric aerosol and investigate the potential sources of PM pollution at a small insular coastal city in the background marine environment of the NAS during summer and winter. To do so we measured the concentrations, size distributions, as well as the elemental composition of the atmospheric aerosol particles in Mytilene, a representatively small coastal city in the region, and related them with transported air masses from different regions.

4.3. Methods

4.3.1. Study areas and meteorology

Measurement campaigns were conducted in the city of Mytilene (39° 10' N, 26° 20' E), which is the capital on the island of Lesbos. The island is located in the region of the NAS, as shown in Fig. 4.1, and is very close to Turkey. In total, two campaigns were carried out: one during winter from 27 January to 24 February 2014 (DOY 27 – 55), and one during summer from 24 June to 15 July 2014 (DOY 175 – 195).

Mytilene is a small densely populated city (ca. 1647 people/km²; 30,000 inhabitants in total) which serves as the main port of the island of Lesbos. The main air pollution sources in the city include the port activities, the thermal power plant located at the suburbs of the city, and the international airport, which is located ca. 8 km away from the city (cf. Psanis et al., 2017, for details). Another major contributor to air pollution is traffic, which can be a significant source at many locations of the city as a result of the narrow roads that cause high congestions, especially during rush hours. PM concentrations were measured simultaneously at two measurement sites

installed at the centre (at Sappous Square of Mytilene, SSM) and at the port (at the Port Authorities of Mytilene, PAM) of the city, as shown in Fig. 4.1.

A number of meteorological parameters, including temperature, relative humidity, wind speed and direction, were provided by the meteorological station located at the airport of the island. To identify the origin of the air masses reaching the measurement sites during the campaigns, we calculated back-trajectories using the NOAA HYSPLIT model (Stein et al., 2015; Rolph et al., 2017). Back trajectories were obtained at ground level. In order to estimate the impact of long range transport of anthropogenic air pollution and desert dust, we also determined back trajectories at a height of 500 and 2500 m a.g.l. over the sampling sites. In addition, days with desert dust episodes were identified using the online NMMB/BSC-dust transport model (Pérez et al., 2011; Haustein et al., 2012) and the SKIRON/Dust model (Spyrou et al., 2010). Finally, the simulated boundary layer height was derived from ECMWF reanalysis data, with a temporal resolution of 6 h and a spatial resolution of 0.75° (Uppala et al., 2005).

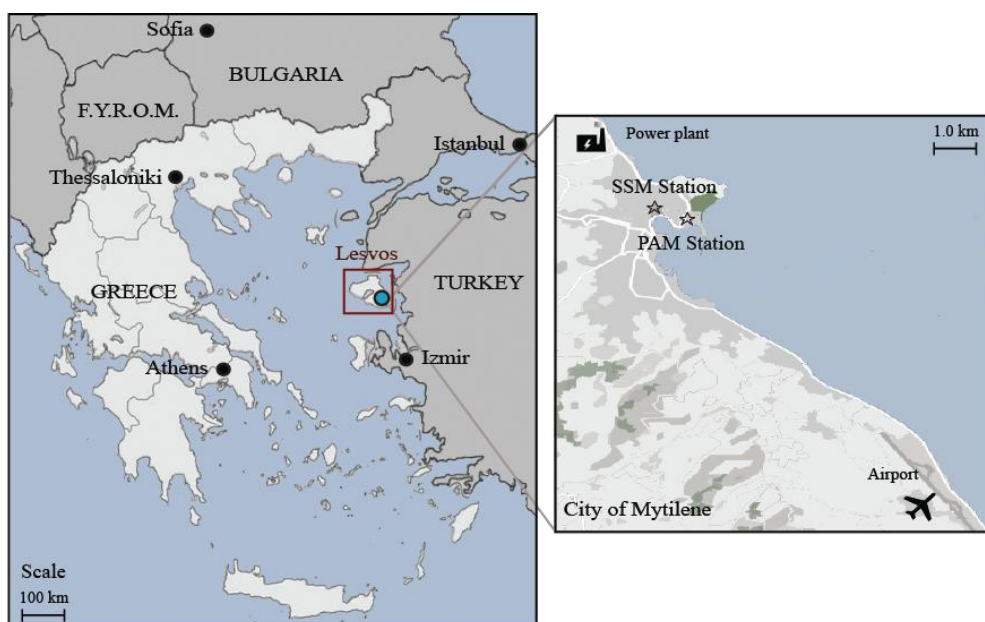


Figure 4.1: Map of Greece showing the islands of Lesvos ($39^\circ 10' N$, $26^\circ 20' E$) and the cities of high population density (up to 1 million inhabitants) in the Eastern Mediterranean area (black solid circles). The detailed map on the right, show the city of Mytilene, the airport, the power plant and the monitoring stations, at the centre (Sappous Square, SSM) and at the port (Port Authorities, PAM) of the city.

4.3.2. Measurements and analytical methods

Total Suspended Particle (TSP) samples were collected at both sites (SSM and PAM) every 8 h during the winter and summer campaigns, using a custom-made sampler operated at a flow rate of 13 lpm. The TSP sampling periods were scheduled during the day (between 7:00 and 14:00), the evening (between 15:00 and 22:00) and the night (between 23:00 and 6:00 the next morning). In addition to TSP samples, particle mass size distributions in the range from 0.1 to 3.2 μm were measured at SSM using a Micro-Orifice Uniform Deposit Impactor (MOUDI; Model 110R; MSP Corporation, Shoreview, MN) operated at a flow rate of 30 lpm for 48 h continuously for each sample. The different stages of the MOUDI had 50% particle cut sizes of 18, 10, 5.6, 3.2, 1.8, 1.0, 0.56, 0.32, 0.18, and 0.10 μm . Using these measurements we also determined the mass concentrations of particles having sizes in the range $0.1\mu\text{m} < d_p < 1.8\mu\text{m}$ and $0.1\mu\text{m} < d_p < 1.0\mu\text{m}$, which provide good approximations of $\text{PM}_{2.0}$ and $\text{PM}_{1.0}$, respectively. Finally, particle number size distributions (in the range between 10 and 500 nm) were measured with a Scanning Mobility Particles Sizer (SMPS; TSI Model 3034) at SSM, and the associated number concentrations were determined by integrating the measurements.

A total of 47 TSP samples (27 corresponding to the winter and 20 to the summer campaign), as well as 19 $\text{PM}_{2.0}$ and $\text{PM}_{1.0}$ samples (9 corresponding to the winter and 10 to the summer campaign) were collected respectively every 8 and 48 h on quartz filters (Whatman QM-A quartz filters 47 mm in diameter, 2 μm pore size, Part No.Z675032). Prior to sampling, the filters were heated at 450°C for 12 h to remove any organic residues. An electronic microbalance with a resolution of 0.01 mg (Kern & Sohn Model 770) was used to weigh the filters under controlled temperature and moisture conditions ($20\pm 2^\circ\text{C}$ and $50\pm 5\%$ RH) before and after sampling. After collection and final weighing, the samples were wrapped in aluminium foils, sealed in plastic containers and stored in a freezer at -20°C until analysed. The majority of the TSP, $\text{PM}_{2.0}$ and $\text{PM}_{1.0}$ samples collected during the two sampling periods were further analysed for a number of elements (i.e., Na, Cl, S, Ca, Ti, K, Cr, Mg, Mn, Fe, Ni, Zn, Ba, Cu and As) using a high resolution energy dispersive X-ray fluorescence spectrometer (Model PANalytical Epsilon 5). Calculated limits of detection (LOD) for the above-mentioned elements ranged from 1×10^{-5} to 3×10^{-2} $\mu\text{g m}^{-3}$, with

precisions ranging from 0.2 to 19%. Details of the XRF analysis and quantification are described in Manousakas et al. (2017).

4.4 Results and discussion

4.4.1 Particle mass concentrations

In general, particle mass concentrations were higher in winter compared to summer. As shown in Fig. 4.2, the measured average concentrations of TSP, PM_{2.0} and PM_{1.0} at SSM were higher by ca. 32%, 26% and 36%, respectively, during winter than during the summer. This observation is consistent with similar measurements from other cities reported in the literature (Carbone et al., 2010; Triantafyllou and Biskos, 2012; Perrino et al., 2014; Mamali et al., 2018), and can be attributed to i) the additional emissions from domestic heating during winter, and ii) the lower dilution associated to the weaker winds and the lower boundary layer heights (ca. 39%; i.e., average values calculated by WRF-Chem model) in winter compared to summer (cf. Table 4.1).

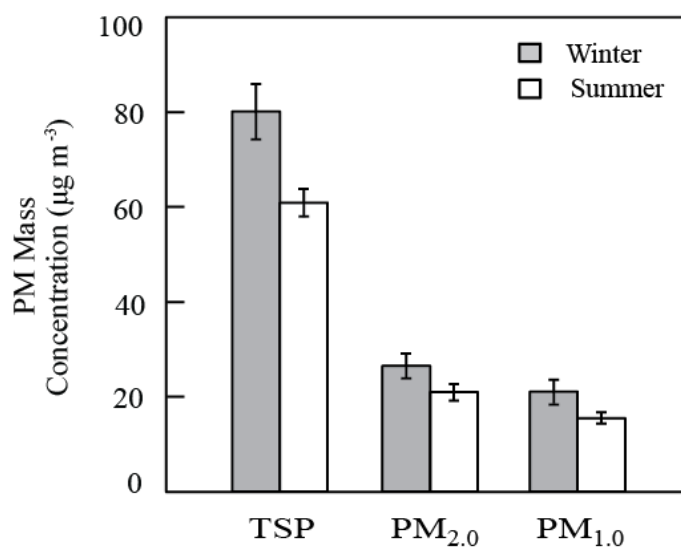


Figure 4.2: Mass concentrations of TSP, PM_{2.0} and PM_{1.0} measured at SSM during winter and summer.

Average TSP concentrations at the two sampling sites during summer were $61\mu\text{g m}^{-3}$ at SSM and $79\mu\text{g m}^{-3}$ at PAM (cf. dashed lines in Fig. C1a in the Appendix C), with the difference being statistically significant as indicated by the Student's t-test

using a cut-off p-value of 0.05. This difference can be attributed to the higher emissions from the enhanced activities at PAM during summer (compared to winter) and the fact that ship emissions did not affect significantly the city centre (i.e. SSM) due to the northern winds that prevailed during the summer period (cf. also Kotrikla et al., 2017). In contrast, the respective values during winter were 80 and 84 $\mu\text{g m}^{-3}$ (cf. dashed lines in Fig. C2a), and those were not statistically significantly different, suggesting that the two sampling sites are similarly affected by all the local sources in this case. The $\text{PM}_{2.0}$ and $\text{PM}_{1.0}$ concentrations recorded at the SSM site had average values of 26 and 21 $\mu\text{g m}^{-3}$ during winter and 21 and 15 $\mu\text{g m}^{-3}$ during summer, respectively (cf. dashed lines in Figs. C1b and C2b). These measurements are lower (by ca. 10-40% in winter and 18-40% in summer) compared to those observed in urban environments of larger cities in Greece, such as Thessaloniki and Athens (Eleftheriadis et al., 2014a; Voutsas et al., 2014; Tolis et al., 2015) as a result of the lower anthropogenic activity (e.g., traffic and heating), but still very close to the mean annual limit values set by the EU for $\text{PM}_{2.5}$.

Table 4.1: Statistics of average hourly wind speed and boundary layer height during the winter and summer sampling periods.

	Wind speed (m s^{-1})		Boundary layer height (m)	
	Winter	Summer	Winter	Summer
Average	2.3	4.1	662	980
St. dev.	1.2	1.9	371	328
Min	1.0	1.0	56	378
Max	5.8	9.3	1514	1741

PM measurements are affected by local sources, but can also be attributed to long-range transport of polluted air masses. As indicated by back trajectory calculations, in ca. 57% of the cases during winter and 80% during summer, the observed air masses were in the polluted region of Northeastern Turkey and the Black Sea ca. 30 h before reaching the measurement sites in our study (cf. Fig. C3a and C3b). Consequently, summer concentrations of PM in the city are affected by the industrial and domestic sources (Elbir, 2003; Odabasi et al., 2010; Koçak et al., 2011) of the Eastern region of Turkey and by the shipping emissions from the nearby waterways connecting the

Black Sea to the Mediterranean and from there to the rest of the globe (Kesgin and Vardar, 2001; Deniz and Durmuşoğlu, 2008).

Days with favourable synoptic conditions for Saharan Dust transport over the North Aegean region were also observed (cf. periods identified by the gray-shaded areas in Figs. C1 and C2 and results of back-trajectory analysis and of the SKIRON Model shown respectively in Figs. C4 and C5). In all cases the transportation of natural dust occurred over small-scale dust events (i.e., events during which the particle reached values of 200–1000 $\mu\text{g m}^{-3}$; Draxler et al., 2001; Escudero et al., 2006). During days with desert dust transport, the TSP, $\text{PM}_{2.0}$ and $\text{PM}_{1.0}$ concentrations were in average ca. 40% higher compared to the days when the air quality was affected primarily by local emissions (cf. Fig. 4.3). This is not surprising given that the Eastern Mediterranean is frequently affected by long-range dust transport (Gkikas et al., 2013; Floutsi et al., 2016), with reports showing that particle concentrations can increase by up to 120% at other rural/coastal sites of the region (e.g., Edermli and Finokalia in the eastern Mediterranean; Gerasopoulos et al., 2006; Koçak et al., 2007; Lazaridis et al., 2008; Vasilatou et al., 2017).

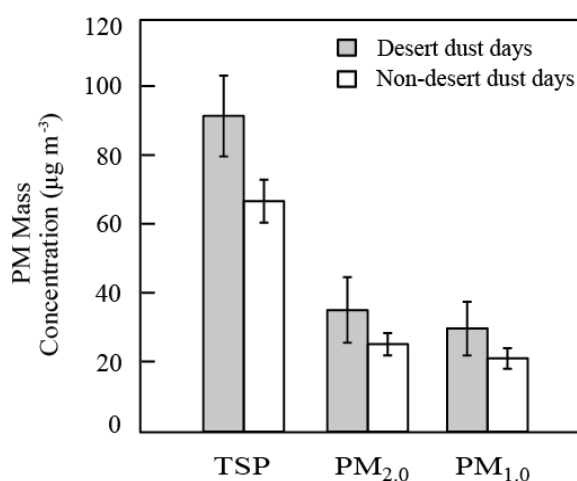


Figure 4.3: Mass concentrations of TSP, $\text{PM}_{2.0}$ and $\text{PM}_{1.0}$ during the days with or without desert dust sources measured at SSM of Mytilene during winter.

The contribution of the finest particle fraction to TSP and of $\text{PM}_{1.0}$ to $\text{PM}_{2.0}$, reflected by the ratios of $\text{PM}_{2.0}/\text{TSP}$ and $\text{PM}_{1.0}/\text{PM}_{2.0}$, are shown in Table 4.2. Fine particles comprise a small fraction of total particle mass ($\text{PM}_{2.0}/\text{TSP}$) in both periods, with an average value of 0.34 and a relatively small range, suggesting that natural

sources (i.e., desert dust transport, local soil dust re-suspension or sea-salt particles) contribute significantly to the particulate matter load in the atmosphere over the city. This is consistent with observations in other Mediterranean coastal cities (Alastuey et al., 2005; Koçak et al., 2007; Galindo et al., 2013; Romano et al., 2016), corroborating that this is a generalized regional pattern. The smaller fractions during both periods are affected largely by anthropogenic sources as indicated by the relatively high average $PM_{1.0}/PM_{2.0}$ ratios (0.80 in winter and 0.75 in summer; Alastuey et al., 2005). Considering also that the variability of this ratio is small for the entire period during both measuring campaigns, the importance of anthropogenic sources in the atmosphere of Mytilene is high in both cases.

Table 4.2: Concentration ratios of the different PM fractions measured at Mytilene during winter and summer period.

	Winter		Summer	
	Whole period		Whole period	
	$PM_{2.0}/$ TSP	$PM_{1.0}/$ $PM_{2.0}$	$PM_{2.0}/$ TSP	$PM_{1.0}/$ $PM_{2.0}$
Average	0.34	0.80	0.34	0.75
Min	0.23	0.45	0.24	0.50
Max	0.54	0.89	0.46	0.88

Figure 4.4 shows the average mass distributions of particles having diameters from 0.1 to 3.2 μm measured by the MOUDI during the two seasons at SSM. In both cases the size distributions exhibit two modes: one in the submicron range with a mean size between 0.18 and 1.0 μm , and one corresponding to coarser particles with sizes > 1.0 μm . The mean size of the particles derived from these measurements is smaller (ca. 0.6 μm) during winter and larger (ca. 1.2 μm) during summer, with more particles residing in the submicron region during winter. This corroborates the higher importance of anthropogenic combustion sources (that produce smaller particles compared to natural sources; Lin and Lee, 2004) during the cold period, which is also supported by the elemental analysis of the PM samples discussed in section 4.4.2 below.

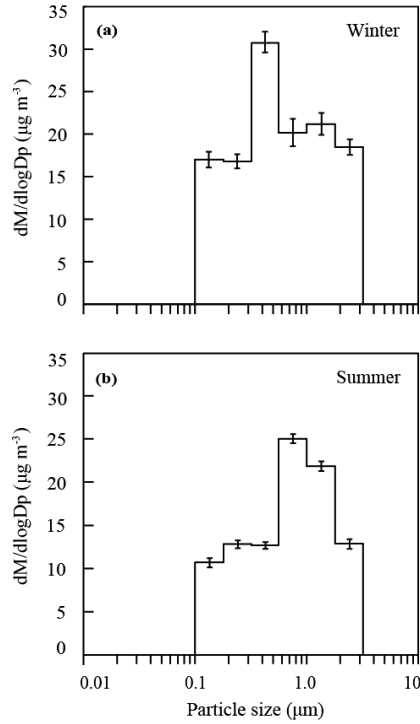


Figure 4.4: Mass size distributions of particles having diameters in the size range 0.1-3.2 μm measured at SSM during (a) winter and (b) summer.

4.4.2 PM chemical composition

Variation in the chemical composition of TSP, $\text{PM}_{2.0}$ and $\text{PM}_{1.0}$ samples collected at the two measurement sites (SSM and PAM) during summer and winter are provided in Tables 4.3 and 4.4. Average values of all elements in both periods are much lower than those reported from measurements at urban sites in Thessaloniki and Athens (Karanasiou et al., 2007; Terzi et al., 2010), with Na, S, Ca, Fe, K and Cl being the most abundant elements at both sites and seasons.

In order to compare the elemental composition and the sources of PM observed during the two seasons, we used a range of tools including the Student's t-test (with p-value 0.05), correlation analysis of elemental concentrations in the TSP (Table 4.5) as well as in $\text{PM}_{2.0}$ and $\text{PM}_{1.0}$ (Table 4.6) samples, and calculations of the enrichment factor (EFs) for each element and season. The EF of an element X for each PM sample was determined by (IAEA, 1992):

$$\text{EF} = \frac{(X/C)_{\text{PMsample}}}{(X/C)_{\text{Crust}}} \quad (1)$$

where C is a reference element of crustal origin, which is usually chosen among Al, Si, Sc, Mn, Ti, Fe (Reimann and Caritat, 2000; Sutherland, 2000). In all cases

presented here we used Ti as a reference element, whereas the elementary composition of the Earth's crust was taken from Wedepohl (1995). The EF values for each element in the samples collected at the two measurement sites (SSM and PAM) are shown in Figure 4.5. EF values larger than 10 suggest that anthropogenic sources dominate the investigated samples, while EF values lower than 5 indicate that elements are of crustal origin. EF values between 5 and 10 correspond to elements that originate from both natural and anthropogenic sources. The results of these analyses suggested that the main PM sources were the marine environment (sea-salt particles), re-suspension of polluted soil particles and road dust, as well as emissions from traffic and residential heating. More detailed discussion on each of these sources is provided below.

Table 4.3: Average and the standard deviation of elemental concentrations (in ng m^{-3}) in TSP mass at the monitoring sites SSM and PAM in winter and summer.

	Winter		Summer	
	<i>n</i> (8)	<i>n</i> (7)	<i>n</i> (10)	<i>n</i> (10)
	TSP SSM (ng m^{-3})	TSP PAM (ng m^{-3})	TSP SSM (ng m^{-3})	TSP PAM (ng m^{-3})
	Av \pm Std	Av \pm Std	Av \pm Std	Av \pm Std
Na	1118 \pm 1351	1823 \pm 2284	672 \pm 396	1338 \pm 470
S	960 \pm 409	1550 \pm 495	1004 \pm 393	1620 \pm 635
Ca	631 \pm 298	1250 \pm 551	1285 \pm 645	5010 \pm 2260
K	374 \pm 256	510 \pm 285	211 \pm 119	623 \pm 397
Fe	239 \pm 198	619 \pm 526	656 \pm 1309	1611 \pm 1069
Cl	169 \pm 193	352 \pm 649	99 \pm 67	1610 \pm 971
Mg	68 \pm 52	209 \pm 76	226 \pm 136	634 \pm 276
Ba	56 \pm 49	117 \pm 129	125 \pm 76	166 \pm 67
Zn	56 \pm 77	88 \pm 130	11 \pm 21	25 \pm 28
Mn	6 \pm 11	33 \pm 31	20 \pm 35	46 \pm 26
Ti	13 \pm 10	27 \pm 13	36 \pm 27	151 \pm 114
Cu	6 \pm 4	10 \pm 6	7 \pm 17	15 \pm 33
V	1 \pm 2	4 \pm 3	4 \pm 5	9 \pm 6
Cr	1 \pm 1	11 \pm 14	32 \pm 67	23 \pm 11
As	18 \pm 9	23 \pm 10	6 \pm 7	10 \pm 5

n: number of samples

Sea-salt was an important fraction of atmospheric aerosol sampled in the marine coastal environment of Mytilene. The abundant presence of marine elements (Na and Cl) were mainly found in TSP, as expected, due to the coarse size of sea-salt particles, which yields relatively low mean $\text{PM}_{2.0}/\text{TSP}$ ratios (ranging from 0.15 to 0.18; cf. Tables 4.3 and 4.4) obtained for these elements during both seasons. The higher

concentrations of Na and Cl at the PAM (p-value of 0.05) suggest that this site is more affected by the sea spray in comparison to SSM, which can be explained by its closer proximity to the open sea. During summer, the mean Cl/Na concentration ratio (ca. 1.2) at PAM was close to the typical sea water ratio of 1.8 (Bowen, 1979), indicating that fresh sea-salt aerosol impacted the site. However, the Cl/Na ratios were very low at SSM in summer and at both sites in winter (0.15 at SSM and 0.19 at PAM). These low values can be explained by the depletion of Cl by the chemical reaction of sea-salt particles with gaseous pollutants (such as nitric and sulfuric acid), leading to the removal of Cl and the formation of particulate nitrate or sulfate species (i.e., NaNO_3 , Na_2SO_4 ; cf. Eleftheriadis et al., 1998).

Table 4.4: Average and standard deviation of elemental concentrations (in ng m^{-3}) of the $\text{PM}_{2.0}$ and $\text{PM}_{1.0}$ samples collected at the monitoring site SSM in winter and summer.

	Winter		Summer	
	<i>n</i> (9)	<i>n</i> (9)	<i>n</i> (10)	<i>n</i> (10)
	$\text{PM}_{2.0}\text{SSM}$ (ng m^{-3})	$\text{PM}_{1.0}\text{SSM}$ (ng m^{-3})	$\text{PM}_{2.0}\text{SSM}$ (ng m^{-3})	$\text{PM}_{1.0}\text{SSM}$ (ng m^{-3})
	Av±Std	Av±Std	Av±Std	Av±Std
Na	182±58	79±37	124±44	80±31
S	402±141	354±128	255±95	227±85
Ca	73±43	33±40	157±67	95±37
K	178±107	157±97	30±21	19±12
Fe	27±7	8±4	45±38	18±11
Cl	29 ±40	1±4	15±11	1±1
Mg	17±14	5±10	35±15	19±6
Ba	11±4	7±3	3±3	2±3
Zn	9±3	4±1	3±2	2±1
Mn	2 ±1	1±1	4±1	3±1
Ti	1±1	0.5±0.5	6±4	3±1
Cu	3±4	3±3	1±0.5	0.4±0.5
V	0.6±0.3	0.6±0.3	1±1	1±1
Cr	1±1	1±1	3±1	2±1
As	3±1	2±1	2±1	1±1

n: number of samples

More recently, in a source apportionment study conducted in two Greek urban centres (Athens and Thessaloniki), Diapouli et al. (2017a) have reported Cl depletion and significant contribution from secondary species in the sea-salt chemical profiles. While we cannot provide evidence for these reactions here due to the absence of sulfate and nitrate measurements, the observed low Cl/Na ratios indicate that marine Na is reacting with nitric acid. The low temperatures and high relative humidity

prevailing during the cold period favour the formation of secondary nitrate (Dassios and Pandis, 1999), leading to aging of the marine aerosol at both sites. Here, Na concentrations displayed a good correlation (R^2 ranging from 0.50 to 0.99) with Fe, Zn, Cr, Cu, Mn at both sites during the cold period (Table 4.5). This observation suggests the presence of aged sea-salt, as it is associated with trace elements of anthropogenic origin having spent considerable time mixed with marine air (Ogunsola et al., 1994; Visser et al., 2015).

Enhanced re-suspension of polluted soil particles and road dust is another important source suggested by the elemental composition of the TSP samples collected at both sites and seasons. High concentrations of Ca, Mg, Fe, and Ti were observed in both seasons, with concentrations during summer being significantly higher compared to those in winter (p-value of 0.05), as a result of the more dry conditions (Petaloti et al., 2006; Minguillón et al., 2012b) and of the stronger (by ca. 78%) summer winds. This is in line with mean $PM_{2.0}/TSP$ ratios for these elements, which exhibited lower values in summer (up to 0.18), and the elemental size distribution of most crustal elements, like Ti, which are shifted towards the coarser sizes (1.0 – 1.8 μ m; Fig.4.6), indicating that these elements were related more to the natural sources during this period. This is also supported by the lower EFs (exhibiting values < 5) of Ca, Mg, Fe and Ti in the TSP samples collected at both seasons and for K in summer (Fig. 4.5a and 4.5b), as well as by the good correlations among almost all these elements (i.e. Ca, Mg, Fe, K and Ti) measured in the TSP samples at both sites during summer (R^2 ranging from 0.40 to 0.80; Table 4.5c and 4.5d). The fine and coarse modes (0.32-0.56 μ m and above 1 μ m, respectively) of K concentrations in summer are of similar magnitude (cf. Fig.4.6), indicating significant contribution from soil re-suspension under dry atmospheric conditions (Lü et al., 2012; Bougiatioti et al., 2013). The important contribution of road dust re-suspension was further exhibited by good correlations between Ca and Mg (R^2 ranging from 0.40 to 0.87; Table 4.6), with most of the traffic-related elements (i.e. Cr, Cu and Mn) being in the fine fractions at the SSM site. Ca has been linked to the combustion of lubricating oil, while Mg can be related to the re-suspension of soil dust and sea-salt particles by vehicular traffic (Viana et al., 2008; Wawer et al., 2015).

Table 4.5: Correlation coefficients (R^2) among the TSP elemental concentrations at SSM and PAM during winter (a and b, respectively) and summer (c and d, respectively). Only R^2 equal or higher than 0.40 (p-value of 0.05) are shown.

a) Winter elemental correlations in TSP mass at SSM													c) Summer elemental correlations in TSP mass at SSM															
	Fe	Zn	Cr	Cu	Mn	As	V	S	Na	Ti	Ca	K	Mg	Fe	Zn	Cr	Cu	Mn	As	V	S	Na	Ti	Ca	K	Mg		
Fe	1.00													1.00														
Zn	0.84	1.00													1.00													
Cr	0.88	0.99	1.00											0.95		1.00												
Cu	0.53	0.62		1.00										0.40			1.00											
Mn	0.97	0.86	0.99	0.45	1.00									0.97		0.91		1.00										
As						1.00													1.00									
V							1.00													1.00								
S								1.00													1.00							
Na	0.81	0.99	0.97	0.64	0.82				1.00						0.89		0.43					1.00						
Ti										1.00												0.40	1.00					
Ca										0.51	1.00												0.63	1.00				
K												1.00											0.51	0.73	0.44	1.00		
Mg													1.00										0.51	0.74	0.46	0.67	1.00	

b) Winter elemental correlations in TSP mass at PAM													d) Summer elemental correlations in TSP mass at PAM														
	Fe	Zn	Cr	Cu	Mn	As	V	S	Na	Ti	Ca	K	Mg	Fe	Zn	Cr	Cu	Mn	As	V	S	Na	Ti	Ca	K	Mg	
Fe	1.00													1.00													
Zn	0.65	1.00													1.00												
Cr	0.98	0.79	1.00													1.00											
Cu		0.67	0.40	1.00											0.40		1.00										
Mn	0.59	0.50	0.53		1.00									0.80				1.00									
As						1.00													1.00								
V							1.00													1.00							
S								1.00										0.51		0.55	1.00						
Na	0.63	0.99	0.72	0.59	0.50			0.45	1.00						0.44						0.43	1.00					
Ti										1.00												0.88	0.40	1.00			
Ca											1.00											0.58	0.64	1.00			
K												1.00										0.78	0.54	0.79	1.00		
Mg													1.00									0.47	0.42	0.40	0.43	1.00	

Table 4.6: Correlation coefficients (R^2) between the elemental concentrations of the $PM_{2.0}$ and $PM_{1.0}$ mass at SSM, that were equal or higher than 0.40 (p-value of 0.05) in winter (a and b, respectively) and summer (c and d, respectively).

a) Winter elemental correlations in $PM_{2.0}$ mass at SSM														c) Summer elemental correlations in $PM_{2.0}$ mass at SSM													
	Fe	Zn	Cr	Cu	Mn	As	V	S	Na	Ti	Ca	K	Mg	Fe	Zn	Cr	Cu	Mn	As	V	S	Na	Ti	Ca	K	Mg	
Fe	1.00													1.00													
Zn	0.43	1.00												0.75	1.00												
Cr	0.43		1.00											0.40	0.46	1.00											
Cu	0.40		0.99	1.00													1.00										
Mn	0.65		0.59	0.57	1.00									0.62	0.71	0.45	0.47	1.00									
As						1.00													1.00								
V							1.00											0.57		1.00							
S								1.00													1.00						
Na	0.69	0.49	0.55	0.50	0.60				1.00					0.69				0.82			0.72	1.00					
Ti										1.00				0.64				0.61			0.46	0.64	1.00				
Ca	0.56		0.95	0.93	0.65	0.47					1.00			0.89	0.74	0.70	0.40	0.87		0.55	0.89	0.80	1.00				
K								0.75				1.00		0.93			0.40	0.71		0.61	0.63	0.77	0.58	1.00			
Mg	0.41		0.80	0.76	0.47				0.53		0.69		1.00	0.73	0.58	0.53	0.40	0.70		0.46	0.73	0.90	0.89	0.63	1.00		

b) Winter elemental correlations in $PM_{1.0}$ mass at SSM														d) Summer elemental correlations in $PM_{1.0}$ mass at SSM													
	Fe	Zn	Cr	Cu	Mn	As	V	S	Na	Ti	Ca	K	Mg	Fe	Zn	Cr	Cu	Mn	As	V	S	Na	Ti	Ca	K	Mg	
Fe	1.00													1.00													
Zn	0.70	1.00													1.00												
Cr			1.00													1.00											
Cu			0.99	1.00												0.41	1.00										
Mn	0.78	0.62	0.47	0.46	1.00									0.67			0.51	1.00									
As			0.40			1.00													1.00								
V							1.00													1.00							
S								1.00													1.00						
Na	0.41		0.88	0.89	0.50				1.00					0.63								1.00					
Ti	0.84	0.59			0.72	0.46				1.00					0.40					0.40	0.40		1.00				
Ca	0.40		0.77	0.78	0.58						1.00						0.40	0.63		0.57	0.97		1.00				
K								0.72				1.00										0.44		1.00			
Mg	0.40		0.56	0.53	0.42				0.54		0.70		1.00				0.40			0.65			0.70		1.00		

Traffic-related PM elements such as Cr, V and Mn were detected in all three PM fractions (TSP, PM_{2.0} and PM_{1.0}) and Ba in TSP, with the concentrations being significantly higher (p-value of 0.05) in summer compared to 1 winter (Tables 4.3 and 4.4). This is to be expected since vehicular traffic is an important contributor to the local emissions, becoming stronger in the busy summer holiday season. In addition, correlations among Fe, Zn, Cr, Cu, and Mn were stronger in the TSP rather than the fine fractions, as a result of the contribution of non-exhaust emissions (tire and brake wear and road dust re-suspension), which generally appear more often at the coarse fractions (Eleftheriadis and Colbeck, 2001; Pio et al., 2013; Pant and Harrison, 2013). The contribution of the non-exhaust emissions is also supported by the PM_{2.0}/TSP ratios for these elements, which were very low (ranging from 0.03 and 0.20) in summer, suggesting the production of mechanical abrasion particles. Significant enrichment with respect to crustal composition (EFs>10) was observed for all traffic-related elements (i.e. Zn, Cu, Cr, and Ba) for all PM fractions in both measurement sites and seasons (Fig. 4.5a and 4.5b), clearly pointing to an anthropogenic origin of these species.

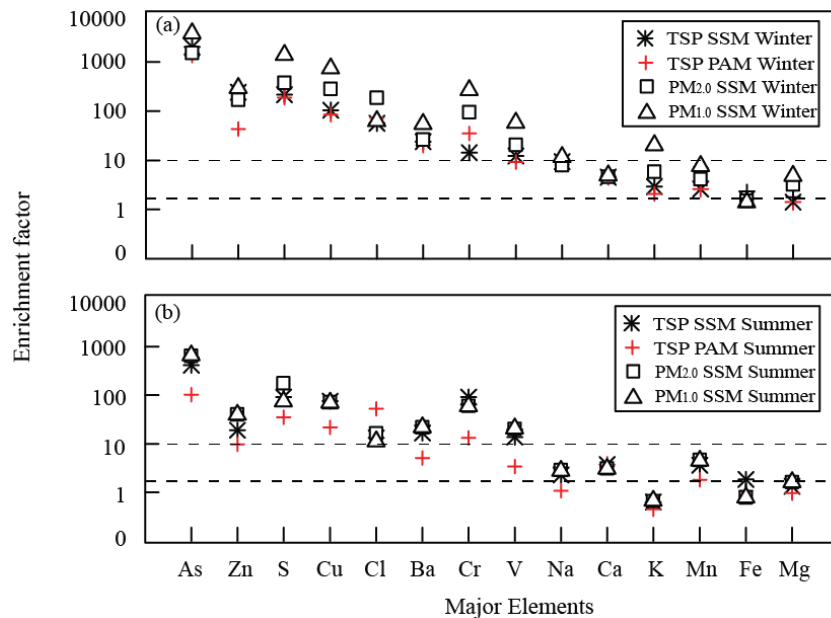


Figure 4.5: Enrichment factors for the major elements in TSP mass at SSM and PAM and in PM_{2.0} and PM_{1.0} at SSM in winter (a) and summer (b) period.

In the case of other elements associated with anthropogenic emissions such as As, average concentrations in all three PM fractions were at least two times higher at both sites during winter, indicating contributions from combustion sources such as

residential heating and coal combustion (Bem et al., 2003; Sun et al., 2014; Manousakas et al., 2015). In addition to that, high K concentrations, which are indicative of wood combustion emissions (Molnár et al., 2005; Saffari et al., 2013), were also observed at SSM in the winter, suggesting that residential heating in Mytilene partly relies on wood burning. This is also reflected by the corresponding EF values ($5 < EF < 10$) as discussed above (cf. Fig. 4.5), further supporting the association of K with combustion sources, and specifically wood combustion. In addition, the fact that K correlated strongly with S in winter (R^2 ranging from 0.72 to 0.75; Table 4.6), also suggests that sources such as biomass burning are important contributors to PM pollution in the city (Liu et al., 2000; Minguillón et al., 2012a). Attribution of K concentrations to anthropogenic combustion in winter is further supported by the fact that higher elemental concentrations are observed at smaller particle sizes (i.e., from 0.32 to 0.56 μm) as shown in Fig.4.6 (Zhao et al., 2011).

The high concentration levels and the high EFs (values >10) for S at both sites and seasons indicate that its sources, which are commonly related to anthropogenic activities, are important contributors to PM pollution in the city. The anthropogenic origin of S is also supported by its size distributions (Fig. 4.6) which exhibited peaks in the fine mode (at 0.32 – 0.56 μm) during both seasons. S-containing aerosol particles may very well be attributed to local shipping emissions and the subsequent formation of sulfates as a result of the increased photochemical activity, or to long range transport of S-containing particles (Zhang et al., 2010; Lü et al., 2012; Becagli et al., 2012). Higher $\text{PM}_{2.0}/\text{TSP}$ ratio for S is determined in winter, but the opposite is observed in summer, indicating that it is related to anthropogenic and more specifically to S-containing fuel combustion in winter. According to the correlation analysis, average S concentrations at PAM can partly be attributed to fuel combustion from shipping emissions (Daher et al., 2013; Johnson et al., 2014), as the concentrations of the element associated with those of V and Mn during the summer period (Table 4.5), but not at the SSM site as mentioned above (cf. section 4.4.1).

Contribution of long-range transported polluted air masses to the air quality of Mytilene was observed during both seasons (cf. section 4.1 and Figs. C3a and C3b). This is indicated by the higher concentrations of some crustal (ca. K, Ca, Ti, Mg and Fe) and anthropogenic elements during the transport events, in comparison to the days

influenced mainly by local emissions. More specifically, elemental concentrations in the TSP samples increased by ca. 50% for K, Ca, Ti, Mg and 90% for Zn and As during the regional transport events in summer, while the associated increase in winter was estimated to be ca. 45% for K, Ca, Ti, Fe and 40% for Zn and S. The observed higher summer contributions associated with long-range transported polluted air masses are also indicated by the correlations between S and crustal components (i.e., Ca, Mg) or Na during summer (Table 4.5 and 4.6), which may be related to the long-range transport of dust along with sea-salt and secondary sulfates as were observed by Diapouli et al. (2017b).

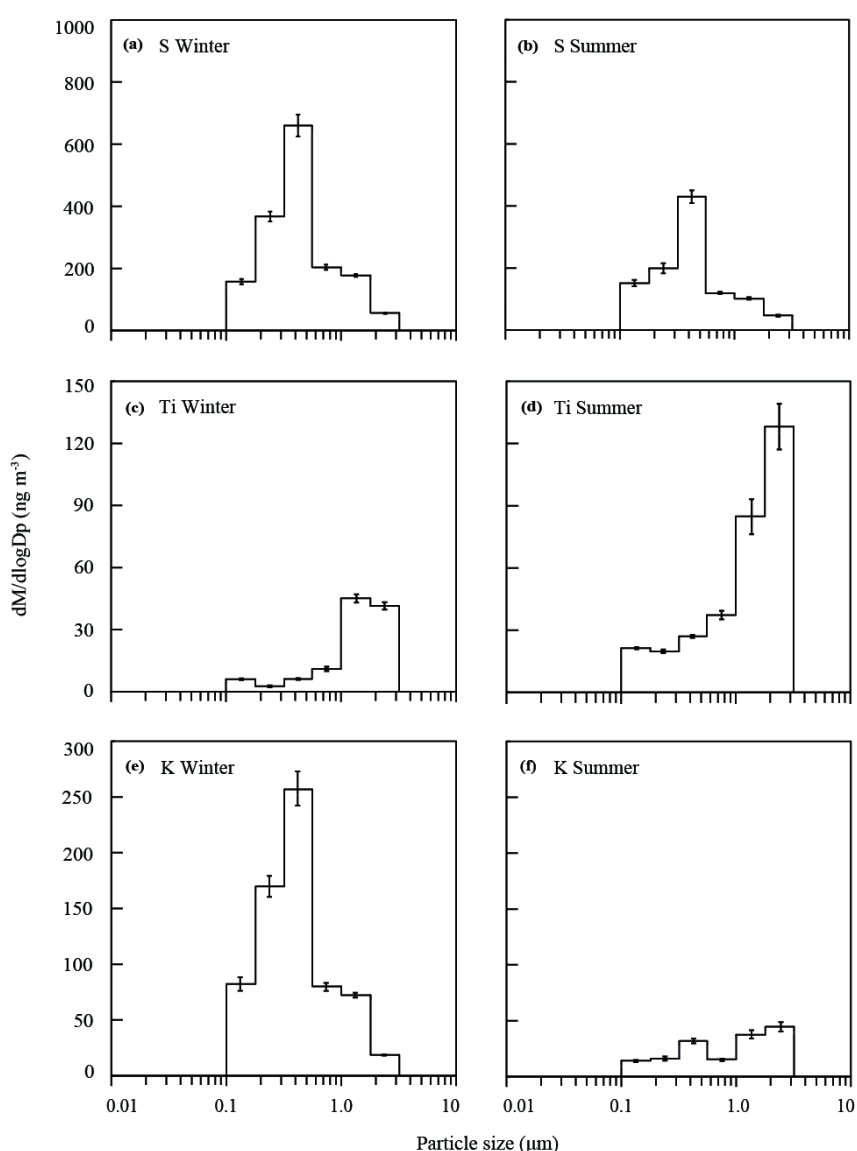


Figure 4.6: Elemental size distributions of S, Ti and K measured at the monitoring site SSM during winter (a, c and e, respectively) and summer (b, d and f, respectively).

4.4.3 Particle number size distributions and concentrations

Figure 4.7 shows the average diurnal evolution of the normalized particle number size distributions, and the associated number concentrations measured at SSM during the winter and summer periods. Although the average concentration levels (having values of 1.4×10^4 and 1.0×10^4 particles cm^{-3} during winter and summer, respectively) were up to a factor of 2 lower than those observed in large urban cities of the region (Diapouli et al., 2011; Siakavaras et al., 2016), we observed a seasonal variation that is typical for an urban site with higher number concentrations in winter (ca. 34%).

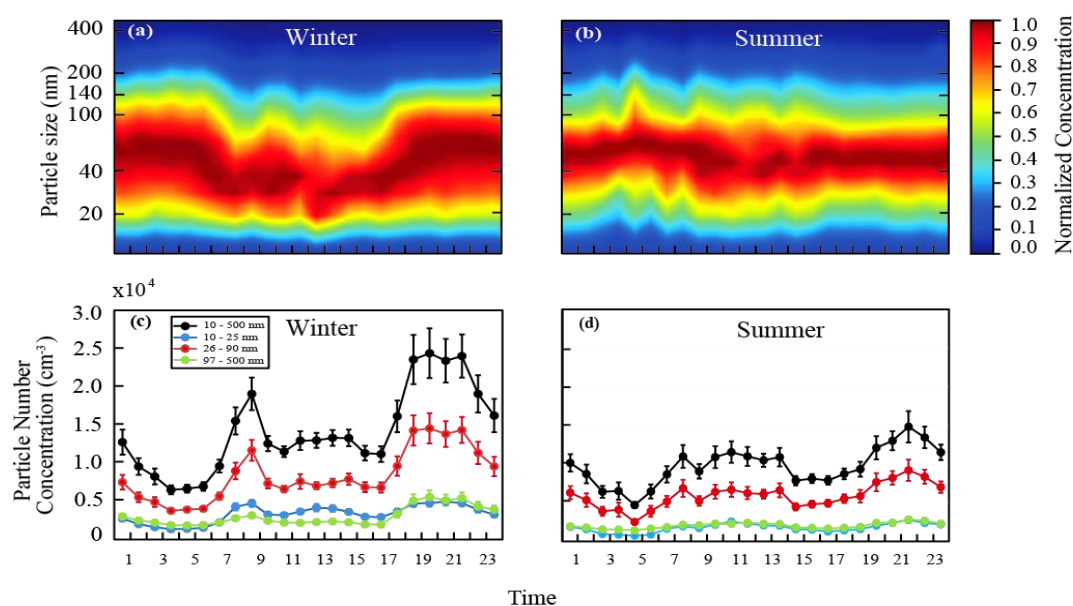


Figure 4.7: Diurnal evolution of the normalized particle number size distributions and of the average number concentrations of particles having sizes in the range 10-500 nm (black line), 10-25 nm (blue line), 26-90 nm (red line) and 97-500 nm (green line), measured at SSM during winter (a, and c, respectively) and summer (b, and d, respectively).

The dominance of Aitken mode particles was evident in both periods (cf. Figs. 4.7a to 4.7d), indicating that the atmospheric aerosol is strongly influenced by traffic emissions (Harris and Maricq, 2001; Wu et al., 2008). Despite that, however, some distinct differences in the evolution of the size distributions measured in winter and summer can be observed. First, number concentrations corresponding to the early morning traffic between 7.00 and 9.00 had a more pronounced increase (reaching values up to 1.8×10^4 particles cm^{-3}) in winter than in summer, most likely due to contribution of the emissions from domestic heating during wintertime. Second, number concentrations decreased by 1.5 times whereas the mean particle size shifted

from ca. 70 to 40 nm after the morning peak during winter. In contrast, during the summer, the size distributions remained almost unchanged, which could be partly explained by the absence of heating emissions. Third, the number concentrations in the evenings (after 17.00) exhibited a similar pattern to that in the morning hours in both periods, which can be attributed to the evening traffic. However, mean total number concentrations during the winter evenings (Fig. 4.7c) were 1.5-fold higher (p-value of 0.05) than those observed in summer, which can be partly attributed to domestic emissions such as heating (in the winter) and cooking, as well as to temperature inversions that occur over the wider region of the Mediterranean area during the winter night hours as reported by Sindosi et al. (2003).

Total number concentrations during days with desert dust transport (which were about 10% of the sampling days) exhibited a strong increase (by ca.40%; Fig.C6) during summer and a weak increase (by ca. 12%) during the winter. The situation was similar also during days with long range transport of anthropogenic air pollution. This difference on the impact of long range transport emissions between summer and winter can be supported by the fact that the additional local emissions (such as domestic heating) and the unstable atmospheric conditions (weaker atmospheric dilution; see section 4.4.1) increase the significance of local emissions in winter, therefore reducing the difference with the long-range transported air masses.

4.5 Conclusions

In this paper we report, for the first time, measurements of the atmospheric aerosol at a representative small insular coastal city in the NAS, namely the city of Mytilene, during the warm and the cold period. Particle mass and number concentration levels in the city are up to a factor of 2 lower compared to those observed in larger cities in the region. Mass concentrations of TSP, PM_{2.0} and PM_{1.0} as well as the average total number concentrations were higher (by ca. 32, 26, 36 and 44%, respectively) in winter compared to summer, which can be attributed to the additional emissions from domestic heating, and to the weaker atmospheric dilution associated to the lower average values of wind speed (ca. mean difference of 56%) and boundary layer height.

Higher particulate concentrations were recorded at the site located at the port of the city (i.e., PAM) only in summer due to enhanced port activities, and not at the site located at the city centre (i.e., SSM) as the prevailing wind directions did not favour the transport of air masses to the direction of city centre. A similar observation can be made for the higher contribution of sea-salt particles at PAM because of its higher proximity to the open sea, in comparison to SSM site.

Re-suspension of polluted soil particles and non-exhaust traffic emission sources are important contributors mainly in the TSP samples at both sites and seasons. Re-suspension of polluted soil particles is more significant in summer, as shown by the higher concentrations of Ca, Mg, Fe, and Ti, due to the drier conditions. High mass and number concentrations in the Aitken mode during heavy traffic hours, as well as strong correlations among anthropogenic elements like Fe, Zn, Cr, Cu, and Mn, suggest that traffic is one of the main contributors to PM pollution. The smaller PM fractions during both periods were also affected largely by other anthropogenic activities such as wood and fuel combustion (i.e. residential heating and shipping emissions), as indicated by high concentrations of K and S. These heating sources are also reflected by a more pronounced increase of number concentrations in winter than in summer.

In addition to the local sources, high contribution of long-range transported polluted air masses was observed in summer compared to winter. This contribution was further supported by the higher concentrations and the strong relationship among some crustal and anthropogenic elements that were recorded during the long-range transport events, as well as by the diurnal variability of the size distribution measurements that are more pronounced in winter.

Chapter 5

Assessment of factors influencing PM mass concentration measured by gravimetric & beta attenuation techniques at a suburban site

5.1 Abstract

Near real-time atmospheric particulate matter (PM) monitors are extensively used in air quality networks given their ability to provide continuous measurements with minimal attention by the operator. Their principle of operation is based on measurement of a physical parameter that is quantitatively linked to the PM mass concentration. Significant discrepancies between these measurements and those obtained by the reference gravimetric method, conducted in regions with diverse climatic conditions, have been reported in the literature. In this study we compare systematic PM_{2.5} and PM₁₀ gravimetric (GM) and beta attenuation (BAM) measurements performed at a suburban site in Athens, Greece, over a period of 4 years (2009-2012). In general, BAM and GM datasets exhibited similar temporal variation for both PM size fractions. An overestimation of the BAM measurements, which was ~30% for the PM_{2.5} and ~10% for the PM₁₀ data, was observed. Good linear correlations between GM and BAM data were observed, with estimated Pearson coefficients being 0.79 for the PM_{2.5} and 0.85 for the PM₁₀ measurements. The respective fitted equations through the entire dataset were $BAM = 0.71 \cdot GM + 6.2$, and $BAM = 0.77 \cdot GM + 4.1$. Better correlation between GM and BAM measurements was observed during the cold rather than the warm period. Discrepancies between BAM and GM PM_{2.5} measurements increased with increasing available water vapor, suggesting that the aerosol bound water has a strong effect on the measurements. The effect of filter material used for GM measurements (i.e., quartz, glass fiber, or Teflon) was also examined for the PM_{2.5} dataset. Best correlation between BAM and GM data was observed when glass fiber, which is incidentally the material of the BAM filter tape, was used in the GM measurements. When the BAM to GM relationship was examined by further categorizing the data by

the season (i.e., cold and warm period) for different filter types, the relationships that were fitted to the data for the two seasons were similar when Teflon filters were used, but quite diverse when quartz and glass fiber filters were employed in the GM measurements. Finally, the variability of the ratio between the two measurement techniques was found to be potentially dependent on the availability of the volatility or stability in the aerosol phase of species such as ammonium nitrate.

5.2 Introduction

Inhaled particles can cause a number of respiratory, cardiovascular, circulatory and nervous diseases including chronic bronchitis, and asthma, alveolar inflammation, cardiac arrhythmia, as well as hypertrophy (Seaton et al., 1995; Schwarze et al., 2006). It is not surprising, therefore, that particulate matter (PM) pollution in urban environments has been associated with increased morbidity and mortality rates in several epidemiological investigations (e.g., Katsouyanni et al., 2001; Puett et al., 2011; Wang et al., 2013; Ostro et al., 2015). The documented detrimental effects of particulate matter pollution to human health have drawn attention to the need for integrated mitigation strategies, including the establishment of air quality guidelines, continuous and accurate monitoring of PM concentrations and effective control of population exposure.

A number of air quality directives have been set by the US Environmental Protection Agency (US-EPA) and the European Commission (EC) since the early 1980's. The first air quality guidelines established by the EC introduced threshold values for "black smoke" which was determined by measuring the light reflectance from PM loads collected on paper filters (Wolff and Perry, 2010). Since then, the EC legislation has been reviewed many times, following the evidence from epidemiological and toxicological studies. The most recent EC Directive (2008/50/EC; EU-Commission, 2008) includes daily and annual limit values for ambient PM₁₀ concentration, as well as an annual target value for PM_{2.5}.

Apart from setting the threshold PM values, another objective of the directives are to establish standardized techniques for measuring PM mass concentrations in order to ensure the quality and uniformity of the data. The use of near real-time PM monitors

has been supported in US and European air quality networks over the past decades mainly due to their ability to provide continuous measurements with minimal human intervention. All types of PM gravimetric samplers, including the sampler recommended by EPA, can provide accurate measurements, considering a 10% variation of mean concentration (Yanosky and MacIntosh, 2001). In contrast to the gravimetric (GM) method, i.e. the reference method for measuring PM concentrations, there are no standardized techniques for near real-time observations. As a result, international policy-making bodies such as the EC Working Group on PM, support actions towards comparability and equivalence among methods for measuring PM mass concentrations (US-EPA, 1999; EC, 2010).

The most commonly used near real-time techniques for measuring PM are the Tapered-Element Oscillating Microbalance (TEOM) and Beta Attenuation (BAM) method. Several studies have compared indirect/near real-time BAM with direct GM particle mass concentration measurements and identified a number of parameters that lead to overestimation of the mass concentration determined by the former (e.g., Chang et al., 2001; Salminen and Karlsson, 2003; Lazaridis et al., 2008; Shin et al., 2011, 2012). These differences often depend on meteorological conditions and therefore exhibit seasonal variability (Gębicki and Szymańska, 2012). In addition, variations in the aerosol chemical composition can induce differences between BAM and GM measurements.

Considering that both meteorological conditions and chemical composition exhibit spatial and temporal variability, calibration parameterization is mandatory for different locations and seasons. One important factor contributing to the discrepancy between BAM and GM measurements is the amount of material (e.g., water and/or other semi-volatile compounds) that can be evaporated from (Chang et al., 2001; Takahashi et al., 2008; Shin et al., 2011, 2012) or adsorbed on the filter or the particle-sample matrix. The filter type is among the most important contributors to the difference between the referred methods, due to their efficiency for releasing or adsorbing water or semi-volatile species such as nitrate salts, during periods of high atmospheric stability (Perrino et al., 2013). Additionally, the influence of ambient humidity conditions on different filter types can lead to non-linear hysteresis effects during the equilibration procedure of filters (Brown et al., 2006).

Price et al. (2003) found that particle bound water may be the major factor in the observed discrepancy between the gravimetric and the TEOM real time monitor, when operating at 50°C. The water content of particles collected on filters depends on the relative humidity (RH) of the sampled air as well as the chemical composition of the particles. GM samples are collected in ambient conditions but are then weighed at ~50% RH. BAM measurements on the other hand are performed in ambient conditions but in order to prevent water condensing on the filter tape, the inlet tube of BAM monitors is typically heated until the moisture content of the sampled air reduced to 35% or below a specified limit, which vary and depend on the different site locations and meteorological conditions (Gobeli, 2008). These differences in sampling/measurement conditions between the BAM and the GM method can significantly affect quantitative agreement between the two methods.

In the present study we report on systematic PM_{2.5} measurements performed at a suburban site in Athens, Greece, during the period 2009-2012, using BAM Thermo ESM Andersen FH62I-R monitors and the Gravimetric Reference method according to the EN12341 Standard. The effect of factors such as the meteorological conditions and the type of filter material used for sampling was investigated. Our analysis focuses more on PM_{2.5} observations because they have not been studied so extensively as PM₁₀ measurements, and in addition they exhibit increased health risks in relation to coarse particles (Kampa and Castanas, 2008). It should be noted that given the documented differences in the chemical composition of coarse and fine airborne particles in the Mediterranean area (Lazaridis et al., 2005, 2006), the comparability of BAM and GM data can differ significantly for these two particle size fractions.

5.3 Methodology

5.3.1 The study area

PM measurements by GM and BAM methods were performed from January 2009 to December 2012 at two co-located monitoring stations in the suburban area of Agia Paraskevi in Athens, Greece. The reference GM measurements were conducted at the DEM station (N37°59'42''.00; E23°48'57''.60) of the National Center for Scientific Research (NCSR) “Demokritos”, which is part of the Global Atmosphere Watch

(GAW) and ACTRIS networks. The BAM measurements were performed at a National Monitoring Network (NMN) station, operated by the Hellenic Ministry of Environment, Energy & Climate Change (N37°59'42''.39; E23°49'09''.90) also situated inside the NCSR “Demokritos” campus, at a distance of 315 m from DEM station. The NCSR “Demokritos” campus is located in the north-east of the city of Athens, at the foothills of Hymettus Mountain and at an altitude of 270 m above sea level. The site is characterized by rich vegetation of pine trees. Both stations have a distance of approximately 400 m from the Hymettus Peripheral road and 1 km from a regular traffic avenue (Fig. 5.1). The background nature of this suburban area ensures that parallel measurements were conducted under the same meteorological conditions and were influenced from the same sources. The uncertainty introduced to the data by the variability in concentrations due to the small distance between the two sites can be therefore considered insignificant. The area exhibits low PM concentrations (Triantafyllou and Biskos, 2012; MinEnv, 2013; Eleftheriadis et al., 2014; Kostenidou et al., 2015) and is representative of suburban background conditions.



Figure 5.1: Map showing the location of the monitoring stations operated by NCSR “Demokritos” (DEM Station) and the National Monitoring Network (NMN Station) at the suburban area of Agia Paraskevi in Athens, Greece.

5.3.2 Measurements and Methods

Two BAM instruments (Thermo ESM Andersen FH62I-R) were used for the monitoring of PM₁₀ and PM_{2.5} concentrations. The instruments utilize the radiometric principle of beta attenuation by a 2-beam compensation method. Particles are collected at a flow rate of 1 m³ h⁻¹ on a glass-fiber filter tape and exposed to a low level (50 mCi) beta radiation emitted by an ⁸⁵Kr source. The radiation attenuated by the particle loadings on the filter tape is continuously monitored and converted to PM mass concentrations (Baron and Willeke, 2001). The accumulated particle mass is also monitored. The concentration range of the BAM monitors is set in the range 0–1 × 10³ μg m⁻³. Measurements at the Ministry of Environment stations employed for this study, were obtained by BAM monitors equipped with a heated inlet maintained at 28 ± 2 °C.

PM₁₀ and PM_{2.5} GM measurements were performed using custom-made low-volume reference gravimetric samplers. Three types of filters were used throughout the measurement period: teflon, quartz and glass fiber. Filters were weighed before and after sampling by a microbalance (Sartorius Model BP 211 D) of 0.01 mg accuracy. Prior to weighing, the filters were conditioned at 20±1 °C and 50±5% RH for 48 h, according to the EN12341 (1998) guidelines. PM concentrations generally corresponded to 24-h sampling, but in some cases we used longer sampling periods of up to 72 h.

Meteorological conditions (i.e., temperature, RH, as well as wind speed and direction) were monitored throughout the measurement period. Back-trajectory analysis by HYSPLIT model (Draxler, and Rolph, 2013) was also used in order to investigate the effect of the origin of air masses arriving at the stations. The near real-time concentrations measured by the BAM monitors were averaged based on the duration of the GM measurements, and classified in two main groups depending on the sampling period. The first group included measurements conducted during the cold period (i.e., from 16 October to 15 April) and the second during the warm period (i.e., from 16 April to 15 October).

5.4 Results and discussion

5.4.1 PM_{2.5} measurements

5.4.1.1 Concentration levels

PM_{2.5} concentrations measured by the GM and BAM methods (referred to as the GM PM_{2.5} and BAM PM_{2.5} measurements, respectively, from this point onwards) are presented in Fig. 5.2. In general, the two data sets exhibited similar temporal variation. The measured PM_{2.5} concentration levels ranged from 2 to 82 $\mu\text{g m}^{-3}$ for the GM method, and from 5 to 52 $\mu\text{g m}^{-3}$ for the BAM method. Two of the three highest concentrations ($> 50 \mu\text{g m}^{-3}$) measured by the GM method corresponded to Sahara dust long range transport episodes. BAM measurements were not available for these days.

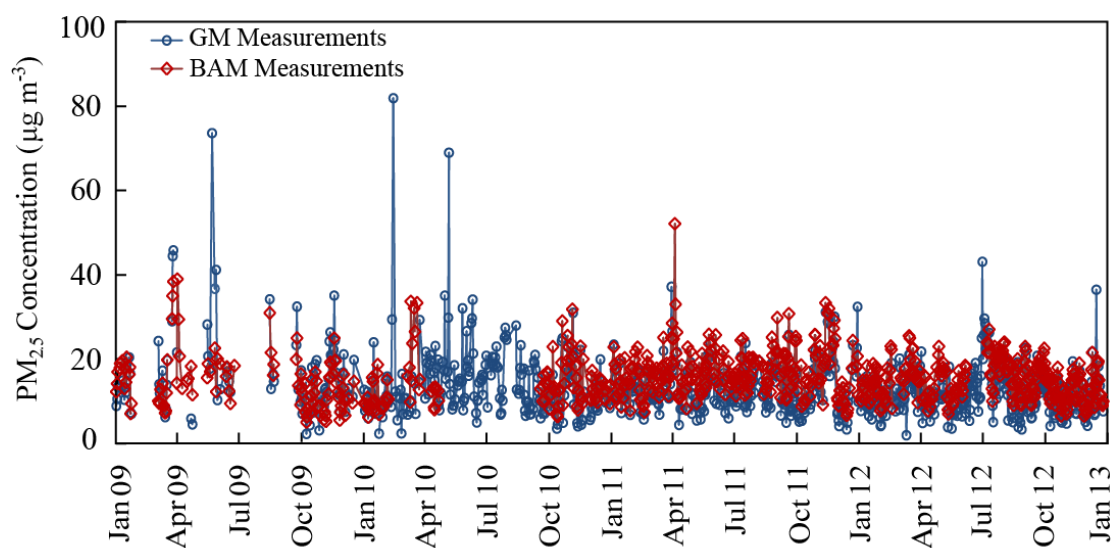


Figure 5.2: Time series of PM_{2.5} mass concentrations measured by gravimetric (blue circles) and beta attenuation (red diamonds) methods at Agia Paraskevi from 2009 to 2012.

The mean PM concentrations measured by the GM and BAM methods for each year are shown in Table 5.1. The BAM PM_{2.5}/GM PM_{2.5} concentration ratio for the entire study period indicated that the BAM levels were on average approximately 30% higher than the respective GM values (ANOVA, p -value < 0.05). This overestimation is more pronounced during the warm period. The BAM PM_{2.5} to GM

PM_{2.5} relationship exhibited significant day-to-day variability, suggesting that various factors may affect the measured concentration levels.

Table 5.1: Descriptive statistics for the GM PM_{2.5} and BAM PM_{2.5} concentrations measured at Agia Paraskevi from 2009 to 2012.

		GM PM _{2.5}		BAM PM _{2.5}		BAM PM _{2.5} / GM PM _{2.5}
	Year	Number of samples (N)	Mean ± St. Deviation (µg m ⁻³)	Number of samples (N)	Mean ± St. Deviation (µg m ⁻³)	Mean ± St. Deviation
Entire Period	2009	95	16.5 ± 10.5	102	14.7 ± 6.7	1.02 ± 0.47
	2010	212	14.6 ± 9.2	103	14.1 ± 6.0	1.25 ± 0.46
	2011	254	13.0 ± 5.3	255	17.0 ± 5.6	1.36 ± 0.32
	2012	324	12.4 ± 5.5	285	14.7 ± 4.3	1.33 ± 0.37
	2009-2012	885	13.5 ± 7.3	745	15.4 ± 5.5	1.29 ± 0.40
Warm Period	2009	29	18.6 ± 14.4	31	15.8 ± 5.5	1.19 ± 0.63
	2010	116	16.0 ± 8.9	23	12.9 ± 3.3	1.15 ± 0.44
	2011	132	12.4 ± 4.4	132	17.1 ± 4.3	1.45 ± 0.37
	2012	163	13.2 ± 6.0	136	15.9 ± 4.4	1.42 ± 0.47
	2009-2012	412	14.0 ± 7.5	292	16.2 ± 4.5	1.40 ± 0.46
Cold Period	2009	66	15.5 ± 8.1	71	14.3 ± 7.2	0.95 ± 0.36
	2010	96	12.9 ± 9.4	80	14.5 ± 6.6	1.28 ± 0.47
	2011	122	13.8 ± 6.1	123	17.0 ± 6.8	1.27 ± 0.23
	2012	161	11.5 ± 4.8	149	13.6 ± 4.0	1.24 ± 0.23
	2009-2012	445	13.0 ± 7.0	423	14.9 ± 6.1	1.21 ± 0.33

5.4.1.2 Correlation between BAM and GM measurements

Good correlation was observed between BAM PM_{2.5} and GM PM_{2.5}, as depicted in Fig. 5.3a (Pearson coefficient was 0.79 for the entire period, and 0.72 and 0.84 for the

warm and cold seasons, respectively). Best linear fits were calculated for all data and each period separately: $BAM = 0.71 \cdot GM + 6.2$ (entire period); $BAM = 0.62 \cdot GM + 8.3$ (warm period); $BAM = 0.77 \cdot GM + 4.7$ (cold period). Although the trends in the warm- and cold-period data are similar, the differences in the fitted equations highlight the need for seasonal calibration of BAM data through reference gravimetric measurements.

Correlation between BAM $PM_{2.5}$ and GM $PM_{2.5}$ data was also examined depending on the filter type used in the GM measurements (Fig. 5.3(b)-(d)). A slightly better correlation was observed when glass fiber filters were used for the GM samples (estimated Pearson correlation coefficients were 0.82 and 0.80 for the Teflon and the quartz filters, respectively). This agreement was anticipated, considering that the BAM monitor employs a glass fiber filter tape. The equation that fitted the data best in the case of glass fiber filters presented the highest slope ($BAM = 0.79 \cdot GM + 5.3$). The corresponding best linear fits in the case of Teflon and quartz filters were $BAM = 0.75 \cdot GM + 6.1$ and $BAM = 0.64 \cdot GM + 4.5$, respectively.

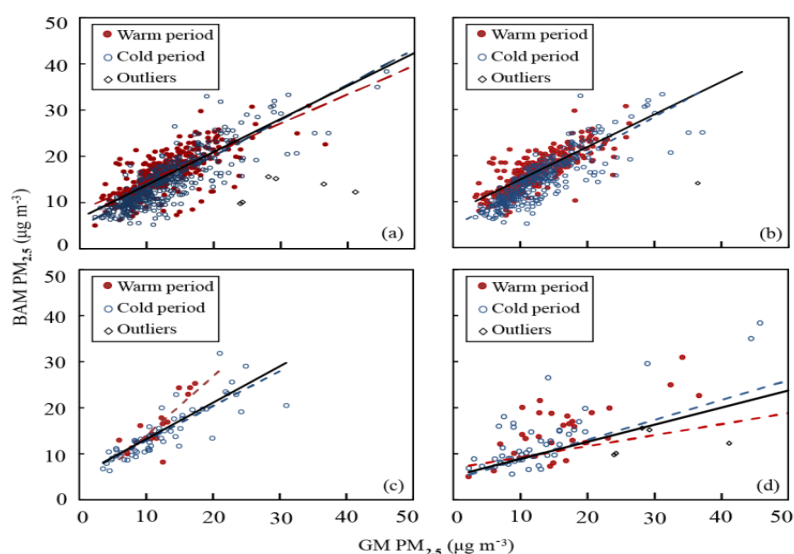


Figure 5.3: Linear correlation between BAM $PM_{2.5}$ and GM $PM_{2.5}$ measurements for (a) all the data, and when (b) Teflon, (c) Glass fiber and (d) Quartz were used in the GM measurements. Red and blue circles correspond to measurements during the warm and the cold period, respectively. Outliers are depicted by diamond-shaped data points. The black line represents the linear fit for all data, while red and blue dashed lines are the fitted equations to the warm and cold season data, respectively.

For all filter types, better correlations were obtained for the cold rather than the warm period. The largest difference between cold and warm period correlation

relationships was observed for glass fiber samples, followed by quartz samples. These discrepancies may be attributed to the different water uptake of each filter type. Glass fiber filters, which are used as standard filter material in BAM measurements, are moisture sensitive.

Quartz filters on the other hand present lower water uptake, whereas Teflon filters are generally hydrophobic (Baron and Willeke, 2001). The results indicate that the selection of the filter substrate may influence the measured PM levels and that filter material should be taken into account when calibrating BAM with GM measurements.

The relation between BAM PM_{2.5} and GM PM_{2.5} measurements was also examined in relation to the origin of air masses arriving at the site, which is an indicator of different types of aerosols (with respect to chemical composition and size distribution). Sahara dust long-range transport events were identified during only 4% of the measurement days and did not affect the relationships between BAM PM and GM PM measurements. The rest of the measurements were separated into three groups depending on the conditions: (i) days of calm conditions, representative of local aerosol (with more than 50% of hourly wind speed values below 1 ms⁻¹), (ii) days with south/west wind directions representative of polluted aerosols coming from the city center, and (iii) days with north/east wind directions representative of “cleaner” aerosols coming from the sea. No change in the BAM/GM relationships was observed, suggesting that the linear regression equations obtained for warm and cold period are representative for the investigated site, and may be used for calibration of BAM monitors.

5.4.1.3 Effect of meteorological and sampling conditions

To further investigate whether the seasonal variability in the differences between BAM and GM measurements is attributed to water evaporation, we tried to estimate the water content of the samples. This depends on the ability of the particles to hold water under given RH conditions, i.e. their hygroscopicity (Colbeck, 2008; Bezantakos et al., 2013), which mainly depends on their chemical composition: inorganic particles are more hygroscopic whereas soot and organic particles can take up significantly lower amounts of water. In addition, the material of the sampling

medium may also take up water during sampling. Glass fiber and quartz filters have a slightly alkaline surface and are therefore affected by humidity, while membrane filters such as Teflon exhibit lower moisture absorption. The amount of liquid water in the atmosphere that can be absorbed by the particles and the filters is:

$$e = RH \cdot e_s \quad (5.1)$$

where RH is the mean relative humidity (%) in the atmosphere during sampling, and e_s the maximum water vapor pressure (mbar). For a given temperature, T (K), e_s can be estimated by the modified empirical Magnus – Tetens relation (Salby, 1996):

$$\log e_s = 9.4041 - \frac{2354}{T} \quad (5.2)$$

The estimated water vapor pressure can be normalized by the GM $PM_{2.5}$ measured concentration, and the resulting value represents the potentially available water for interaction with each unit of sampled mass.

The monthly averaged BAM $PM_{2.5}$ to GM $PM_{2.5}$ concentration ratio, along with the respective temperature and relative humidity conditions, is shown in Fig. 5.4. The BAM $PM_{2.5}$ /GM $PM_{2.5}$ ratio was consistently higher than 1.3 when the RH decreased below 60% and the temperature was higher than 20 °C. The lowest values of the BAM $PM_{2.5}$ /GM $PM_{2.5}$ concentration ratio (i.e., around 1.2) were observed during the

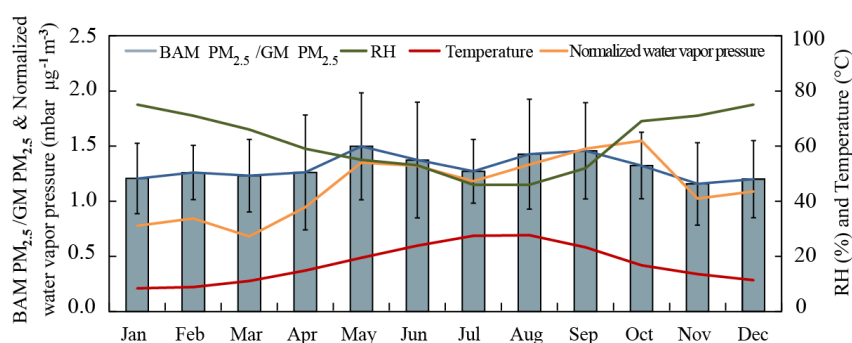


Figure 5.4: Variation of the monthly averaged BAM $PM_{2.5}$ to GM $PM_{2.5}$ concentration ratio (bars and blue line) and of the corresponding temperature (red line), relative humidity (green line) and the water vapor pressure normalized by $PM_{2.5}$ concentrations (orange line).

cold period when ambient temperature was around or below 10 °C and RH was above 70%. The lowest values of the BAM $PM_{2.5}$ /GM $PM_{2.5}$ concentration ratio (i.e., around 1.2) were observed during the cold period when ambient temperature was around or

below 10 °C and RH was above 70%. Given that a heating inlet was employed at the BAM monitor (in order to bring the sample to a standard temperature of 28 °C) and not in the GM measurements, the lower values of the ratio during the cold period may be related to the evaporation of water and loss of volatile aerosol compounds during heating of the sampled air. During the warm period, volatile aerosol compounds are not present when sample air enters the inlet due to high ambient air temperatures. As shown in Fig. 5.4, the normalized water vapor pressure exhibits a seasonal variation that is very similar with that of the BAM PM_{2.5}/GM PM_{2.5} ratio. This similarity indicates that the samples' water content strongly affects the discrepancies observed between BAM and GM measurements.

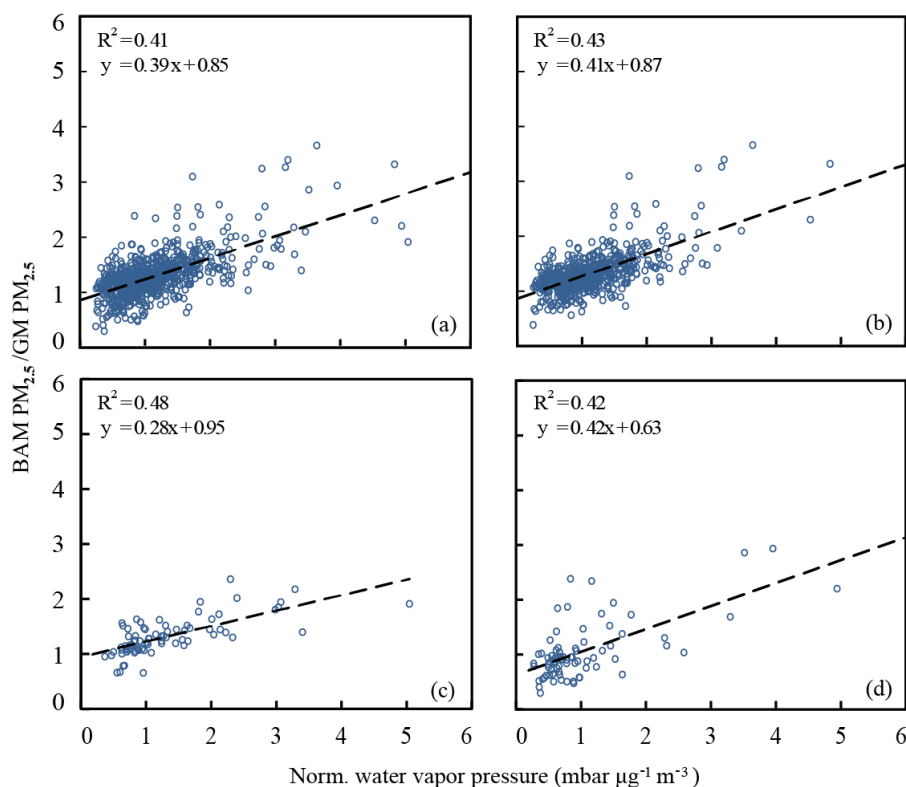


Figure 5.5: Correlation between the BAM PM_{2.5}/GM PM_{2.5} ratio and the normalized water vapor pressure, for (a) the entire data set and separately when (b) Teflon, (c) glass fiber, and (d) quartz filters were used in the GM measurements. The dashed line show best fit regression models.

The relationship between the BAM PM_{2.5}/GM PM_{2.5} ratio and the normalized water vapor pressure, for the entire data set and for the measurements using the different filter types, is shown in Fig. 5.5. BAM to GM concentration ratios exhibited an

increasing trend with normalized water vapor pressure in all cases. It is interesting to note that the curve fitted through the measurements is steeper when Teflon filters (which are highly hydrophobic) are used in the GM measurements (Fig. 5.5b).

In order to evaluate the other issues of possible gain or loss of water and/or other species, further analysis of the parameters involved was conducted. As already shown, temperature or RH alone cannot explain the discrepancy between BAM and GM measurements, as well as the normalized available water content does (Fig. 5.4). Temperature is a critical parameter for semi volatile species like ammonium nitrate as expected from basic thermodynamic considerations (Dassios and Pandis, 1999). Pandolfi et al. (2012) observed that temperature is the only parameter showing a relatively high correlation with NO_3 . The temperature range between 15 and 22°C has been also shown to play a role in the ambient levels of the semi volatile species according to model calculations and ambient data for Riverside CA, US (Aw and Kleeman, 2003). Although these effects are difficult to quantify, conditioning of filters and PM samples at 20°C and 50% RH sets some reference conditions at which the discrepancy between BAM and GM measurements can be evaluated, thereby providing a systematic way of its characterization.

Useful information about the structure of the variability of the BAM to GM ratio can be derived when we examine this ratio against RH over three temperature ranges 0-10°C, 11-22°C and greater than 22°C. Scatter plots of this exercise are shown in Fig. 5.6.

Despite the high scatter we observe that the linear fit lines display no significant trend of the discrepancy at high and low temperatures and that the mean value across the whole of the RH range is similar to the ratios shown in Table 5.1, with BAM measurements constantly overestimating the GM $\text{PM}_{2.5}$ concentration. When the mean temperature is within the range 11-22°C we have a significant number of data where BAM measurements underestimate the $\text{PM}_{2.5}$ concentration at high RH and a linear trend becomes significant ($p < 0.01$). This trend appearing for the temperature range studied can be attributed to the loss of nitrate. This assumption is supported by the fact that ammonium nitrate salts are found in the urban atmosphere in significant concentrations. Other semi volatile species can also cause an equivalent discrepancy under these conditions (see discussion below).

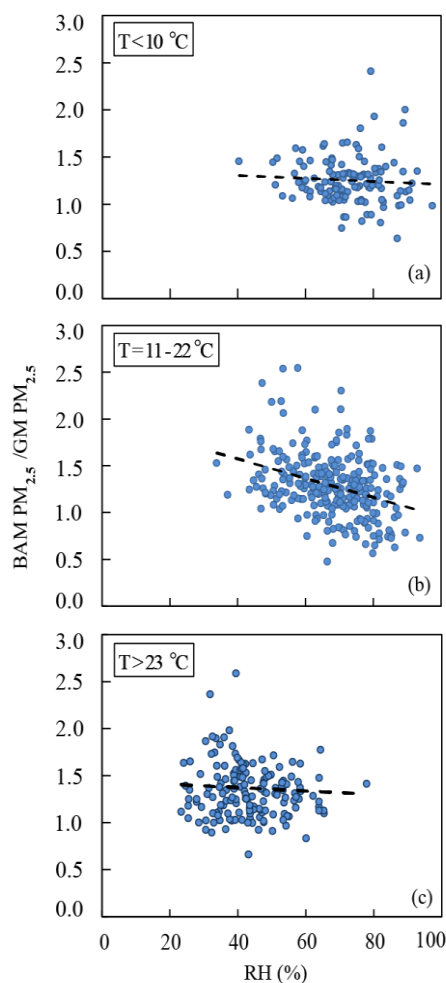


Figure 5.6: Correlation between the BAM $PM_{2.5}/GM PM_{2.5}$ ratio and the relative humidity when Teflon filters were used in the GM measurements and the ambient temperature was (a) less than $10^{\circ}C$, (b) between 11 and $22^{\circ}C$, and (c) higher than $22^{\circ}C$. The dashed line show best-fit regression models.

The dataset for the Teflon measurements shown in Fig. 5.7 is evaluated in the same way against the normalized water content over the same temperature ranges. The temperature range between 11 and $22^{\circ}C$ does not display a distinct behavior as that in the measurements shown in Fig. 5.6. The available water does not seem to depend on RH for all three temperature ranges, while the overestimation of $PM_{2.5}$ concentration by the BAM measurements is always correlated with liquid water, with the correlation coefficient becoming stronger for higher temperatures. This feature indicates that BAM systems retain or accumulate liquid water due to condensation on the measured sample, while conditioning of filters during GM measurements removes liquid water more efficiently. On the other hand, the difference in the water content does not

explain alone the dependence of the BAM/GM ratio to RH as shown in Fig. 5.6b. It is reasonable to explore the possibility of evaporation/condensation of other semi volatile species such as organics and ammonium nitrate, which may be in transition from particulate to gaseous phase at these temperature and RH ranges. Especially for ammonium nitrate, the particle phase is favored at high RH and lower temperatures.

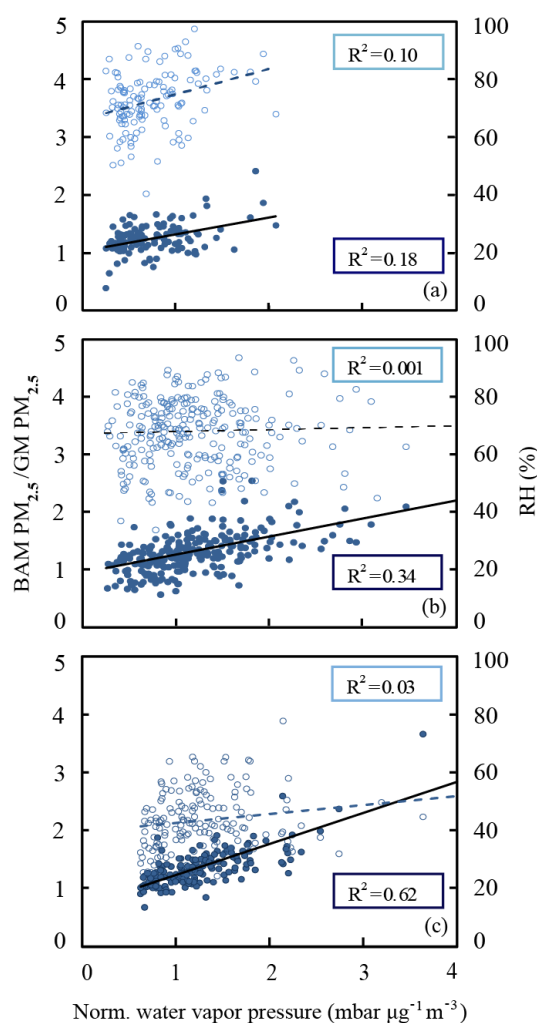


Figure 5.7: Correlation between the normalized water vapor pressure and the BAM PM_{2.5}/GM PM_{2.5} ratio (blue solid circles), or the relative humidity (blue open circles), when the ambient temperature was (a) less than 10 °C, (b) between 11 and 22°C, and (c) higher than 22°C. The black solid line and the blue dashed line represent best linear fit for the correlations between the normalized water vapor pressure and the BAM PM_{2.5}/GM PM_{2.5} ratio and the relative humidity, respectively. These correlations include the PM_{2.5} samples collected on Teflon filters.

During our study period, estimated ammonium nitrate levels inferred from earlier measurements at the same site (Eleftheriadis et al., 2014 reporting total NH₄ and NO₃

to be on average $1.3 \mu\text{g m}^{-3}$ and $1.4 \mu\text{g m}^{-3}$, respectively) are expected in general to be below $2 \mu\text{g m}^{-3}$. This in turn is a 10-15% of the $\text{PM}_{2.5}$ mass concentration. During periods when maximum ammonium nitrate concentrations are expected in the particulate phase due to high RH (Dassios and Pandis, 1999), dissociation due to BAM inlet heating and retention in the GM filter at ambient and conditioning temperatures $< 20^\circ\text{C}$ can explain the lower BAM/GM ratios observed in Fig. 5.6b. The temperature difference between the heated inlet (28°C) and the equilibrium temperature for filters during gravimetric analysis can induce an increased evaporation of NH_4NO_3 as well as aerosol particle water during BAM measurements while GM measurements remain unaffected.

The analysis presented here for PTFE filters could not be repeated for an equivalent number of data for the GF and Quartz filter due to a smaller number of samples on these filters. The data available display either similar behaviour with PTFE filters or absence of correlation.

Based on the above observations, it is proposed that when equivalence tests are conducted the results are checked against the normalized water content in order to remove seasonal discrepancies external to the conditioning of the aerosol samples. A method of drying the incoming aerosol before a BAM system instead of heating would also facilitate towards reducing the effect of water vapor condensation and loss of aerosol due to heating.

5.5 PM_{10} measurements

A less extensive data set with BAM and GM PM_{10} concentration measurements was also obtained during the studied period. All GM PM_{10} measurements were conducted with Teflon filters. Descriptive statistics of this data set are provided in Table 5.2. Mean PM_{10} concentrations measured by the two methods exhibited an average difference of 10% for the entire period (ANOVA, p-value = 0.05). Very good correlation was observed between BAM PM_{10} and GM PM_{10} mass concentration measurements (Fig. 5.8). Different linear regression equations were calculated for the warm and cold season measurements, highlighting the seasonality of BAM to GM relationship.

Table 5.2: Descriptive statistics of PM₁₀ concentrations measured at Agia Paraskevi by beta-attenuation (BAM) and gravimetric method (GM) for the years 2011 and 2012.

Year	GM PM ₁₀		BAM PM ₁₀		BAM PM ₁₀ / GM PM ₁₀
	Number of samples (N)	Mean ± St. Deviation (µg m ⁻³)	Number of samples (N)	Mean ± St. Deviation (µg m ⁻³)	Mean ± St. Deviation (µg m ⁻³)
2011-2012	95	23.4 ± 14.9	67	25.1 ± 6.5	1.10 ± 0.33
2011 (warm period)	48	24.4 ± 7.5	48	24.9 ± 6.3	1.08 ± 0.38
2012 (cold period)	47	22.4 ± 19.8	19	25.7 ± 7.1	1.18 ± 0.15

The obtained results are comparable to those reported by Lazaridis et al. (2008) who have also observed a slight over prediction of the PM₁₀ concentrations measured by a BAM monitor during measurements on the island of Crete, Greece (mean BAM/GM ratio around 1.2). While BAM and GM methods for PM₁₀ measurements are in good agreement, the application of calibration equations, derived through parallel gravimetric measurements at both cold and warm season, can certainly enhance the reliability of the measurements obtained by BAM monitors.

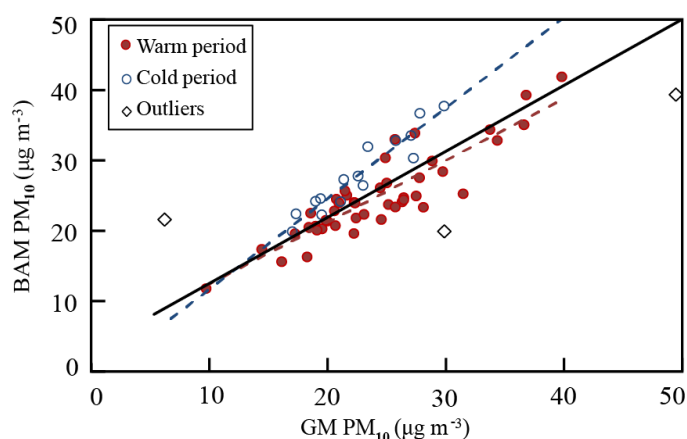


Figure 5.8: Correlation between BAM PM₁₀ and GM PM₁₀ measurements. Red and blue circles correspond to measurements during the warm and the cold period, respectively. Outliers are depicted by the black diamonds. The solid black line ($BAM = 0.77 \cdot GM + 4.1$, $R^2 = 0.72$) represents the best linear fit for the entire data set. The red dashed line ($BAM = 0.88 \cdot GM + 3.6$, $R^2 = 0.80$) and the blue dashed line ($BAM = 1.50 \cdot GM - 6.7$, $R^2 = 0.88$) represent best linear fits for the warm and cold period, respectively.

5.6 Conclusions

This work presents a comparison of PM_{2.5} and PM₁₀ concentration measurements performed by a single type of beta attenuation monitors (Thermo ESM Andersen FH62I-R monitors) and reference gravimetric samplers at a suburban site in Athens, Greece, during a period of four years. Given that the majority of previous similar studies used PM₁₀ measurements, here we focus on PM_{2.5} measurements that have greater human health relevance. BAM and GM measurements showed in general similar temporal variation, for both PM₁₀ and PM_{2.5} fractions, with the former being systematically higher. This difference was more pronounced for PM_{2.5} (on average 30%) compared to the PM₁₀ (on average 10%) measurements. The correlation between BAM and GM measurements was higher during the cold period for both size fractions, with Pearson coefficient being 0.84 for PM_{2.5} and 0.95 for PM₁₀ in the cold period and 0.72 for PM_{2.5} and 0.90 for PM₁₀ in the warm period.

The seasonality in the differences between BAM and GM measurements could be largely explained by a strong effect of temperature and humidity. The BAM PM_{2.5}/GM PM_{2.5} ratio increased with atmospheric water vapor pressure, indicating that the water content of the collected samples has a strong effect on the observed discrepancy between BAM and GM measurements. The filter material used in the GM measurements was identified as another important factor for this discrepancy. The strongest correlation between BAM PM_{2.5} and GM PM_{2.5} measurements and the one having a fitted line with a slope closest to unity were obtained when GM samples were collected on filters made of glass fiber, which is the same material used in the filter tapes in the BAM measurements. The highly hydrophobic Teflon filters were less affected by moisture in comparison to quartz and glass fiber filters, yielding larger discrepancies between BAM and GM measurements when the atmospheric water vapor pressure increased.

Our results show that differences between BAM and GM measurements can vary significantly when determining PM₁₀ and PM_{2.5} concentrations, and that relationship between the two observation methods ought to be determined for each site and season. The measurements also highlight the importance of reporting the meteorological conditions and operational characteristics (i.e., filter materials and sampling temperatures of the BAM monitor inlet and unit) along with the measurements, since

they can strongly affect the results. Considering that inter-comparisons are scarce for the PM_{2.5} fraction, additional measurements, in different climatic regions, are required to obtain a better overall picture for the effects of liquid water condensation and loss of semi volatile species.

Chapter 6

Summary and Future research

6.1 Summary and conclusions

The main goal of this study has been to examine the quantitative (concentration and size) and qualitative (chemical composition) characteristics of the atmospheric aerosols in urban and suburban-background sites in the North Aegean Sea region and to compare them with those of other regions. Furthermore, the discrepancies between two different measurement techniques for two fractions of Particulate Matter (PM; PM₁₀ and PM_{2.5}) were investigated.

Chapter 2 analyzed the temporal variation of PM₁₀ mass concentrations at five urban and ten suburban areas in the two major cities in Greece, namely Athens and Thessaloniki, from 2001 to 2010. In both cities, all urban stations exceeded the EU annual and 24-h PM₁₀ concentration limits (40 and 50 $\mu\text{g m}^{-3}$, respectively) during the entire period that we investigated, having annual average values of 50.1 $\mu\text{g m}^{-3}$ in Athens and 57.7 $\mu\text{g m}^{-3}$ in Thessaloniki. The urban stations in Thessaloniki exhibited higher PM₁₀ concentrations, compared to those in Athens, which can be attributed to the more intensive industrial activity in the city.

With the exception of two stations in Athens, and another two in Thessaloniki, all suburban stations were lower than the EU PM₁₀ limits. The rest of the stations that exhibited higher than EU PM₁₀ limit concentrations are strongly affected by nearby PM sources such as high traffic and agricultural or industrial activity.

An interesting observation was that the annual average PM₁₀ concentrations exhibited an overall decreasing trend in both cities during the entire period investigated. Exceptions to this observation were observed for two stations in Athens and one in Thessaloniki that did not exhibit any statistically significant trend, most likely due to

their proximity to constant PM sources. The seasonal variation was shown to be different between urban and suburban stations in both Athens and Thessaloniki. The PM₁₀ concentrations at the urban stations in Athens were higher during autumn and winter and lower during summer (having values of 46.2, 46 and 42.8 $\mu\text{g m}^{-3}$, respectively), while the highest values at the suburban stations were observed during the spring and the lowest during the winter (having values of 37.7 and 29.8 $\mu\text{g m}^{-3}$, respectively). A possible explanation for this difference is that the urban stations are influenced to a greater extent by domestic heating compared to other sources of PM₁₀ (e.g., traffic). In Thessaloniki, with the exception of one station that does not exhibit any seasonality, seasonal variations were found to be similar both at the urban and the suburban stations, exhibiting highest concentrations during autumn and lowest concentrations in summer.

Chapter 3 provides measurements of the properties of atmospheric particles in the remote environment of the North Aegean Sea (NAS) during the summer period when the meteorological conditions were representative of the Etesian conditions, with the aim to improve understanding on how cross-border air pollution transport affects local air quality.

During these air pollution transportation episodes in the NAS, the particle size distributions exhibited a peak shift towards smaller diameters (i.e., from 100 to ca. 20 nm), while the number concentrations (with a mean value of 2.2×10^3 particles cm^{-3}) increased substantially. The nucleation-mode particles observed during all the pollution transport episodes had starting sizes from ca. 15 to 17 nm and grew with a rate of ca. 9.0 nm h^{-1} , providing a first indication that they have been formed in highly polluted areas and their size was increased during transportation to the NAS. In addition, the estimated concentrations of sulfuric acid during the episodes were in the order of 10^5 molecules cm^{-3} , suggesting that it plays an important role in the formation and growth of the observed nanoparticles. The correlation between $N_{d < 25 \text{ nm}}$ and $[\text{H}_2\text{SO}_4]$ was moderate but became strong ($R^2 = 0.71$) when a time lag of 7 ± 1 h was used between the two data sets.

The fraction of sulfates, nitrates, and ammonium on PM_{1.0} samples exhibited an increase of ca. 60%, whereas the OC/EC ratio was systematically higher during the

particle transport days compared to the rest of the days. In addition, a strong correlation ($R^2 = 0.67$) was observed between OC and EC, suggesting that they have common combustion sources. These observations provide an additional indication that the particles observed in the region of NAS have an urban and/or industrial origin, as also confirmed by analysis of back-trajectories and omega fields.

Analysis in **chapter 4** relates the quantitative (concentration and size) and qualitative (chemical composition) characteristics of atmospheric aerosols at an urban site of a representative small insular coastal city in the NAS, namely the city of Mytilene, during summer and winter. Mean $PM_{2.0}$ and $PM_{1.0}$ concentrations at the city centre were respectively 26 and 21 $\mu\text{g m}^{-3}$ during winter and 21 and 15 $\mu\text{g m}^{-3}$ during summer, and were considerably lower compared to corresponding values recorded in large cities in the region. The measured average concentrations of TSP, $PM_{2.0}$ and $PM_{1.0}$ at SSM were higher by ca. 26-36% and by ca. 44% for number concentrations in winter compared to those in summer, due to the additional emissions from domestic heating and the weaker atmospheric dilution. Higher particulate concentrations were recorded at the site located at the port of the city only in summer due to enhanced port activities, and not at the site located at the city centre as the prevailing wind directions did not favour the transport of air masses to the direction of city centre.

The elemental composition measurements also showed that natural sources contribute sea-salt and resuspended soil in the TSP samples at both sites and seasons. Re-suspension of polluted soil particles is more significant in summer, as shown by the higher concentrations of Ca, Mg, Fe, and Ti, due to the drier conditions. Non-exhaust traffic emission sources were also found to be an important contributor, as indicated by the good correlations ($R^2 = 0.40 - 0.91$) between crustal and traffic-related elements (i.e., Zn, Cr, Cu, and Mn). Anthropogenic sources such as wood and fuel combustion (i.e. residential heating and shipping emissions) contributed to the smaller PM fractions during both periods, as indicated by high concentrations of K and S. These heating sources are also reflected by a more pronounced increase of number concentrations in winter than in summer. In addition to local sources, the contribution of long-range transported polluted air masses to the air quality of Mytilene was observed mostly in summer by the higher concentrations and the strong relationship among some crustal and anthropogenic elements (i.e., K, Ca, Ti, Mg, Fe, As, S) during these events.

Finally, **chapter 5** investigates the comparability and the effect of factors such as the meteorological conditions and the type of filter material of gravimetric (GM) and beta attenuation (BAM) measurements for $PM_{2.5}$ and PM_{10} at a suburban site in Athens, Greece, during a period of four years. Given that the majority of previous similar studies used PM_{10} measurements, here we focus on $PM_{2.5}$ measurements that have higher human health relevance. This supplementary study provides information about the discrepancies of PM sampling techniques in a suburban site in the Eastern Mediterranean area that helps in better understanding of continuous PM measurements.

BAM and GM measurements showed in general similar temporal variation, for both PM_{10} and $PM_{2.5}$ fractions, with the former being systematically higher. This difference was more pronounced for $PM_{2.5}$ (on average 30%) compared to PM_{10} (on average 10%) measurements. The correlation between BAM and GM measurements was higher during the cold period for both size fractions, with Pearson coefficients being 0.84 for $PM_{2.5}$ and 0.95 for PM_{10} in the cold period and 0.72 for $PM_{2.5}$ and 0.90 for PM_{10} in the warm period.

The seasonality in the differences between BAM and GM measurements could be largely explained by a strong effect of temperature and humidity. The BAM $PM_{2.5}$ /GM $PM_{2.5}$ ratio increased with atmospheric water vapor pressure, indicating that the water content of the collected samples has a strong effect on the observed discrepancy between BAM and GM measurements. The filter material used in the GM measurements was identified as another important factor for this discrepancy. The strongest correlation between BAM $PM_{2.5}$ and GM $PM_{2.5}$ measurements, and the one having a fitted line with a slope closest to unity, were obtained when GM samples were collected on filters made of glass fiber, which is the same material used in the filter tapes in the BAM measurements. The highly hydrophobic Teflon filters were less affected by moisture in comparison to quartz and glass fiber filters, yielding larger discrepancies between BAM and GM measurements when the atmospheric water vapor pressure increased.

The results of this study show that differences between BAM and GM measurements can vary significantly when determining PM_{10} and $PM_{2.5}$ concentrations, and that relationships between the two observation methods ought to be determined for each site and season. The measurements also highlight the importance of reporting the meteorological conditions and operational characteristics (i.e., filter materials and sampling temperatures of the BAM monitor inlet and unit) along with the measurements, since they can strongly affect the results. Considering that inter-comparisons are scarce for the $PM_{2.5}$ fraction, additional measurements, in different climatic regions, are required to obtain a better overall picture for the effects of liquid water condensation and loss of semi volatile species.

6.2 Future research

This study provides information on the air quality in urban and remote sites in the region of North Aegean Sea (NAS). Based on the results of this study, this section provides further research directions.

The region of NAS is characterized by particular synoptic meteorological conditions that favor the transportation of air masses from distant sources. Apart from fixed distance sources, shipping emissions have an important impact on sulphur deposition in PM concentrations mainly in the warm period. This observation lead to further study and control of sulphur and nitrogen compounds in particulate matter as well as of sulphur dioxide (SO_2) and nitrogen oxides (NO_x) emissions from shipping activities as have been set by the current International Maritime Organization (IMO; MEPC57, 2008) and the EU (European Directive 2012/33/EU) regulatory requirements.

This thesis is primarily reported measurements of aerosol particles. Simultaneously measurements of particulate matter and gaseous pollutants can take place at a permanent monitoring station, in order to provide a comprehensive picture of ambient air quality in the main cities of NAS. The emissions of greenhouse gases are important but the combination of particles with gaseous pollutants may be more damaging in human health than the effects of gaseous pollutants. Further investigation of the contribution of particulate pollution during desert dust transport events is

needed to understand their impacts on human health and climate in the region of NAS, considering that these dust intrusions usually occur in spring (i.e., March, April, May).

The spatial variability of concentrations from various point sources (e.g. activities of the electric power plant, the airport) can be also evaluated in order to provide additional information about the local sources in the main cities of NAS. Spatial variation by the use of air pollution dispersion models is needed because these models can potentially expand ground monitoring networks due to their broad spatial coverage and give information of various emission sources.

References

Articles

- Aarnio, P., Martikainen, J., Hussein, T., Valkama, I., Vehkamäki, H., Sogacheva, L., Härkönen, J., Karppinen, A., Koskentalo, T., Kukkonen, J., Kulmala, M., 2008. Analysis and evaluation of selected PM₁₀ pollution episodes in the Helsinki Metropolitan Area in 2002. *Atmos. Environ., Fifth International Conference on Urban Air Quality* 42, 3992–4005.
- Alastuey, A., Querol, X., Castillo, S., Escudero, M., Avila, A., Cuevas, E., Torres, C., Romero, P.-M., Exposito, F., García, O., Pedro Diaz, J., Dingenen, R.V., Putaud, J.P., 2005. Characterisation of TSP and PM_{2.5} at Izaña and Sta. Cruz de Tenerife (Canary Islands, Spain) during a Saharan Dust Episode (July 2002). *Atmos. Environ.* 39, 4715–4728.
- Alyuz, U., Alp, K., 2014. Emission inventory of primary air pollutants in 2010 from industrial processes in Turkey. *Sci. Total Environ.* 488, 369–381.
- Anagnostopoulou, C., Zanis, P., Katragkou, E., Tegoulas, I., Tolika, K., 2014. Recent past and future patterns of the Etesian winds based on regional scale climate model simulations. *Clim. Dyn.* 42, 1819–1836.
- Apostolou, E.K., Yannitsaros, A.G., 1977. Atmospheric Pollen in the Area of Athens. *Allergy* 32, 109–117.
- Aranda, A., Díaz-de-Mera, Y., Notario, A., Rodríguez, D., Rodríguez, A., 2015. Fine and ultrafine particles in small cities. A case study in the south of Europe. *Environ. Sci. Pollut. Res.* 22, 18477–18486.

- Argyropoulos, G., Samara, C., Voutsas, D., Kouras, A., Manoli, E., Voliotis, A., Tsakis, A., Chasapidis, L., Konstandopoulos, A., Eleftheriadis, K., 2016. Concentration levels and source apportionment of ultrafine particles in road microenvironments. *Atmos. Environ.* 129, 68–78.
- Aw, J., Kleeman, M.J., 2003. Evaluating the first-order effect of intraannual temperature variability on urban air pollution. *J. Geophys. Res. Atmospheres* 108, 4365.
- Bardouki, H., Liakakou, H., Economou, C., Sciare, J., Smolík, J., Ždímal, V., Eleftheriadis, K., Lazaridis, M., Dye, C., Mihalopoulos, N., 2003. Chemical composition of size-resolved atmospheric aerosols in the eastern Mediterranean during summer and winter. *Atmos. Environ.* 37, 195–208.
- Becagli, S., Sferlazzo, D.M., Pace, G., di Sarra, A., Bommarito, C., Calzolari, G., Ghedini, C., Lucarelli, F., Meloni, D., Monteleone, F., Severi, M., Traversi, R., Udisti, R., 2012. Evidence for heavy fuel oil combustion aerosols from chemical analyses at the island of Lampedusa: a possible large role of ships emissions in the Mediterranean. *Atmos Chem Phys* 12, 3479–3492.
- Bem, H., Gallorini, M., Rizzio, E., Krzemińska, M., 2003. Comparative studies on the concentrations of some elements in the urban air particulate matter in Lodz City of Poland and in Milan, Italy. *Environ. Int.* 29, 423–428.
- Bezantakos, S., Barmounis, K., Giamarelou, M., Bossioli, E., Tombrou, M., Mihalopoulos, N., Eleftheriadis, K., Kalogiros, J., D. Allan, J., Bacak, A., Percival, C.J., Coe, H., Biskos, G., 2013a. Chemical composition and hygroscopic properties of aerosol particles over the Aegean Sea. *Atmos Chem Phys* 13, 11595–11608.
- Birch, M.E., Cary, R.A., 1996. Elemental carbon-based method for occupational monitoring of particulate diesel exhaust: methodology and exposure issues. *Analyst* 121, 1183–1190.

- Birmili, W., Berresheim, H., Plass-Dülmer, C., Elste, T., Gilge, S., Wiedensohler, A., Uhrner, U., 2003. The Hohenpeissenberg aerosol formation experiment (HAFEX): a long-term study including size-resolved aerosol, H₂SO₄, OH, and monoterpenes measurements. *Atmos Chem Phys* 3, 361–376.
- Bougiatioti, A., Bezantakos, S., Stavroulas, I., Kalivitis, N., Kokkalis, P., Biskos, G., Mihalopoulos, N., Papayannis, A., Nenes, A., 2016. Biomass-burning impact on CCN number, hygroscopicity and cloud formation during summertime in the eastern Mediterranean. *Atmos Chem Phys* 16, 7389–7409.
- Bougiatioti, A., Fountoukis, C., Kalivitis, N., Pandis, S.N., Nenes, A., Mihalopoulos, N., 2009. Cloud condensation nuclei measurements in the marine boundary layer of the Eastern Mediterranean: CCN closure and droplet growth kinetics. *Atmos Chem Phys* 9, 7053–7066.
- Bougiatioti, A., Zampas, P., Koulouri, E., Antoniou, M., Theodosi, C., Kouvarakis, G., Saarikoski, S., Mäkelä, T., Hillamo, R., Mihalopoulos, N., 2013. Organic, elemental and water-soluble organic carbon in size segregated aerosols, in the marine boundary layer of the Eastern Mediterranean. *Atmos. Environ.* 64, 251–262.
- Bowen, H.J.M., 1979. *Environmental chemistry of the elements*. Academic Press, London; New York.
- Brown, A.S., Yardley, R.E., Quincey, P.G., Butterfield, D.M., 2006. Studies of the effect of humidity and other factors on some different filter materials used for gravimetric measurements of ambient particulate matter. *Atmos. Environ.* 40, 4670–4678.
- Calvo, A.I., Pont, V., Lioussé, C., Dupré, B., Mariscal, A., Zouiten, C., Gardrat, E., Castera, P., Lacaux, C.G., Castro, A., Fraile, R., 2008. Chemical composition of urban aerosols in Toulouse, France during CAPITOUL experiment. *Meteorol. Atmospheric Phys.* 102, 307–323.

- Cao, J.J., Lee, S.C., Chow, J.C., Watson, J.G., Ho, K.F., Zhang, R.J., Jin, Z.D., Shen, Z.X., Chen, G.C., Kang, Y.M., Zou, S.C., Zhang, L.Z., Qi, S.H., Dai, M.H., Cheng, Y., Hu, K., 2007. Spatial and seasonal distributions of carbonaceous aerosols over China. *J. Geophys. Res. Atmospheres* 112, D22S11.
- Carbone, C., Decesari, S., Mircea, M., Giulianelli, L., Finessi, E., Rinaldi, M., Fuzzi, S., Marinoni, A., Duchi, R., Perrino, C., Sargolini, T., Vardè, M., Sprovieri, F., Gobbi, G.P., Angelini, F., Facchini, M.C., 2010. Size-resolved aerosol chemical composition over the Italian Peninsula during typical summer and winter conditions. *Atmos. Environ.* 44, 5269–5278.
- Chaloulakou, A., Kassomenos, P., Grivas, G., Spyrellis, N., 2005. Particulate matter and black smoke concentration levels in central Athens, Greece. *Environ. Int.* 31, 651–659.
- Chaloulakou, A., Kassomenos, P., Spyrellis, N., Demokritou, P., Koutrakis, P., 2003. Measurements of PM₁₀ and PM_{2.5} particle concentrations in Athens, Greece. *Atmos. Environ.* 37, 649–660.
- Chang, C.T., Tsai, C.J., Lee, C.T., Chang, S.Y., Cheng, M.T., Chein, H.M., 2001. Differences in PM₁₀ concentrations measured by β -gauge monitor and hi-vol sampler. *Atmos. Environ.* 35, 5741–5748.
- Chrysikou, L.P., Samara, C.A., 2009. Seasonal variation of the size distribution of urban particulate matter and associated organic pollutants in the ambient air. *Atmos. Environ.* 43, 4557–4569.
- Civan, M.Y., Kuntasal, Ö.O., Tuncel, G., 2011. Source Apportionment of Ambient Volatile Organic Compounds in Bursa, a Heavily Industrialized City in Turkey. *Environ. Forensics* 12, 357–370.
- Curtius, J., 2006. Nucleation of atmospheric aerosol particles. *Comptes Rendus Phys., Nucleation* 7, 1027–1045.

- Daher, N., Hasheminassab, S., M. Shafer, M., J. Schauer, J., Sioutas, C., 2013. Seasonal and spatial variability in chemical composition and mass closure of ambient ultrafine particles in the megacity of Los Angeles. *Environ. Sci. Process. Impacts* 15, 283–295.
- D’Amato, G., Baena-Cagnani, C.E., Cecchi, L., Annesi-Maesano, I., Nunes, C., Ansotegui, I., D’Amato, M., Liccardi, G., Sofia, M., Canonica, W.G., 2013. Climate change, air pollution and extreme events leading to increasing prevalence of allergic respiratory diseases. *Multidiscip. Respir. Med.* 8, 12.
- Dassios, K.G., Pandis, S.N., 1999a. The mass accommodation coefficient of ammonium nitrate aerosol. *Atmos. Environ.* 33, 2993–3003.
- Deniz, C., Durmuşoğlu, Y., 2008. Estimating shipping emissions in the region of the Sea of Marmara, Turkey. *Sci. Total Environ.* 390, 255–261.
- Deshmukh, D., Deb, M., Tsai, Y.I., Mkoma, S.L., 2011. Water Soluble Ions in PM 2.5 and PM Aerosols in Durg City, Chhattisgarh, India.
- Diapouli, E., Eleftheriadis, K., Karanasiou, A.A., Vratolis, S., Hermansen, O., Colbeck, I., Lazaridis, M., 2011. Indoor and outdoor particle number and mass concentrations in Athens. Sources, sinks and variability of aerosol parameters. pp. 632–642.
- Diapouli, E., Manousakas, M., Vratolis, S., Vasilatou, V., Maggos, T., Saraga, D., Grigoratos, T., Argyropoulos, G., Voutsas, D., Samara, C., Eleftheriadis, K., 2017a. Evolution of air pollution source contributions over one decade, derived by PM₁₀ and PM_{2.5} source apportionment in two metropolitan urban areas in Greece. *Atmos. Environ.* 164, 416–430.
- Diapouli, E., Manousakas, M.I., Vratolis, S., Vasilatou, V., Pateraki, S., Bairachtari, K.A., Querol, X., Amato, F., Alastuey, A., Karanasiou, A.A., Lucarelli, F., Nava, S., Calzolari, G., Gianelle, V.L., Colombi, C., Alves, C., Custódio, D., Pio, C., Spyrou, C., Kallos, G.B., Eleftheriadis, K., 2017b. AIRUSE-LIFE +:

estimation of natural source contributions to urban ambient air PM₁₀ and PM_{2.5} concentrations in southern Europe – implications to compliance with limit values. *Atmos Chem Phys* 17, 3673–3685.

Dockery, D.W., 2001. Epidemiologic evidence of cardiovascular effects of particulate air pollution. *Environ. Health Perspect.* 109, 483–486.

Dockery, D.W., Pope, C.A., Xu, X., Spengler, J.D., Ware, J.H., Fay, M.E., Ferris, B.G., Speizer, F.E., 1993. An association between air pollution and mortality in six U.S. cities. *N. Engl. J. Med.* 329, 1753–1759.

Draxler, R.R., Gillette, D.A., Kirkpatrick, J.S., Heller, J., 2001. Estimating PM₁₀ air concentrations from dust storms in Iraq, Kuwait and Saudi Arabia. *Atmos. Environ.* 35, 4315–4330.

Ehn, M., Vuollekoski, H., Petäjä, T., Kerminen, V.-M., Vana, M., Aalto, P., de Leeuw, G., Ceburnis, D., Dupuy, R., O'Dowd, C.D., Kulmala, M., 2010. Growth rates during coastal and marine new particle formation in western Ireland. *J. Geophys. Res. Atmospheres* 115, D18218.

Elbir, T., 2003. Comparison of model predictions with the data of an urban air quality monitoring network in Izmir, Turkey. *Atmos. Environ.* 37, 2149–2157.

Eleftheriadis, K., Balis, D., Ziomas, I.C., Colbeck, I., Manalis, N., 1998. Atmospheric aerosol and gaseous species in Athens, Greece. *Atmos. Environ.* 32, 2183–2191.

Eleftheriadis, K., Colbeck, I., 2001. Coarse atmospheric aerosol: size distributions of trace elements. *Atmos. Environ.* 35, 5321–5330.

Eleftheriadis, K., Ochsenkuhn, K.M., Lymperopoulou, T., Karanasiou, A., Razos, P., Ochsenkuhn-Petropoulou, M., 2014a. Influence of local and regional sources on the observed spatial and temporal variability of size resolved atmospheric

- aerosol mass concentrations and water-soluble species in the Athens metropolitan area. *Atmos. Environ.* 97, 252–261.
- Emmanouil, C., Drositi, E., Vasilatou, V., Diapouli, E., Krikonis, K., Eleftheriadis, K., Kungolos, A., 2017. Study on particulate matter air pollution, source origin, and human health risk based of PM₁₀ metal content in Volos City, Greece. *Toxicol. Environ. Chem.* 99, 691–709.
- Englert, N., 2004. Fine particles and human health—a review of epidemiological studies. *Toxicol. Lett.*, Proceedings of EUROTOX 2003. The XLI European Congress of Toxicology. *Science for Safety* 149, 235–242.
- Escudero, M., Stein, A., Draxler, R.R., Querol, X., Alastuey, A., Castillo, S., Avila, A., 2006. Determination of the contribution of northern Africa dust source areas to PM₁₀ concentrations over the central Iberian Peninsula using the Hybrid Single-Particle Lagrangian Integrated Trajectory model (HYSPLIT) model. *J. Geophys. Res. Atmospheres* 111, D06210.
- Fenger, J., 2009. Air pollution in the last 50 years – From local to global. *Atmos. Environ.*, *Atmospheric Environment - Fifty Years of Endeavour* 43, 13–22.
- Floutsi, A.A., Korras-Carraca, M.B., Matsoukas, C., Hatzianastassiou, N., Biskos, G., 2016. Climatology and trends of aerosol optical depth over the Mediterranean basin during the last 12 years (2002–2014) based on Collection 006 MODIS-Aqua data. *Sci. Total Environ.* 551, 292–303.
- Galindo, N., Gil-Moltó, J., Varea, M., Chofre, C., Yubero, E., 2013. Seasonal and interannual trends in PM levels and associated inorganic ions in southeastern Spain. *Microchem. J.* 110, 81–88.
- Gębicki, J., Szymańska, K., 2012. Comparative field test for measurement of PM₁₀ dust in atmospheric air using gravimetric (reference) method and β -absorption method (Eberline FH 62-1). *Atmos. Environ.* 54, 18–24.

- Gerasopoulos, E., Kouvarakis, G., Babasakalis, P., Vrekoussis, M., Putaud, J.-P., Mihalopoulos, N., 2006. Origin and variability of particulate matter (PM₁₀) mass concentrations over the Eastern Mediterranean. *Atmos. Environ.* 40, 4679–4690.
- Gkikas, A., Hatzianastassiou, N., Mihalopoulos, N., Katsoulis, V., Kazadzis, S., Pey, J., Querol, X., Torres, O., 2013. The regime of intense desert dust episodes in the Mediterranean based on contemporary satellite observations and ground measurements. *Atmos Chem Phys* 13, 12135–12154.
- Glasius, M., Ketzel, M., Wåhlin, P., Jensen, B., Mønster, J., Berkowicz, R., Palmgren, F., 2006. Impact of wood combustion on particle levels in a residential area in Denmark. *Atmos. Environ.* 40, 7115–7124.
- Goldberg, M.S., Burnett, R.T., Yale, J.-F., Valois, M.-F., Brook, J.R., 2006. Associations between ambient air pollution and daily mortality among persons with diabetes and cardiovascular disease. *Environ. Res.* 100, 255–267.
- Grell, G.A., Peckham, S.E., Schmitz, R., McKeen, S.A., Frost, G., Skamarock, W.C., Eder, B., 2005. Fully coupled “online” chemistry within the WRF model. *Atmos. Environ.* 39, 6957–6975.
- Grivas, G., Chaloulakou, A., Kassomenos, P., 2008. An overview of the PM₁₀ pollution problem, in the Metropolitan Area of Athens, Greece. Assessment of controlling factors and potential impact of long range transport. *Sci. Total Environ.* 389, 165–177.
- Guerreiro, C.B.B., Foltescu, V., de Leeuw, F., 2014. Air quality status and trends in Europe. *Atmos. Environ.* 98, 376–384.
- Hamed, A., Joutsensaari, J., Mikkonen, S., Sogacheva, L., Dal Maso, M., Kulmala, M., Cavalli, F., Fuzzi, S., Facchini, M.C., Decesari, S., Mircea, M., Lehtinen, K.E.J., Laaksonen, A., 2007. Nucleation and growth of new particles in Po Valley, Italy. *Atmos Chem Phys* 7, 355–376.

- Harris, S.J., Maricq, M.M., 2001. Signature size distributions for diesel and gasoline engine exhaust particulate matter. *J. Aerosol Sci.* 32, 749–764.
- Harrison, R.M., Yin, J., Mark, D., Stedman, J., Appleby, R.S., Booker, J., Moorcroft, S., 2001. Studies of the coarse particle (2.5–10 μ m) component in UK urban atmospheres. *Atmos. Environ.* 35, 3667–3679.
- Haustein, K., Pérez, C., Baldasano, J.M., Jorba, O., Basart, S., Miller, R.L., Janjic, Z., Black, T., Nickovic, S., Todd, M.C., Washington, R., Müller, D., Tesche, M., Weinzierl, B., Esselborn, M., Schladitz, A., 2012. Atmospheric dust modeling from meso to global scales with the online NMMB/BSC-Dust model – Part 2: Experimental campaigns in Northern Africa. *Atmos Chem Phys* 12, 2933–2958.
- Hoek, G., Boogaard, H., Knol, A., de Hartog, J., Slottje, P., Ayres, J.G., Borm, P., Brunekreef, B., Donaldson, K., Forastiere, F., Holgate, S., Kreyling, W.G., Nemery, B., Pekkanen, J., Stone, V., Wichmann, H.-E., van der Sluijs, J., 2010. Concentration Response Functions for Ultrafine Particles and All-Cause Mortality and Hospital Admissions: Results of a European Expert Panel Elicitation. *Environ. Sci. Technol.* 44, 476–482.
- Hoet, P.H., Brüske-Hohlfeld, I., Salata, O.V., 2004. Nanoparticles – known and unknown health risks. *J. Nanobiotechnology* 2, 12.
- Houthuijs, D., Breugelmans, O., Hoek, G., Vaskövi, É., Miháliková, E., Pastuszka, J.S., Jirik, V., Sachelarescu, S., Lolova, D., Meliefste, K., Uzunova, E., Marinescu, C., Volf, J., de Leeuw, F., van de Wiel, H., Fletcher, T., Lebret, E., Brunekreef, B., 2001. PM₁₀ and PM_{2.5} concentrations in Central and Eastern Europe: *Atmos. Environ.* 35, 2757–2771.
- Jacob, D., Jacob, 1999. *Introduction to Atmospheric Chemistry.* , Princeton University Press Princeton, New Jersey.

- Jacobson, M.Z., 2001. Strong radiative heating due to the mixing state of black carbon in atmospheric aerosols. *Nature* 409, 695–697.
- Jimoda, L.A., 2012. Effects of particulate matter on human health, the ecosystem, climate and materials: A review. *Facta Univ. - Ser. Work. Living Enviromental Prot.* 9, 27–44.
- Johnson, G.R., Juwono, A.M., Friend, A.J., Cheung, H.-C., Stelcer, E., Cohen, D., Ayoko, G.A., Morawska, L., 2014. Relating urban airborne particle concentrations to shipping using carbon based elemental emission ratios. *Atmos. Environ.* 95, 525–536.
- Kalivitis, N., Birmili, W., Stock, M., Wehner, B., Massling, A., Wiedensohler, A., Gerasopoulos, E., Mihalopoulos, N., 2008. Particle size distributions in the Eastern Mediterranean troposphere. *Atmos Chem Phys* 8, 6729–6738.
- Kallos, G., Astitha, M., Katsafados, P., Spyrou, C., 2007. Long-Range Transport of Anthropogenically and Naturally Produced Particulate Matter in the Mediterranean and North Atlantic: Current State of Knowledge. *J. Appl. Meteorol. Climatol.* 46, 1230–1251.
- Kallos, G., Kotroni, V., Lagouvardos, K., Papadopoulos, A., 1998. On the Long-Range transport of air pollutants from Europe to Africa. *Geophys. Res. Lett.* 25, 619–622.
- Kalnay, E., Kanamitsu, M., Kistler, R., Collins, W., Deaven, D., Gandin, L., Iredell, M., Saha, S., White, G., Woollen, J., Zhu, Y., Leetmaa, A., Reynolds, R., Chelliah, M., Ebisuzaki, W., Higgins, W., Janowiak, J., Mo, K.C., Ropelewski, C., Wang, J., Jenne, R., Joseph, D., 1996. The NCEP/NCAR 40-Year Reanalysis Project. *Bull. Am. Meteorol. Soc.* 77, 437–471.
- Kambezidis, H., Kassomenos, P., Kiriaki, E., 1986. Smoke concentration levels in a monitoring network in Athens, Greece. *Atmospheric Environ.* 1967 20, 601–604.

- Kampa, M., Castanas, E., 2008. Human health effects of air pollution. *Environ. Pollut.*, Proceedings of the 4th International Workshop on Biomonitoring of Atmospheric Pollution (With Emphasis on Trace Elements) 151, 362–367.
- Kanakidou, M., Seinfeld, J.H., Pandis, S.N., Barnes, I., Dentener, F.J., Facchini, M.C., Van Dingenen, R., Ervens, B., Nenes, A., Nielsen, C.J., Swietlicki, E., Putaud, J.P., Balkanski, Y., Fuzzi, S., Horth, J., Moortgat, G.K., Winterhalter, R., Myhre, C.E.L., Tsigaridis, K., Vignati, E., Stephanou, E.G., Wilson, J., 2005. Organic aerosol and global climate modelling: a review. *Atmos Chem Phys* 5, 1053–1123.
- Karaca, F., Anil, I., Alagha, O., 2009. Long-range potential source contributions of episodic aerosol events to PM₁₀ profile of a megacity. *Atmos. Environ.* 43, 5713–5722.
- Karanasiou, A.A., Sitaras, I.E., Siskos, P.A., Eleftheriadis, K., 2007. Size distribution and sources of trace metals and n-alkanes in the Athens urban aerosol during summer. *Atmos. Environ.* 41, 2368–2381.
- Kaskaoutis, D.G., Kambezidis, H.D., Nastos, P.T., Kosmopoulos, P.G., 2008. Study on an intense dust storm over Greece. *Atmos. Environ.* 42, 6884–6896.
- Kato, S., Pochanart, P., Kajii, Y., 2001. Measurements of ozone and nonmethane hydrocarbons at Chichi-jima island, a remote island in the western Pacific: long-range transport of polluted air from the Pacific rim region. *Atmos. Environ.* 35, 6021–6029.
- Katsouyanni, K., Touloumi, G., Samoli, E., Gryparis, A., Le Tertre, A., Monopoli, Y., Rossi, G., Zmirou, D., Ballester, F., Boumghar, A., Anderson, H.R., Wojtyniak, B., Paldy, A., Braunstein, R., Pekkanen, J., Schindler, C., Schwartz, J., 2001. Confounding and effect modification in the short-term effects of ambient particles on total mortality: results from 29 European cities within the APHEA2 project. *Epidemiol. Camb. Mass* 12, 521–531.

- Kesgin, U., Vardar, N., 2001. A study on exhaust gas emissions from ships in Turkish 12 Straits. *Atmos. Environ.* 35, 1863–1870.
- Ketzel, M., Omstedt, G., Johansson, C., Düring, I., Pohjola, M., Oetl, D., Gidhagen, L., Wåhlin, P., Lohmeyer, A., Haakana, M., Berkowicz, R., 2007. Estimation and validation of PM_{2.5}/PM₁₀ exhaust and non-exhaust emission factors for practical street pollution modelling. *Atmos. Environ.* 41, 9370–9385.
- Klimont, Z., Smith, S.J., Cofala, J., 2013. The last decade of global anthropogenic sulfur dioxide: 2000–2011 emissions. *Environ. Res. Lett.* 8, 014003.
- Koçak, M., Mihalopoulos, N., Kubilay, N., 2007. Contributions of natural sources to high PM₁₀ and PM_{2.5} events in the eastern Mediterranean. *Atmos. Environ.* 41, 3806–3818.
- Koçak, M., Theodosi, C., Zampas, P., Im, U., Bougiatioti, A., Yenigun, O., Mihalopoulos, N., 2011. Particulate matter (PM₁₀) in Istanbul: Origin, source areas and potential impact on surrounding regions. *Atmos. Environ., Modeling of Air Quality Impacts, Forecasting and Interactions with Climate.* 45, 6891–6900.
- Koliadima, A., Athanasopoulou, A., Karaiskakis, G., 1998. Particulate Matter in Air of the Cities of Athens and Patras (Greece): Particle-Size Distributions and Elemental Concentrations. *Aerosol Sci. Technol.* 28, 292–300.
- Kopanakis, I., Eleftheriadis, K., Mihalopoulos, N., Lydakis-Simantiris, N., Katsivela, E., Pentari, D., Zampas, P., Lazaridis, M., 2012. Physico-chemical characteristics of particulate matter in the Eastern Mediterranean. *Atmospheric Res.* 106, 93–107.
- Kostenidou, E., Florou, K., Kaltsonoudis, C., Tsiflikiotou, M., Vratolis, S., Eleftheriadis, K., Pandis, S.N., 2015. Sources and chemical characterization of

organic aerosol during the summer in the eastern Mediterranean. *Atmos Chem Phys* 15, 11355–11371.

Kotrikla, A.M., Korras-Carraca, M.B., Dimou, K., Triantafyllou, E., Fameli, K.M., Psanis, C., Floutsi, A.A., Biskos, G., 2017. Air Pollution Modeling in a North Aegean City: Effects of the Transportation System on Local Air Quality, in: Karacostas, T., Bais, A., Nastos, P.T. (Eds.), *Perspectives on Atmospheric Sciences*, Springer Atmospheric Sciences. Springer International Publishing, pp. 1093–1098.

Kotroni, V., Lagouvardos, K., Lalas, D., 2001. The effect of the island of Crete on the Etesian winds over the Aegean Sea. *Q. J. R. Meteorol. Soc.* 127, 1917–1937.

Koulouri, E., Saarikoski, S., Theodosi, C., Markaki, Z., Gerasopoulos, E., Kouvarakis, G., Mäkelä, T., Hillamo, R., Mihalopoulos, N., 2008. Chemical composition and sources of fine and coarse aerosol particles in the Eastern Mediterranean. *Atmos. Environ.* 42, 6542–6550.

Kouvarakis, G., Doukelis, Y., Mihalopoulos, N., Rapsomanikis, S., Sciare, J., Blumthaler, M., 2002. Chemical, physical, and optical characterization of aerosols during PAUR II experiment. *J. Geophys. Res. Atmospheres* 107, 8141.

Krecl, P., Ström, J., Johansson, C., 2008. Diurnal variation of atmospheric aerosol during the wood combustion season in Northern Sweden. *Atmos. Environ.* 42, 4113–4125.

Kubilay, N., Nickovic, S., Moulin, C., Dulac, F., 2000. An illustration of the transport and deposition of mineral dust onto the eastern Mediterranean. *Atmos. Environ.* 34, 1293–1303.

Kuklinska, K., Wolska, L., Namiesnik, J., 2015. Air quality policy in the U.S. and the EU – a review. *Atmospheric Pollut. Res.* 6, 129–137. \

- Kulmala, M., Petäjä, T., Mönkkönen, P., Koponen, I.K., Dal Maso, M., Aalto, P.P., Lehtinen, K.E.J., Kerminen, V.-M., 2005. On the growth of nucleation mode particles: source rates of condensable vapor in polluted and clean environments. *Atmos Chem Phys* 5, 409–416.
- Lazaridis, M., Dzumbova, L., Kopanakis, I., Ondracek, J., Glytsos, T., Aleksandropoulou, V., Voulgarakis, A., Katsivela, E., Mihalopoulos, N., Eleftheriadis, K., 2008. PM₁₀ and PM_{2.5} Levels in the Eastern Mediterranean (Akrotiri Research Station, Crete, Greece). *Water, Air, Soil Pollut.* 189, 85–101.
- Lazaridis, M., Eleftheriadis, K., Smolik, J., Colbeck, I., Kallos, G., Drossinos, Y., Zdimal, V., Vecera, Z., Mihalopoulos, N., Mikuska, P., Bryant, C., Housiadas, C., Spyridaki, A., Astitha, M., Havranek, V., 2006. Dynamics of fine particles and photo-oxidants in the Eastern Mediterranean (SUB-AERO). *Atmos. Environ.* 40, 6214–6228.
- Lazaridis, M., Spyridaki, A., Solberg, S., Smolík, J., Zdimal, V., Eleftheriadis, K., Aleksandropoulou, V., Hov, O., Georgopoulos, P.G., 2005. Mesoscale modeling of combined aerosol and photo-oxidant processes in the Eastern Mediterranean. *Atmos Chem Phys* 5, 927–940.
- Lelieveld, J., Berresheim, H., Borrmann, S., Crutzen, P.J., Dentener, F.J., Fischer, H., Feichter, J., Flatau, P.J., Heland, J., Holzinger, R., Korrman, R., Lawrence, M.G., Levin, Z., Markowicz, K.M., Mihalopoulos, N., Minikin, A., Ramanathan, V., Reus, M. de, Roelofs, G.J., Scheeren, H.A., Sciare, J., Schlager, H., Schultz, M., Siegmund, P., Steil, B., Stephanou, E.G., Stier, P., Traub, M., Warneke, C., Williams, J., Ziereis, H., 2002. Global Air Pollution Crossroads over the Mediterranean. *Science* 298, 794–799.
- Lelieveld, J., Evans, J.S., Fnais, M., Giannadaki, D., Pozzer, A., 2015. The contribution of outdoor air pollution sources to premature mortality on a global scale. *Nature* 525, 367–371.

- Lin, J.J., Lee, L.-C., 2004. Characterization of the concentration and distribution of urban submicron (PM₁) aerosol particles. *Atmos. Environ.* 38, 469–475.
- Liu, X., Espen, P.V., Adams, F., Cafmeyer, J., Maenhaut, W., 2000. Biomass Burning in Southern Africa: Individual Particle Characterization of Atmospheric Aerosols and Savanna Fire Samples. *J. Atmospheric Chem.* 36, 135–155.
- Lomax, R.G., 2007. An introduction to statistical concepts. 2nd Ed., Lawrence Erlbaum Associates.
- Löndahl, J., Massling, A., Pagels, J., Swietlicki, E., Vaclavik, E., Loft, S., 2007. Size-Resolved Respiratory-Tract Deposition of Fine and Ultrafine Hydrophobic and Hygroscopic Aerosol Particles During Rest and Exercise. *Inhal. Toxicol.* 19, 109–116.
- Lü, S., Zhang, R., Yao, Z., Yi, F., Ren, J., Wu, M., Feng, M., Wang, Q., 2012a. Size distribution of chemical elements and their source apportionment in ambient coarse, fine, and ultrafine particles in Shanghai urban summer atmosphere. *J. Environ. Sci.* 24, 882–890.
- Lü, S., Zhang, R., Yao, Z., Yi, F., Ren, J., Wu, M., Feng, M., Wang, Q., 2012b. Size distribution of chemical elements and their source apportionment in ambient coarse, fine, and ultrafine particles in Shanghai urban summer atmosphere. *J. Environ. Sci.* 24, 882–890.
- Mamali, D., Mikkilä, J., Henzing, B., Spoor, R., Ehn, M., Petäjä, T., Russchenberg, H., Biskos, G., 2018. Long-term observations of the background aerosol at Cabauw, The Netherlands. *Sci. Total Environ.* 625, 752–761.
- Manalis, N., Grivas, G., Protonotarios, V., Moutsatsou, A., Samara, C., Chaloulakou, A., 2005. Toxic metal content of particulate matter (PM₁₀), within the Greater Area of Athens. *Chemosphere* 60, 557–566.

- Manoli, E., Chelioti-Chatzidimitriou, A., Karageorgou, K., Kouras, A., Voutsas, D., Samara, C., Kampanos, I., 2017. Polycyclic aromatic hydrocarbons and trace elements bounded to airborne PM₁₀ in the harbor of Volos, Greece: Implications for the impact of harbor activities. *Atmos. Environ.* 167, 61–72.
- Manoli, E., Voutsas, D., Samara, C., 2002. Chemical characterization and source identification/apportionment of fine and coarse air particles in Thessaloniki, Greece. *Atmos. Environ.* 36, 949–961.
- Manousakas, M., Diapouli, E., Papaefthymiou, H., Kantarelou, V., Zarkadas, C., Kalogridis, A.-C., Karydas, A.-G., Eleftheriadis, K., 2017a. XRF characterization and source apportionment of PM₁₀ samples collected in a coastal city. *X-Ray Spectrom.* 1–11.
- Manousakas, M., Diapouli, E., Papaefthymiou, H., Migliori, A., Karydas, A.G., Padilla-Alvarez, R., Bogovac, M., Kaiser, R.B., Jaksic, M., Bogdanovic-Radovic, I., Eleftheriadis, K., 2015. Source apportionment by PMF on elemental concentrations obtained by PIXE analysis of PM₁₀ samples collected at the vicinity of lignite power plants and mines in Megalopolis, Greece. *Nucl. Instrum. Methods Phys. Res. Sect. B Beam Interact. Mater. At.* 349, 114–124.
- Manousakas, M., Papaefthymiou, H., Diapouli, E., Migliori, A., Karydas, A.G., Bogdanovic-Radovic, I., Eleftheriadis, K., 2017b. Assessment of PM_{2.5} sources and their corresponding level of uncertainty in a coastal urban area using EPA PMF 5.0 enhanced diagnostics. *Sci. Total Environ.* 574, 155–164.
- Mantis, J., Chaloulakou, A., Samara, C., 2005. PM₁₀-bound polycyclic aromatic hydrocarbons (PAHs) in the Greater Area of Athens, Greece. *Chemosphere* 59, 593–604.
- Masclat, P., Pistikopoulos, P., Beyne, S., Mouvier, G., 1988. Long range transport and gas/particle distribution of polycyclic aromatic hydrocarbons at a remote site in the Mediterranean Sea. *Atmospheric Environ.* 1967 22, 639–650.

- Matthaios, V.N., Triantafyllou, A.G., Koutrakis, P., 2017. PM₁₀ episodes in Greece: Local sources versus long-range transport—observations and model simulations. *J. Air Waste Manag. Assoc.* 67, 105–126.
- McMurry, P.H., 2000. A review of atmospheric aerosol measurements. *Atmos. Environ.* 34, 1959–1999.
- Medina, S., Plasencia, A., Ballester, F., Mücke, H.G., Schwartz, J., Apheis group, 2004. Apheis: public health impact of PM₁₀ in 19 European cities. *J. Epidemiol. Community Health* 58, 831–836.
- Mihalopoulos, N., Stephanou, E., Kanakidou, M., Pilitsidis, S., Bousquet, P., 1997. Tropospheric aerosol ionic composition in the Eastern Mediterranean region. *Tellus B* 49, 314–326.
- Mikkonen, S., Romakkaniemi, S., Smith, J.N., Korhonen, H., Petäjä, T., Plass-Duelmer, C., Boy, M., McMurry, P.H., Lehtinen, K.E.J., Joutsensaari, J., Hamed, A., Mauldin III, R.L., Birmili, W., Spindler, G., Arnold, F., Kulmala, M., Laaksonen, A., 2011a. A statistical proxy for sulphuric acid concentration. *Atmos Chem Phys* 11, 11319–11334.
- Minguillón, M.C., Querol, X., Baltensperger, U., Prévôt, A.S.H., 2012a. Fine and coarse PM composition and sources in rural and urban sites in Switzerland: Local or regional pollution? *Sci. Total Environ.* 427, 191–202.
- Minguillón, M.C., Rivas, I., Aguilera, I., Alastuey, A., Moreno, T., Amato, F., Sunyer, J., Querol, X., 2012b. Within-city contrasts in PM composition and sources and their relationship with nitrogen oxides. *J. Environ. Monit.* 14, 2718–2728.
- Molnár, P., Gustafson, P., Johannesson, S., Boman, J., Barregård, L., Sällsten, G., 2005. Domestic wood burning and PM_{2.5} trace elements: Personal exposures, indoor and outdoor levels. *Atmos. Environ.* 39, 2643–2653.

- Moussiopoulos, N., Vlachokostas, C., Tsilingiridis, G., Douros, I., Hourdakias, E., Naneris, C., Sidiropoulos, C., 2009. Air quality status in Greater Thessaloniki Area and the emission reductions needed for attaining the EU air quality legislation. *Sci. Total Environ.* 407, 1268–1285.
- Odabasi, M., Bayram, A., Elbir, T., Seyfioglu, R., Dumanoglu, Y., Ornektekin, S., 2010. Investigation of Soil Concentrations of Persistent Organic Pollutants, Trace Elements, and Anions Due to Iron–Steel Plant Emissions in an Industrial Region in Turkey. *Water. Air. Soil Pollut.* 213, 375–388.
- Ogunsola, O.J., Oluwole, A.F., Asubiojo, O.I., Olaniyi, H.B., Akeredolu, F.A., Akanle, O.A., Spyrou, N.M., Ward, N.I., Ruck, W., 1994. Traffic pollution: preliminary elemental characterisation of roadside dust in Lagos, Nigeria. *Sci. Total Environ., Highway Pollution* 146–147, 175–184.
- Ostro, B., Broadwin, R., Green, S., Feng, W., Lipsett, M., 2006. Fine particulate air pollution and mortality in nine California counties: results from CALFINE. *Environ Health Perspect* 114:29–33.
- Ostro, B., Tobias, A., Karanasiou, A., Samoli, E., Querol, X., Rodopoulou, S., Basagaña, X., Eleftheriadis, K., Diapouli, E., Vratolis, S., Jacquemin, B., Katsouyanni, K., Sunyer, J., Forastiere, F., Stafoggia, M., 2015. The risks of acute exposure to black carbon in Southern Europe: results from the MED-PARTICLES project. *Occup Env. Med* 72, 123–129.
- Pandolfi, M., Amato, F., Reche, C., Alastuey, A., Otjes, R.P., Blom, M.J., Querol, X., 2012. Summer ammonia measurements in a densely populated Mediterranean city. *Atmos Chem Phys* 12, 7557–7575.
- Pant, P., Harrison, R.M., 2013. Estimation of the contribution of road traffic emissions to particulate matter concentrations from field measurements: A review. *Atmos. Environ.* 77, 78–97.

- Papanastasiou, D.K., Melas, D., 2008. Statistical characteristics of ozone and PM₁₀ levels in a medium-sized Mediterranean city. *Int. J. Environ. Pollut.* 36, 127–138.
- Paraskevopoulou, D., Liakakou, E., Gerasopoulos, E., Mihalopoulos, N., 2015. Sources of atmospheric aerosol from long-term measurements (5years) of chemical composition in Athens, Greece. *Sci. Total Environ.* 527, 165–178.
- Paraskevopoulou, D., Liakakou, E., Gerasopoulos, E., Theodosi, C., Mihalopoulos, N., 2014. Long-term characterization of organic and elemental carbon in the PM_{2.5} fraction: the case of Athens, Greece. *Atmos Chem Phys* 14, 13313–13325.
- Pateraki, S., Maggos, T., Michopoulos, J., Flocas, H.A., Asimakopoulos, D.N., Vasilakos, C., 2008. Ions species size distribution in particulate matter associated with VOCs and meteorological conditions over an urban region. *Chemosphere* 72, 496–503.
- Peng, J.F., Hu, M., Wang, Z.B., Huang, X.F., Kumar, P., Wu, Z.J., Guo, S., Yue, D.L., Shang, D.J., Zheng, Z., He, L.Y., 2014. Submicron aerosols at thirteen diversified sites in China: size distribution, new particle formation and corresponding contribution to cloud condensation nuclei production. *Atmos Chem Phys* 14, 10249–10265.
- Penner, J.E., Chuang, C.C., Grant, K., 1998. Climate forcing by carbonaceous and sulfate aerosols. *Clim. Dyn.* 14, 839–851.
- Pérez, C., Haustein, K., Janjic, Z., Jorba, O., Huneus, N., Baldasano, J.M., Black, T., Basart, S., Nickovic, S., Miller, R.L., Perlwitz, J.P., Schulz, M., Thomson, M., 2011. Atmospheric dust modeling from meso to global scales with the online NMMB/BSC-Dust model – Part 1: Model description, annual simulations and evaluation. *Atmos Chem Phys* 11, 13001–13027.

- Perrino, C., Canepari, S., Catrabone, M., 2013. Comparing the Performance of Teflon and Quartz Membrane Filters Collecting Atmospheric PM: Influence of Atmospheric Water. *Aerosol Air Qual. Res.* 137–147.
- Perrino, C., Catrabone, M., Torre, S.D., Rantica, E., Sargolini, T., Canepari, S., 2014. Seasonal variations in the chemical composition of particulate matter: a case study in the Po Valley. Part I: macro-components and mass closure. *Environ. Sci. Pollut. Res.* 21, 3999–4009.
- Petaloti, C., Maggos, T., Bartzis, J.G., 2006a. Airborne particulate matter in Greece-physical and chemical characteristics. *Fresenius Environ. Bull.* 15, 859–865.
- Petaloti, C., Triantafyllou, A., Kouimtzis, T., Samara, C., 2006b. Trace elements in atmospheric particulate matter over a coal burning power production area of western Macedonia, Greece. *Chemosphere, Environmental Chemistry* 65, 2233–2243.
- Pikridas, M., Bougiatioti, A., Hildebrandt, L., Engelhart, G.J., Kostenidou, E., Mohr, C., Prévôt, A.S.H., Kouvarakis, G., Zampas, P., Burkhardt, J.F., Lee, B.-H., Psichoudaki, M., Mihalopoulos, N., Pilinis, C., Stohl, A., Baltensperger, U., Kulmala, M., Pandis, S.N., 2010. The Finokalia Aerosol Measurement Experiment – 2008 (FAME-08): an overview. *Atmos Chem Phys* 10, 6793–6806.
- Pikridas, M., Tasoglou, A., Florou, K., Pandis, S.N., 2013. Characterization of the origin of fine particulate matter in a medium size urban area in the Mediterranean. *Atmos. Environ.* 80, 264–274.
- Pio, C., Mirante, F., Oliveira, César, Matos, M., Caseiro, A., Oliveira, Cristina, Querol, X., Alves, C., Martins, N., Cerqueira, M., Camões, F., Silva, H., Plana, F., 2013. Size-segregated chemical composition of aerosol emissions in an urban road tunnel in Portugal. *Atmos. Environ.* 71, 15–25.

- Pope III, C.A., 2000. Epidemiology of fine particulate air pollution and human health: biologic mechanisms and who's at risk? *Environ. Health Perspect.* 108, 713–723.
- Pope III, C.A., Thun, M.J., Namboodiri, M.M., Dockery, D.W., Evans, J.S., Speizer, F.E., Heath, C.W., 1995. Particulate Air Pollution as a Predictor of Mortality in a Prospective Study of U.S. Adults. *Am. J. Respir. Crit. Care Med.* 151, 669–674.
- Poupkou, A., Zanis, P., Nastos, P., Papanastasiou, D., Melas, D., Tourpali, K., Zerefos, C., 2011. Present climate trend analysis of the Etesian winds in the Aegean Sea. *Theor. Appl. Climatol.* 106, 459–472.
- Price, M., Bulpitt, S., Meyer, M.B., 2003. A comparison of PM₁₀ monitors at a Kerbside site in the northeast of England. *Atmos. Environ.* 37, 4425–4434.
- Proias, G.T., Moustiris, K.P., Larissi, I.K., Nastos, P.T., Paliatsos, A.G., 2012. Ambient PM₁₀ concentrations and the impact of wind at an urban site in central Greece. *Fresenius Environ. Bull.* 21, 1935–1941.
- Psanis, C., Triantafyllou, E., Giamarelou, M., Manousakas, M., Eleftheriadis, K., Biskos, G., 2017. Particulate matter pollution from aviation-related activity at a small airport of the Aegean Sea Insular Region. *Sci. Total Environ.* 596–597, 187–193.
- Puett, R.C., Hart, J.E., Suh, H., Mittleman, M., Laden, F., 2011. Particulate Matter Exposures, Mortality, and Cardiovascular Disease in the Health Professionals Follow-up Study. *Environ. Health Perspect.* 119, 1130–1135.
- Querol, X., Alastuey, A., Ruiz, C.R., Artiñano, B., Hansson, H.C., Harrison, R.M., Buringh, E., ten Brink, H.M., Lutz, M., Bruckmann, P., Straehl, P., Schneider, J., 2004. Speciation and origin of PM₁₀ and PM_{2.5} in selected European cities. *Atmos. Environ.*, Contains Special Issue section on Measuring the composition of Particulate Matter in the EU 38, 6547–6555.

- Querol, X., Pey, J., Minguillón, M.C., Pérez, N., Alastuey, A., Viana, M., Moreno, T., Bernabé, R.M., Blanco, S., Cárdenas, B., Vega, E., Sosa, G., Escalona, S., Ruiz, H., Artíñano, B., 2008. PM speciation and sources in Mexico during the MILAGRO-2006 Campaign. *Atmospheric Chem. Phys. Discuss.* 7, 10589–10629.
- Reimann, C., Caritat, P. de, 2000. Intrinsic Flaws of Element Enrichment Factors (EFs) in Environmental Geochemistry. *Environ. Sci. Technol.* 34, 5084–5091.
- Rolph, G., Stein, A., Stunder, B., 2017. Real-time Environmental Applications and Display sYstem: READY. *Environ. Model. Softw.* 95, 210–228.
- Romano, S., Burlizzi, P., Perrone, M.R., 2016. Experimental determination of short- and long-wave dust radiative effects in the Central Mediterranean and comparison with model results. *Atmospheric Res.* 171, 5–20.
- Saffari, A., Daher, N., Samara, C., Voutsas, D., Kouras, A., Manoli, E., Karagkiozidou, O., Vlachokostas, C., Moussiopoulos, N., Shafer, M.M., Schauer, J.J., Sioutas, C., 2013. Increased Biomass Burning Due to the Economic Crisis in Greece and Its Adverse Impact on Wintertime Air Quality in Thessaloniki. *Environ. Sci. Technol.* 47, 13313–13320.
- Salby, M.L., 1996. *Fundamentals of Atmospheric Physics*, 1st Edition, Elsevier, U.S.A.
- Salma, I., Borsós, T., Weidinger, T., Aalto, P., Hussein, T., Dal Maso, M., Kulmala, M., 2011. Production, growth and properties of ultrafine atmospheric aerosol particles in an urban environment. *Atmos Chem Phys* 11, 1339–1353.
- Salminen, K., Karlsson, V., 2003. Comparability of low-volume PM₁₀ sampler with β -attenuation monitor in background air. *Atmos. Environ.* 37, 3707–3712.
- Samara, C., 2005. Chemical mass balance source apportionment of TSP in a lignite-burning area of Western Macedonia, Greece. *Atmos. Environ.* 39, 6430–6443.

- Samara, C., Kouimtzis, T., Tsitouridou, R., Kanias, G., Simeonov, V., 2003. Chemical mass balance source apportionment of PM₁₀ in an industrialized urban area of Northern Greece. *Atmos. Environ.* 37, 41–54.
- Samara, C., Voutsas, D., 2005. Size distribution of airborne particulate matter and associated heavy metals in the roadside environment. *Chemosphere* 59, 1197–1206.
- Samara, C., Voutsas, D., Kouimtzis, T., Bournis, N., Tsani, E., 1990. Characterization of airborne particulate matter in Thessaloniki, Greece. *Toxicol. Environ. Chem.* 29, 107–119.
- Sarigiannis, D.A., Kyriakou, S., Kermenidou, M., Karakitsios, S.P., 2017. The Reactive Oxidative Potential from Biomass Emitted Particulate Matter (PM₁₀, PM_{2.5} & PM₁) and Its Impact on Human Health. *Fresenius Environ. Bull.* 26, 188–195.
- Schwarze, P.E., Øvreivik, J., Låg, M., Refsnes, M., Nafstad, P., Hetland, R.B., Dybing, E., 2006. Particulate matter properties and health effects: consistency of epidemiological and toxicological studies. *Hum. Exp. Toxicol.* 25, 559–579.
- Sciare, J., Bardouki, H., Moulin, C., Mihalopoulos, N., 2003. Aerosol sources and their contribution to the chemical composition of aerosols in the Eastern Mediterranean Sea during summertime. *Atmos Chem Phys* 3, 291–302.
- Sciare, J., Oikonomou, K., Favez, O., Liakakou, E., Markaki, Z., Cachier, H., Mihalopoulos, N., 2008. Long-term measurements of carbonaceous aerosols in the Eastern Mediterranean: evidence of long-range transport of biomass burning. *Atmos Chem Phys* 8, 5551–5563.
- Seaton, A., Godden, D., MacNee, W., Donaldson, K., 1995. Particulate air pollution and acute health effects. *The Lancet* 345, 176–178.

- Shin, S.E., Jung, C.H., Kim, Y.P., 2012. Estimation of the optimal heated inlet air temperature for the beta-ray absorption method: analysis of the PM₁₀ concentration difference by different methods in coastal areas. *Adv. Environ. Res.* 1, 69–82.
- Shin, S.E., Jung, C.H., Kim, Y.P., 2011. Analysis of the Measurement Difference for the PM₁₀ Concentrations between Beta-ray Absorption and Gravimetric Methods at Gosan. *Aerosol Air Qual. Res.* 11, 846–853.
- Siakavaras, D., Samara, C., Petrakakis, M., Biskos, G., 2016. Nucleation events at a coastal city during the warm period: Kerbside versus urban background measurements. *Atmos. Environ.* 140, 60–68.
- Sillanpää, M., Frey, A., Hillamo, R., Pennanen, A.S., Salonen, R.O., 2005. Organic, elemental and inorganic carbon in particulate matter of six urban environments in Europe. *Atmos Chem Phys* 5, 2869–2879.
- Sindosi, O.A., Katsoulis, B.D., Bartzokas, A., 2003. An objective definition of air mass types affecting Athens, Greece; the corresponding atmospheric pressure patterns and air pollution levels. *Environ. Technol.* 24, 947–962.
- Smolík, J., Ždímal, V., Schwarz, J., Lazaridis, M., Havárnek, V., Eleftheriadis, K., Mihalopoulos, N., Bryant, C., Colbeck, I., 2003. Size resolved mass concentration and elemental composition of atmospheric aerosols over the Eastern Mediterranean area. *Atmos Chem Phys* 3, 2207–2216.
- Spyrou, C., Mitsakou, C., Kallos, G., Louka, P., Vlastou, G., 2010. An improved limited area model for describing the dust cycle in the atmosphere. *J. Geophys. Res. Atmospheres* 115, D17211.
- Stafoggia, M., Schneider, A., Cyrys, J., Samoli, E., Andersen, Z.J., Bedada, G.B., Bellander, T., Cattani, G., Eleftheriadis, K., Faustini, A., Hoffmann, B., Jacquemin, B., Katsouyanni, K., Massling, A., Pekkanen, J., Perez, N., Peters, A., Quass, U., Yli-Tuomi, T., Forastiere, F., UF&HEALTH Study Group,

2017. Association Between Short-term Exposure to Ultrafine Particles and Mortality in Eight European Urban Areas. *Epidemiol. Camb. Mass* 28, 172–180.
- Stein, A.F., Draxler, R.R., Rolph, G.D., Stunder, B.J.B., Cohen, M.D., Ngan, F., 2015. NOAA's HYSPLIT Atmospheric Transport and Dispersion Modeling System. *Bull. Am. Meteorol. Soc.* 96, 2059–2077.
- Sun, Y., Hu, X., Wu, J., Lian, H., Chen, Y., 2014. Fractionation and health risks of atmospheric particle-bound As and heavy metals in summer and winter. *Sci. Total Environ.* 493, 487–494.
- Sutherland, R.A., 2000. Bed sediment-associated trace metals in an urban stream, Oahu, Hawaii. *Environ. Geol.* 39, 611–627.
- Takahashi, K., Minoura, H., Sakamoto, K., 2008. Examination of discrepancies between beta-attenuation and gravimetric methods for the monitoring of particulate matter. *Atmos. Environ.* 42, 5232–5240.
- Talwar, B., Bharati, A., 2012. Chemical characterization of PM₁ around an Industrial area. *J. Environ. Occup. Sci.* 1, 43.
- Terzi, E., Anatolaki, C., Samara, C., Tsitouridou, R., 2008. Mass closure of total suspended particles over the coal burning power production area of western Macedonia, Greece. *J. Atmospheric Chem.* 59, 171–186.
- Terzi, E., Argyropoulos, G., Bougatioti, A., Mihalopoulos, N., Nikolaou, K., Samara, C., 2010. Chemical composition and mass closure of ambient PM₁₀ at urban sites. *Atmos. Environ.* 44, 2231–2239.
- Theodosi, C., Grivas, G., Zarmas, P., Chaloulakou, A., Mihalopoulos, N., 2011. Mass and chemical composition of size-segregated aerosols (PM₁, PM_{2.5}, PM₁₀) over Athens, Greece: local versus regional sources. *Atmos Chem Phys* 11, 11895–11911.

- Theophanides, M., Anastassopoulou, J., Vasilakos, C., Maggos, T., Theophanides, T., 2007. Mortality and pollution in several greek cities. *J. Environ. Sci. Health Part A* 42, 741–746.
- Thöni, L., Yurukova, L., Bergamini, A., Ilyin, I., Matthaei, D., 2011. Temporal trends and spatial patterns of heavy metal concentrations in mosses in Bulgaria and Switzerland: 1990–2005. *Atmos. Environ.* 45, 1899–1912.
- Tolis, E., Saraga, D., Ammari, G., Gkanas, E., Gougoulas, T., Papaioannou, C., Sarioglou, A., Kougioumtzidis, E., Skemperi, A., Bartzis, J., 2014. Chemical characterization of particulate matter (PM) and source apportionment study during winter and summer period for the city of Kozani, Greece. *Open Chem.* 12, 643–651.
- Tolis, E.I., Saraga, D.E., Lytra, M.K., Papathanasiou, A.C., Bougaidis, P.N., Prekas-Patronakis, O.E., Ioannidis, I.I., Bartzis, J.G., 2015. Concentration and chemical composition of PM_{2.5} for a one-year period at Thessaloniki, Greece: A comparison between city and port area. *Atmos. Environ.* 113, 197–207.
- Tombrou, M., Bossioli, E., Kalogiros, J., Allan, J., Bacak, A., Biskos, G., Coe, H., Dandou, A., Kouvarakis, G., Mihalopoulos, N., Protonotariou, A.P., Szabó-Takács, B., Triantafyllou, E., 2013. Physical and Chemical Processes of Polluted Air Masses During Etesians: Aegean-Game Airborne Campaign – An Outline, in: *Advances in Meteorology, Climatology and Atmospheric Physics*, Springer Atmospheric Sciences. Springer, Berlin, Heidelberg, pp. 1239–1244.
- Tombrou, M., Bossioli, E., Kalogiros, J., Allan, J.D., Bacak, A., Biskos, G., Coe, H., Dandou, A., Kouvarakis, G., Mihalopoulos, N., Percival, C.J., Protonotariou, A.P., Szabó-Takács, B., 2015. Physical and chemical processes of air masses in the Aegean Sea during Etesians: Aegean-GAME airborne campaign. *Sci. Total Environ.* 506, 201–216.
- Triantafyllou, A.G., 2001. PM₁₀ pollution episodes as a function of synoptic climatology in a mountainous industrial area. *Environ. Pollut.* 112, 491–500.

- Triantafyllou, E., Biskos, G., 2012. Overview of the Temporal Variation of PM₁₀ Mass Concentrations in the two Major Cities in Greece: Athens and Thessaloniki. *Global Nest*. 14, N4, 431-441.
- Triantafyllou, E., Giamarelou, M., Bossioli, E., Zampas, P., Theodosi, C., Matsoukas, C., Tombrou, M., Mihalopoulos, N., Biskos, G., 2016. Particulate pollution transport episodes from Eurasia to a remote region of northeast Mediterranean. *Atmos. Environ.* 128, 45–52.
- Tsitouridou, R., Samara, C., 1993. First results of acidic and alkaline constituents determination in air particulates of Thessaloniki, Greece. *Atmospheric Environ. Part B Urban Atmosphere* 27, 313–319.
- Tsitouridou, R., Voutsas, D., Kouimtzis, T., 2003. Ionic composition of PM₁₀ in the area of Thessaloniki, Greece. *Chemosphere* 52, 883–891.
- Tyrlis, E., Lelieveld, J., 2013. Climatology and Dynamics of the Summer Etesian Winds over the Eastern Mediterranean. *J. Atmospheric Sci.* 70, 3374–3396.
- Tyrlis, E., Lelieveld, J., Steil, B., 2013. The summer circulation over the eastern Mediterranean and the Middle East: influence of the South Asian monsoon. *Clim. Dyn.* 40, 1103–1123.
- Uppala, S.M., Kållberg, P.W., Simmons, A.J., Andrae, U., Bechtold, V.D.C., Fiorino, M., Gibson, J.K., Haseler, J., Hernandez, A., Kelly, G.A., Li, X., Onogi, K., Saarinen, S., Sokka, N., Allan, R.P., Andersson, E., Arpe, K., Balmaseda, M.A., Beljaars, A.C.M., Berg, L.V.D., Bidlot, J., Bormann, N., Caires, S., Chevallier, F., Dethof, A., Dragosavac, M., Fisher, M., Fuentes, M., Hagemann, S., Hólm, E., Hoskins, B.J., Isaksen, L., Janssen, P. a. E.M., Jenne, R., McNally, A.P., Mahfouf, J.-F., Morcrette, J.-J., Rayner, N.A., Saunders, R.W., Simon, P., Sterl, A., Trenberth, K.E., Untch, A., Vasiljevic, D., Viterbo, P., Woollen, J., 2005. The ERA-40 re-analysis. *Q. J. R. Meteorol. Soc.* 131, 2961–3012.

- Vardoulakis, S., Kassomenos, P., 2008. Sources and factors affecting PM₁₀ levels in two European cities: Implications for local air quality management. *Atmos. Environ.*, Fifth International Conference on Urban Air Quality 42, 3949–3963.
- Vasilatou, V., Manousakas, M., Gini, M., Diapouli, E., Scoullou, M., Eleftheriadis, K., 2017. Long Term Flux of Saharan Dust to the Aegean Sea around the Attica Region, Greece. *Front. Mar. Sci.* 4.
- Vassilakos, C., Saraga, D., Maggos, T., Michopoulos, J., Pateraki, S., Helmis, C.G., 2005. Temporal variations of PM_{2.5} in the ambient air of a suburban site in Athens, Greece. *Sci. Total Environ.* 349, 223–231.
- Viana, M., Kuhlbusch, T.A.J., Querol, X., Alastuey, A., Harrison, R.M., Hopke, P.K., Winiwarter, W., Vallius, M., Szidat, S., Prévôt, A.S.H., Hueglin, C., Bloemen, H., Wåhlin, P., Vecchi, R., Miranda, A.I., Kasper-Giebl, A., Maenhaut, W., Hitzenberger, R., 2008. Source apportionment of particulate matter in Europe: A review of methods and results. *J. Aerosol Sci.* 39, 827–849.
- Visser, S., Slowik, J.G., Furger, M., Zotter, P., Bukowiecki, N., Canonaco, F., Flechsig, U., Appel, K., Green, D.C., Tremper, A.H., Young, D.E., Williams, P.I., Allan, J.D., Coe, H., Williams, L.R., Mohr, C., Xu, L., Ng, N.L., Nemitz, E., Barlow, J.F., Halios, C.H., Fleming, Z.L., Baltensperger, U., Prévôt, A.S.H., 2015. Advanced source apportionment of size-resolved trace elements at multiple sites in London during winter. *Atmos Chem Phys* 15, 11291–11309.
- Voutsas, D., Samara, C., Kouimtzi, T., Ochsenkühn, K., 2002. Elemental composition of airborne particulate matter in the multi-impacted urban area of Thessaloniki, Greece. *Atmos. Environ.* 36, 4453–4462.
- Voutsas, D., Samara, C., Manoli, E., Lazarou, D., Tzoumaka, P., 2014a. Ionic composition of PM_{2.5} at urban sites of northern Greece: secondary inorganic aerosol formation. *Environ. Sci. Pollut. Res.* 21, 4995–5006.

- Voutsas, D., Samara, C., Manoli, E., Lazarou, D., Tzoumaka, P., 2014b. Ionic composition of PM_{2.5} at urban sites of northern Greece: secondary inorganic aerosol formation. *Environ. Sci. Pollut. Res.* 21, 4995–5006.
- Vrekoussis, M., Richter, A., Hilboll, A., Burrows, J.P., Gerasopoulos, E., Lelieveld, J., Barrie, L., Zerefos, C., Mihalopoulos, N., 2013. Economic crisis detected from space: Air quality observations over Athens/Greece. *Geophys. Res. Lett.* 40, 458–463.
- Wang, T., Li, G., Sun, J., Buys, N., Liu, H., Liu, M., Ni, M., Li, B., Liang, X., Pan, X., 2013. Association between ambient particulate matter and daily cause-specific mortality in Tanggu, Tianjin Binhai New Area, China. *Int. J. Environ. Health Res.* 23, 205–214.
- Wark, K., Warner, C.F., Davis, W.T., 1997. *Air Pollution: Its Origin and Control*. 3rd Ed. Pearson, Menlo Park, Calif.
- Wedepohl, K.H., 1995. The composition of the continental crust. *Geochim. Cosmochim. Acta* 59, 1217–1232.
- Weijers, E.P., Khlystov, A.Y., Kos, G.P.A., Erisman, J.W., 2004. Variability of particulate matter concentrations along roads and motorways determined by a moving measurement unit. *Atmos. Environ.* 38, 2993–3002.
- Wu, Z., Hu, M., Lin, P., Liu, S., Wehner, B., Wiedensohler, A., 2008. Particle number size distribution in the urban atmosphere of Beijing, China. *Atmos. Environ.* 42, 7967–7980.
- Xu, L., Chen, X., Chen, J., Zhang, F., He, C., Zhao, J., Yin, L., 2012. Seasonal variations and chemical compositions of PM_{2.5} aerosol in the urban area of Fuzhou, China. *Atmospheric Res.* 104, 264–272.
- Yanosky, J.D., MacIntosh, D.L., 2001. A comparison of four gravimetric fine particle sampling methods. *J. Air Waste Manag. Assoc.* 51, 878–884.

Yotova, G.I., Tsitouridou, R., Tsakovski, S.L., Simeonov, V.D., 2016. Urban air quality assessment using monitoring data of fractionized aerosol samples, chemometrics and meteorological conditions. *J. Environ. Sci. Health Part A* 51, 544–552.

Zhang, W., Zhuang, G., Guo, J., Xu, D., Wang, W., Baumgardner, D., Wu, Z., Yang, W., 2010. Sources of aerosol as determined from elemental composition and size distributions in Beijing. *Atmospheric Res., Special Section: Little Alaska Weather Symposium 2008* 95, 197–209.

Zhao, J., Zhang, F., Xu, Y., Chen, J., 2011. Characterization of water-soluble inorganic ions in size-segregated aerosols in coastal city, Xiamen. *Atmospheric Res.* 99, 546–562.

Zikovsky, L., Leduc, R., Badillo, M., 1987. Comparison of measured distributions of concentrations of trace elements in air particulates with normal and lognormal probability functions. *Int. J. Environ. Stud.* 29, 175–179.

Books

Baron, P.A., Willeke, K., 2001. *Aerosol Measurement: Principles, Techniques, and Applications*, 3rd Ed. Wiley, New York.

Boubel, R.W., Fox, D.L., Turner, D.B., Stern, A.C., 1994. *Fundamentals of air pollution*. 3rd Ed. Academic Press, U.S.A.

Colbeck, I., 2008. *Environmental Chemistry of Aerosols* - Wiley Online Library [WWW Document]. URL <http://onlinelibrary.wiley.com/book/10.1002/9781444305388> (accessed 8.31.17).

Colbeck, I., Lazaridis, M., 2014. *Aerosol Science: Technology and Applications*. 1st Ed. Wiley, New York.

Colls, J., 2002. *Air Pollution*. 2nd Ed. Spon Press, London and New York.

- Cooper, C.D., Alley, F.C., 2002. Air pollution control: A design approach. 3rd Ed. Waveland Press, Inc., London
- Dodds, W.K., Whiles, M.R., 2010. Freshwater Ecology Concepts and Environmental Applications of Limnology: A volume in Aquatic Ecology. 2nd Ed. Academic Press, USA.
- Finlayson-Pitts, B.J., Pitts, J.J.N., 1986. Atmospheric Chemistry: Fundamentals and Experimental Techniques. John Wiley & Sons, New York.
- Hinds, W.C., 1999. Aerosol Technology: Properties, Behavior, and Measurement of Airborne Particles. Wiley, New York.
- Jacobson, M.Z., 2002. Atmospheric Pollution: History, Science, and Regulation. Cambridge University Press, Cambridge, UK ; New York.
- Malm, W.C., 1999. Introduction to Visibility. Cooperative Institute for Research in the Atmosphere, NPS Visibility Program, Colorado State University.
- Seinfeld, J.H., Pandis, S.N., 2006. Atmospheric Chemistry and Physics: From Air Pollution to Climate Change. 2nd Ed. John Wiley & Sons, Inc., New York.
- Verma, H.R., 2007. Atomic and Nuclear Analytical Methods - XRF, Mössbauer, XPS, NAA and Ion-Beam Spectroscopic Techniques. Springer Libri, New York.

Other sources

- ACGIH. 1998. Particle Size-Selective Sampling for Particulate Air Contaminants. Cincinnati, OH: American Conference of Government Industrial Hygienists.
- Draxler, R.R., Hess, G., 1998. An overview of the HYSPLIT_4 modeling system for trajectories, dispersion, and deposition.
- Draxler, R.R., Rolph, G.D., 2003. HYSPLIT (Hybrid Single Particle Lagrangian Intergrated Trajectory) Model Access via NOAA ARL READY

Website. NOAA Air Resources Laboratory, Silver Spring, MD
<http://www.arl.noaa.gov/ready/hysplit4.html>.

Draxler, R.R., Rolph, G.D., 2013. HYSPLIT (HYbrid Single-particle Lagrangian Integrated Trajectory). Model Access via NOAA ARL READY Website. NOAA Air Resources Laboratory, Silver Spring, MD. [WWW Document]. URL <http://ready.arl.noaa.gov/HYSPLIT.php> (accessed 9.27.17).

EC, 2010. Guide to the Demonstration of Equivalence of Ambient Air Monitoring Methods. Retrieved February 10, 2014 from <http://ec.europa.eu/environment/air/quality/legislation/pdf/equivalence.pdf>.

EPA, 2004. U.S. Environmental Protection Agency. Air Quality Criteria for Particulate Matter (Final Report, 2004).

Esworthy, R., 2013. Air Quality: EPA's 2013 Changes to the Particulate Matter (PM) Standard. Air Qual. 47.

EU-Commission, 2008. Council directive 2008/50/EC of 21 May 2008 relating to the ambient air quality and cleaner air for Europe. Off. J. L. 152 (1).

European Council Directive 1999/30/EC, 1999, relating to limit values for sulphur dioxide, nitrogen dioxide and oxides of nitrogen, particulate matter and lead in ambient air. Official Journal of the European Communities, L163, 41–60.

European Directive 2012/33/EU. Directive 2012/33/EU of the European Parliament and of the Council of 21 November 2012 amending Council Directive 1999/32/EC as regards the sulphur content of marine fuels, L 327/2.

Gobeli, D., 2008. Met One Instruments BAM-1020 Beta Attenuation Mass Monitor US-EPA PM_{2.5} Federal Equivalent Method Field Test Results. Air Waste Management Association Conference (Jan. 2008) Kansas city, Missouri, USA.

Hellenic Statistical Authority, 2011. Press Release: “Temporarily Results of Population census in Greece through 10 to 24 May 2011” (accessed July 2011). Available at <http://www.statistics.gr>.

- HMECC, 2010. (Hellenic Ministry of Environment Energy & Climate Change), Directorate of air quality, (2010), Atmospheric pollution in Athens – 2009 (in Greek). Available at <http://www.ypeka.gr/Default.aspx?tabid=490&language=el-GR>.
- IAEA, 1992. Sampling and analytical methodologies for instrumental neutron activation analysis of airborne particulate matter (No. IAEA-TCS--4). International Atomic Energy Agency.
- ICRP, 1994. Human Respiratory Tract Model for Radiological Protection. ICRP Publication 66. Ann. ICRP 24 (1-3).
- IPCC, 2013. Intergovernmental panel on Climate Change. Climate Change 2013: The physical science basis- Summary for policymakers (WG1).
- IPCC, 2007. Intergovernmental panel on Climate Change. Climate Change 2007: The Physical Science Basis, Summary for Policymakers. Contribution of Working Group I to the Fourth Assessment Report of the Intergovernmental Panel on Climate Change.
- ISO. 1995. Air Quality-Particle Size Fraction Definitions for Health-Related Sampling, ISO Standard 7708. Geneva: International Standards Organisation.
- MEPC57, 2008. From 31 March to 4 April 2008; Marine Environmental Protection Committee; International Maritime Organization: Geneva, Switzerland, 2008.
- MinEnv, 2013. Hellenic Ministry of Environment, Energy and Climate Change: Annual Air Pollution Report. www.ypeka.gr.
- RCM, 2007. (Region of Central Macedonia). Directorate of Environment and Public Works, (2007), Atmospheric pollution in Thessaloniki – 2006 (in Greek). Available at <http://www.ypeka.gr/Default.aspx?tabid=490&language=el-GR>.
- US-EPA, 1999. Ambient Air Monitoring Reference and Equivalent Methods, Code of Federal Regulations (CFR) Title 40, Part 53. US-EPA, Washington, DC

(revised July 1999). [WWW Document]. URL
<https://www.gpo.gov/fdsys/granule/CFR-2002-title40-vol5/CFR-2002-title40-vol5-part53> (accessed 9.26.17).

WHO, 2013. Health effects of particulate matter. Policy implications for countries in eastern Europe, Caucasus and central Asia.

WHO, 2006. WHO Air quality guidelines - global update 2005 [WWW Document]. WHO. URL

Wolff, H., Perry, L., 2010. Policy Monitor Trends in Clean Air Legislation in Europe: Particulate Matter and Low Emission Zones. *Rev. Environ. Econ. Policy* 4, 293–308.

Appendix A

Table A1: Information of the sampling stations at the two largest cities in Greece. The last column indicates the operator of each air quality network.

City	Station	Characterization	Elevation (m.a.s.l.)	Longitude	Latitude	Operated by
Athens	Piraeus (PIR)	Urban traffic	20	23° 38' 51''	37° 56' 36''	MEPPPW*
	Aristotelous St. (ARI)	Urban traffic	95	23° 43' 39''	37° 59' 16''	
	Maroussi (MAR)	Urban traffic	145	23° 47' 14''	38° 01' 51''	
	Lykovrissi (LYK)	Suburban traffic	210	23° 46' 35''	38° 04' 11''	
	Thrakomacedones (THR)	Suburban background	550	23° 45' 29''	38° 08' 37''	
	Agia Paraskevi (AGP)	Suburban background	290	23° 49' 10''	37° 59' 42''	
Thessaloniki	Kordelio (KOD)	Urban - ...Industrial	52	22.9°	40.7°	DEPWCMD**
	Agia Sofia (AGS)	Urban	20	22.9°	40.6°	
	Kalamaria (KAL)	Suburban	50	22.9°	40.6°	
	Panorama (PAO)	Suburban	330	23°	40.6°	
	Sindos (SIN)	Suburban - Industrial	14	22.8°	40.7°	

*MEPPPW: Air Quality Department of the Ministry of Environment Physical Planning and Public Works

**DEPWCMD: Department of Environment and Public Works of Central Macedonia District in Thessaloniki

Statistical Analysis in Athens from 2001 to 2010

Table A2: Descriptive statistics (Mean, Standard Deviation, N total values, Min and Max) for average PM₁₀ concentrations ($\mu\text{g m}^{-3}$) and the exceedances (Ex.D.; more than 35 days) of the EU 24-h limit value ($50 \mu\text{g m}^{-3}$) at the monitoring stations in Athens.

		Descriptive Statistics and exceedances of EU PM ₁₀ limits for PM ₁₀ concentrations in Athens stations 2001 - 2010										
Station		Year										
		2001	2002	2003	2004	2005	2006	2007	2008	2009	2010	2001-2010
PIR	Mean	57.7	62.5	54.3	56.3	54.9		46.7	33.3	32.3	44.1	49.1
	S.D	19.8	20.6	21.6	22.7	34.6		16.3	16.7	19.5	20.3	
	(N)	(300)	(275)	(83)	(110)	(70)	-	(279)	(322)	(302)	(222)	
	Min	18	23	19	20	24		16	11	12	13	
	Max	135	157	159	166	236		118	107	185	169	
	Ex.D.	172	201	43	57	29		103	46	30	62	
MAR	Mean	55.5				45.7	48.3	48.5	48.4	43.5	40.6	47.2
	S.D	23.9				22.4	27.2	20	21.9	23.2	19.5	
	(N)	(359)	-	-	-	(335)	(335)	(348)	(349)	(303)	(340)	
	Min	7				12	9	18	19	13	12	
	Max	167				175	331	203	175	208	260	
	Ex.D.	195				104	108	134	124	68	63	
ARI	Mean	55.6	54.8	56.4	57.9	52.8	56.7	51.7	56.6	49.3	48.7	54.1
	S.D	24.6	21.5	21.6	24.4	20.3	29.7	19	25.1	26.2	29.7	
	(N)	(358)	(220)	(225)	(152)	(357)	(355)	(328)	(328)	(355)	(305)	
	Min	11	18	18	19	13	14	21	14	20	20	
	Max	219	130	165	166	197	386	139	176	257	421	
	Ex.D.	181	110	115	85	169	178	145	163	122	99	
THR	Mean	31.1	33.9	31.9	33.2	30.5	27.0	21.5	27.2	30.4	36.7	30.3
	S.D	15.5	20.1	17.6	23.3	21.1	25.5	11.9	17.6	18.3	19.0	
	(N)	(357)	(263)	(296)	(297)	(233)	(293)	(304)	(299)	(297)	(283)	
	Min	6	3	6	4	9	2	4	3	8	5	
	Max	99	185	154	244	155	329	101	134	236	164	
	Ex.D.	35	31	33	31	23	10	10	21	22	43	
LYK	Mean	59.7	61.9	58.7	62.9	53.3	58.7	54.8	54.9	42.9	38.6	54.6
	S.D	24.1	27.1	25.6	28.1	25	33.9	22.9	25.1	28.0	26.3	
	(N)	(352)	(303)	(280)	(337)	(275)	(306)	(362)	(306)	(344)	(356)	
	Min	10	12	12	9	9	5	15	8	8	9	
	Max	151	170	214	272	207	438	149	176	289	388	
	Ex.D.	221	184	163	216	124	158	178	147	86	56	

AGP	Mean	46.5	37.7	37.1	39.4	40.7	34	28.4	28.3	25.6	28.2	34.6
	S.D	24.5	18.8	20.8	24.4	21.5	31	12.9	16.9	21.8	16.5	
	(N)	(267)	(311)	(353)	(338)	(295)	(214)	(335)	(315)	(330)	(319)	
	Min	9	8	6	9	12	9	10	6	8	6	
	Max	142	133	203	193	192	396	103	127	292	118	
	Ex.D.	92	49	64	69	67	11	18	20	17	22	

Table A3: The results of Kolmogorov - Smirnov test for PM₁₀ concentrations and log transformed averaged PM₁₀ concentrations in Athens from 2001 to 2010.

		Kolmogorov-Smirnov test for PM₁₀ concentrations in Athens from 2001 to 2010									
Station		Year									
		2001	2002	2003	2004	2005	2006	2007	2008	2009	2010
PIR	PR	.010	.074	.247	.182	.001		.010	.000	.000	.001
	LN	.730	.289	.999	.501	.258		.539	.141	.058	.547
ARI	PR	.000	.022	.006	.042	.001	.000	.001	.000	.000	.000
	LN	.836	.989	.227	.949	.791	.816	.620	.112	.056	.137
MAR	PR	.002				.000	.000	.002	.000	.000	.000
	LN	.267				.805	.327	.505	.262	.056	.421
LYK	PR	.051	.000	.004	.002	.002	.000	.001	.000	.000	.000
	LN	.033	.280	.311	.880	.384	.218	.352	.502	.212	.224
THR	PR	.005	.000	.006	.000	.000	.000	.000	.000	.000	.000
	LN	.054	.179	.361	.307	.061	.116	.056	.204	.383	.286
AGP	PR	.000	.000	.000	.000	.000	.000	.000	.000	.000	.000
	LN	.300	.220	.349	.052	.849	.057	.216	.047	.025	.300

PR.: Previously data

LN: Lognormal data

Statistical analysis of annual variation in Athens

Table A4: The results of Levene's test of log-transformed annual-averaged PM₁₀ concentrations in Athens from 2001 to 2010.

Levene's test of log-transformed annual-averaged PM₁₀ concentrations in Athens from 2001 to 2010				
	Levene Statistic	df1	df2	Sig.
LNPIR	5.340	8	1954	.000
LNMAR	3.644	6	2362	.001
LNARI	1.768	9	2973	.069
LNTHR	1.478	9	2913	.150
LNLYK	0.574	9	3211	.819
LNAGP	4.902	9	3067	.000

Table A5: The results of One-way ANOVA procedure for log-transformed (LN) annual averaged PM₁₀ concentrations in Athens from 2001 to 2010.

One-way ANOVA procedure of log-transformed annual-averaged PM₁₀ concentrations in Athens from 2001 to 2010

	F	Sig.
LN ARI	8.013	.000
LN LYK	51.492	.000
LN THR	27.947	.000

Table A6: The Tukey HSD test log-transformed annual-averaged PM₁₀ concentrations at ARI station from 2001 to 2010. The critical level of confidence was 0.05.

Tukey HSD test of log-transformed annual-averaged PM₁₀ concentrations at ARI station

Year	N	1	2	3
2010	305	3.7927 (44.4)		
2009	355	3.8093 (45.1)	3.8093 (45.1)	
2007	328		3.8839 (48.6)	3.8839 (48.6)
2005	357			3.9030 (49.5)
2002	220			3.9302 (50.9)
2001	358			3.9351 (51.2)
2006	355			3.9479 (51.8)
2008	328			3.9503 (51.9)
2003	225			3.9656 (52.7)
2004	152			3.9788 (53.4)
Sig.		.142	.117	.106

Table A7: The Tukey HSD test log-transformed annual-averaged PM₁₀ concentrations at THR station from 2001 to 2010. The critical level of confidence was 0.05.

Tukey HSD test of log-transformed annual-averaged PM₁₀ concentrations at THR station

Year	N	1	2	3	4
2007	304	2.9326 (18.8)			
2006	293		3.1327 (22.9)		
2008	299		3.1468 (23.3)		
2005	234			3.2898 (26.8)	

2009	297			3.3056 (27.3)	
2001	357			3.3185 (27.6)	
2003	296			3.3289 (27.9)	
2004	297			3.3553 (28.6)	
2002	263			3.3843 (29.5)	3.3843 (29.5)
2010	283				3.4886 (32.7)
Sig.		1.000	1.000	.444	.056

Table A8: The Tukey HSD test of log-transformed annual-averaged PM₁₀ concentrations at LYK station from 2001 to 2010. The critical level of confidence was 0.05.

Tukey HSD test of log-transformed annual-averaged PM₁₀ concentrations at LYK station

Year	N	1	2	3	4
2010	356	3.5365 (34.3)			
2009	344	3.6367 (37.9)			
2005	275		3.8821 (48.5)		
2008	306		3.9102 (49.9)	3.9102 (49.9)	
2007	362		3.9194 (50.4)	3.9194 (50.4)	
2006	306		3.9580 (52.4)	3.9580 (52.4)	3.9580 (52.4)
2003	280		3.9796 (53.5)	3.9796 (53.5)	3.9796 (53.5)
2001	352			3.9992 (54.5)	3.9992 (54.5)
2002	303				4.0383 (56.7)
2004	337				4.0545 (57.6)
Sig.		.116	.142	.245	.152

Table A9: The results of Welch ANOVA procedure of log-transformed (LN) annual-averaged PM₁₀ concentrations at PIR, MAR and AGP stations in Athens from 2001 to 2010.

Welch – ANOVA procedure of log-transformed annual-averaged PM₁₀ concentrations in Athens from 2002 to 2008

	F	Sig.
LNPIR	102.380	.000
LNMAR	18.530	.000
LNAGP	53.721	.000

Table A10: The Games-Howell post hoc test of log-transformed annual-averaged PM₁₀ concentrations at PIR station in Athens from 2001 to 2010.

Games-Howell post hoc test of log-transformed annual-averaged PM₁₀ concentrations at PIR from 2001 to 2010

Year	2001	2002	2003	2004	2005	2007	2008	2009	2010
2001		.072	.787	.988	.551	.000	.000	.000	.000
2002	.072		.019	.072	.026	.000	.000	.000	.000
2003	.787	.019		.999	.999	.054	.000	.000	.000
2004	.988	.072	.999		.960	.001	.000	.000	.000
2005	.551	.026	.999	.960		.760	.000	.000	.074
2007	.000	.000	.054	.001	.760		.000	.000	.240
2008	.000	.000	.000	.000	.000	.000		.357	.000
2009	.000	.000	.000	.000	.000	.000	.357		.000
2010	.000	.000	.000	.000	.074	.240	.000	.000	

Table A11: The Games-Howell post hoc test of log-transformed annual-averaged PM₁₀ concentrations at MAR station in Athens from 2004 to 2010.

Games-Howell post hoc test of log-transformed annual-averaged PM₁₀ concentrations at MAR from 2001 to 2010

Year	2001	2005	2006	2007	2008	2009	2010
2001		.000	.000	.009	.001	.000	.000
2005	.000		.927	.115	.364	.662	.026
2006	.000	.969		.732	.961	.097	.000
2007	.007	.103	.732		.998	.001	.000
2008	.002	.422	.961	.998		.005	.000
2009	.000	.747	.097	.001	.005		.774
2010	.000	.026	.000	.000	.000	.774	

Table A12: The Games-Howell post hoc test of log-transformed annual-averaged PM₁₀ concentrations at AGP station from 2001 to 2010.

Games-Howell post hoc test of log-transformed annual-averaged PM₁₀ concentrations at AGP from 2001 to 2010

Year	2001	2002	2003	2004	2005	2006	2007	2008	2009	2010
2001		.000	.000	.002	.226	.000	.000	.000	.000	.000
2002	.000		.988	1.000	.491	.041	.000	.000	.000	.000
2003	.000	.988		.965	.049	.462	.000	.000	.000	.000
2004	.002	1.000	.965		.705	.030	.000	.000	.000	.000

2005	.226	.491	.049	.705		.000	.000	.000	.000	.000
2006	.000	.041	.462	.030	.000		.004	.000	.000	.000
2007	.000	.000	.000	.000	.000	.004		.980	.000	.922
2008	.000	.000	.000	.000	.000	.000	.980		.017	1.000
2009	.000	.000	.000	.000	.000	.000	.000	.017		.048
2010	.000	.000	.000	.000	.000	.000	.922	1.000	.048	

Statistical Analysis in Thessaloniki from 2001 to 2010

Table A13: Descriptive statistics (Mean, Standard Deviation, N total values, Min and Max) for average PM₁₀ concentrations ($\mu\text{g m}^{-3}$) and the exceedances (Exc.D.; more than 35 days) of the EU 24-h limit value ($50 \mu\text{g m}^{-3}$) at all stations in Thessaloniki from 2001 to 2010.

Descriptive Statistics and the exceedances of EU PM₁₀ limits for PM₁₀ concentrations in Thessaloniki stations from 2001 to 2010

Station	Year											
		2001	2002	2003	2004	2005	2006	2007	2008	2009	2010	2001 - 2010
KOD	Mean	69.0	67.7	65.9	64.3	60.6	67.6	56.3	54.2	44.3	41.7	59.2
	S.D	1.6	1.7	1.8	2.9	2.3	2.1	1.5	1.3	21.1	23.9	
	(N)	(303)	(357)	(259)	(120)	(196)	(267)	(353)	(332)	(256)	(269)	
	Min	15	12	10	24	9	19	16	10	9	11	
	Max	213	192	227	167	171	198	165	130	125	206	
	Ex.D.	111	227	183	70	103	167	162	172	80	59	
AGS	Mean	63.5	70.8	63.9	59.5	-	-	46.1	57.0	42.8	46.2	56.2
	S.D	1.8	1.6	1.6	4.1			1.0	1.4	14.4	26.2	
	(N)	(358)	(362)	(332)	(60)			(341)	(335)	(254)	(325)	
	Min	10	14	19	7			19	22	19	12	
	Max	299	244	253	134			141	184	92	257	
	Ex.D	207	277	219	28			105	192	67	96	
SIN	Mean	51.5	47.9	51.3	43.3	44.9	49.9	49.6	46.4	40.1	-	47.2
	S.D	1.3	1.1	1.2	1.0	1.9	1.5	1.1	1.0	14.3		
	(N)	(220)	(363)	(340)	(290)	(143)	(261)	(358)	(322)	(122)		
	Min	18	10	12	2	11	12	11	14	10		
	Max	130	130	206	163	175	172	177	112	97		
	Ex.D	149	127	160	75	42	97	145	123	21		
PAO	Mean	36.9	33.9	33.2	31.7	-	30.4	26.0	26.8	23.4	-	30.3
	S.D	0.8	0.8	1.2	0.7		0.7	0.6	1.5	8.5		
	(N)	(363)	(355)	(282)	(318)		(327)	(358)	(31)	(166)		
	Min	10	5	8	10		9	5	9	4		
	Max	99	85	200	88		78	92	48	59		
	Ex.D	62	43	28	23		25	6	0	3		

KAL	Mean	-	-	-	-	-	-	48.2	35.5	30.7	28.2	35.7
	S.D							1.2	1.0	11.9	14.5	
	(N)							(275)	(286)	(259)	(251)	
	Min							12	11	8	11	
	Max							142	96	81	206	
	Ex.D							104	50	19	7	

Table A14: The results of Kolmogorov-Smirnov test for PM₁₀ concentrations and log transformed (LN) averaged PM₁₀ concentrations in Thessaloniki from 2001 to 2010.

Kolmogorov-Smirnov test for Thessaloniki concentrations from 2001 to 2010

Station		Year									
		2001	2002	2003	2004	2005	2006	2007	2008	2009	2010
KOD	PR.	.000	.004	.172	.017	.006	.003	.000	.128	.012	.000
	LN	.693	.837	.100	.520	.915	.635	.074	.282	.411	.561
AGS	PR.	.000	.000	.001	.066			.000	.011	.023	.000
	LN	.224	.286	.664	.848			.420	.924	.825	.089
SIN	PR.	.000	.000	.034	.008	.006	.000	.000	.481	.339	-
	LN	.358	.353	.066	.389	.502	.244	.357	.243	.037	
PAO	PR.	.017	.020	.001	.010		.004	.150	.848	.482	-
	LN	.395	.182	.343	.235		.661	.026	.660	.145	
KAL	PR.							.011	.000	.000	.000
	LN							.588	.401	.245	.444

PR.: Previously data
LN.: Lognormal data

Statistical analysis of annual variation in Thessaloniki

Table A15: The results of Levene's test of log-transformed (LN) annual-averaged PM₁₀ concentrations in Thessaloniki from 2001 to 2010.

Levene's test of log-transformed annual-averaged PM₁₀ concentrations in Thessaloniki from 2001 to 2010

	Levene Statistic	df1	df2	Sig.
LNKOD	2.282	8	2581	.020
LNPAO	2.086	6	2161	.052
LNAGS	4.525	6	2300	.000
LNSIN	0.837	7	2397	.556
LNKAL	6.423	3	1067	.000

Table A16: The results of One-way ANOVA procedure for log-transformed (LN) annual-averaged PM₁₀ concentrations at SIN and PAO stations in Thessaloniki from 2001 to 2008.

One-way ANOVA procedure of log-transformed annual-averaged PM₁₀ concentrations from 2001 to 2010

	F	Sig.
LNSIN	8.122	.000
LNPAO	34.187	.000

Table A17: The Tukey HSD test of log-transformed (LN) annual-averaged PM₁₀ concentrations at SIN station from 2001 to 2010. The critical level of confidence was 0.05.

Tukey HSD test of log-transformed annual-averaged PM₁₀ concentrations at SIN station

Year	N	1	2	3
2009	122	3.6258 (37.5)		
2004	290	3.6846 (39.9)	3.6846 (39.9)	
2002	363		3.7848 (44.0)	3.7848 (44.0)
2008	306		3.7906 (44.3)	3.7906 (44.3)
2006	261			3.8076 (45.0)
2007	358			3.8205 (45.6)
2001	365			3.8490 (46.9)
2003	340			3.8587 (47.4)
Sig.		.726	.063	.443

Table A18: The Tukey HSD test of log-transformed annual-averaged PM₁₀ concentrations at PAO station from 2001 to 2010. The critical level of confidence was 0.05.

Tukey HSD test of log-transformed annual-averaged PM₁₀ concentrations at PAO station

Year	N	1	2	3
2009	166	3.0805 (21.8)		
2007	358	3.1626 (23.6)		
2006	326		3.3301 (27.9)	
2003	282		3.3811 (29.4)	
2004	318		3.3815 (29.4)	
2002	355		3.4307 (30.9)	3.4307 (30.9)
2001	363			3.5223 (33.9)
Sig.		.252	.076	.143

Table A19: The results of Welch ANOVA procedure of log-transformed (LN) annual-averaged PM₁₀ concentrations at KOD, AGS and KAL stations in Thessaloniki from 2001 to 2010.

Welch – ANOVA procedure of log-transformed annual-averaged PM₁₀ concentrations in Thessaloniki from 2001 to 2008

	F	Sig.
LNKOD	46.482	.000
LNAGS	76.303	.000
LNKAL	87.773	.000

Table A20: The Games-Howell post hoc test of log-transformed (LN) annual-averaged PM₁₀ concentrations at KOD station in Thessaloniki from 2001 to 2010.

Games-Howell post hoc test of log-transformed annual-averaged PM₁₀ concentrations at KOD from 2001 to 2010

Year	2001	2002	2003	2004	2005	2006	2007	2008	2009	2010
2001		.994	.984	.767	.011	1.000	.000	.000	.000	.000
2002	.994		1.000	.989	.119	1.000	.000	.000	.000	.000
2003	.984	1.000		.997	.212	1.000	.000	.000	.000	.000
2004	.767	.989	.997		.940	.972	.329	.078	.000	.000
2005	.011	.119	.212	.940		.099	.996	.825	.000	.000
2006	1.000	1.000	1.000	.972	.099		.000	.000	.000	.000
2007	.000	.000	.000	.329	.996	.000		.994	.000	.000
2008	.000	.000	.000	.078	.825	.000	.994		.000	.000
2009	.000	.000	.000	.000	.000	.000	.000	.000		.830
2010	.000	.000	.000	.000	.000	.000	.000	.000	.830	

Table A21: The Games-Howell post hoc test of log-transformed (LN) annual-averaged PM₁₀ concentrations at AGS station in Thessaloniki from 2001 to 2010.

Games-Howell post hoc test of log-transformed annual-averaged PM₁₀ concentrations at AGS from 2001 to 2010

Year	2001	2002	2003	2007	2008	2009	2010
2001		.001	.966	.000	.434	.000	.000
2002	.001		.020	.000	.000	.000	.000
2003	.966	.020		.000	.033	.000	.000
2007	.000	.000	.000		.000	.432	.961
2008	.434	.000	.033	.000		.000	.000

2009	.000	.000	.000	.432	.000		.979
2010	.000	.000	.000	.961	.000	.979	

Table A22: The Games-Howell post hoc test of log-transformed (LN) annual-averaged PM₁₀ concentrations at KAL station in Thessaloniki from 2001 to 2010.

**Games-Howell post hoc test of log-transformed
annual-averaged PM₁₀ concentrations at KAL
from 2001 to 2010**

Year	2007	2008	2009	2010
2007		.000	.000	.000
2008	.000		.110	.000
2009	.000	.011		.027
2010	.000	.000	.027	

Statistical analysis of seasonal variation in Athens

Table A23: The results of Levene's test of log-transformed (LN) seasonal-averaged PM₁₀ concentrations in Athens from 2001 to 2010.

**Levene's test of log-transformed seasonal-averaged PM₁₀ concentrations
in Athens from 2001 to 2010**

	Levene statistic	df1	df2	Sig.
LNPIR	8.776	3	1959	.000
LNMAR	55.447	3	2365	.000
LNARI	59.073	3	2979	.000
LNTHR	25.369	3	3217	.000
LNLYK	55.738	3	3073	.000
LNAGP	11.659	3	2919	.000

Table A24: The results of Welch ANOVA procedure of log-transformed (LN) seasonal-averaged PM₁₀ concentrations in Athens stations from 2001 to 2010.

**Welch – ANOVA procedure of log-transformed seasonal-averaged PM₁₀
concentrations in Athens from 2001 to 2010**

	Statistic - F	df1	df2	Sig.
LNPIR	3.013	3	1056.680	.029
LNMAR	7.694	3	1273.968	.000
LNARI	15.129	3	1606.068	.000

LNTHR	71.552	3	1435.000	.000
LNLYK	3.863	3	1725.573	.009
LNAGP	117.465	3	1703.995	.000

Table A25: The Games-Howell post hoc test of log-transformed (LN) seasonal-averaged PM₁₀ concentrations at PIR, MAR, ARI, THR, LYK and AGP stations in Athens from 2001 to 2010.

Games-Howell post hoc test of seasonal-averaged PM₁₀ concentrations at PIR, MAR, ARI, THR, LYK and AGP from 2001 to 2010

LNPIR		Spr	Sum	Aut	Win
	Spr.		.019	.232	.508
	Sum.	.019		.676	.501
	Aut.	.232	.676		.984
	Win	.508	.501	.984	
LNMAR		Spr	Sum	Aut	Win
	Spr.		.012	.992	.261
	Sum.	.012		.018	.000
	Aut.	.992	.018		.478
	Win	.261	.000	.478	
LNARI		Spr	Sum	Aut	Win
	Spr.		.005	.006	.961
	Sum.	.005		.000	.008
	Aut.	.006	.000		.100
	Win	.961	.008	.100	
LNTHR		Spr	Sum	Aut	Win
	Spr.		.947	.000	.000
	Sum.	.947		.000	.000
	Aut.	.000	.000		.000
	Win.	.000	.000	.000	.000
LNLYK		Spr	Sum	Aut	Win
	Spr.		.168	.057	.011
	Sum.	.168		.861	.341
	Aut.	.057	.861		.782

	Win.	.011	.341	.782	
LNAGP		Spr	Sum	Aut	Win
	Spr.		.039	.013	.000
	Sum.	.039		.000	.000
	Aut.	.013	.000		.000
	Win.	.000	.000	.000	

Statistical analysis of seasonal variation in Thessaloniki

Table A26: The results of Levene's test of log-transformed (LN) seasonal-averaged PM₁₀ concentrations in Thessaloniki from 2001 to 2010.

Levene's test of log-transformed seasonal-averaged PM₁₀ concentrations in Thessaloniki from 2001 to 2010

	Levene Statistic	df1	df2	Sig.
LNKOD	46.335	3	2706	.000
LNPAO	13.655	3	2164	.000
LNAGS	29.998	3	2303	.000
LNSIN	13.976	3	2401	.000
LNKAL	12.965	3	1067	.000

Table A27: The results of Welch ANOVA procedure of log-transformed (LN) seasonal-averaged PM₁₀ concentrations at all the stations in Thessaloniki from 2001 to 2010.

Welch – ANOVA procedure of log-transformed seasonal-averaged PM₁₀ concentrations in Thessaloniki from 2001 to 2010

	Statistic - F	df1	df2	Sig.
LNKOD	17.744	3	1477.787	.000
LNPAO	4.654	3	1151.392	.003
LNAGS	20.291	3	1258.870	.000
LNSIN	26.925	3	1296.969	.000
LNKAL	12.054	3	450.756	.000

Table A28: The Games-Howell post hoc test of log-transformed (LN) seasonal-averaged PM₁₀ concentrations at all the stations in Thessaloniki from 2001 to 2010.

Games-Howell post hoc test of seasonal-averaged PM₁₀ concentrations at KOD, AGS, PAO, SIN and KAL from 2001 to 2010

LNKOD		Spr	Sum	Aut	Win
--------------	--	------------	------------	------------	------------

	Spr.		.220	.004	.000
	Sum.	.220		.000	.000
	Aut.	.004	.000		.815
	Win	.000	.000	.815	
LNPAO		Spr	Sum	Aut	Win
	Spr.		.865	.352	.055
	Sum.	.865		.080	.005
	Aut.	.352	.080		.873
	Win	.055	.005	.873	
LNAGS		Spr	Sum	Aut	Win
	Spr.		.637	.000	.003
	Sum.	.637		.000	.000
	Aut.	.000	.000		.429
	Win	.003	.000	.429	
LNSIN		Spr	Sum	Aut	Win
	Spr.		.002	.000	.010
	Sum.	.002		.000	.997
	Aut.	.000	.000		.000
	Win	.010	.997	.000	
LNKAL		Spr	Sum	Aut	Win
	Spr.		.984	.042	.000
	Sum.	.984		.017	.000
	Aut.	.042	.017		.518
	Win	.000	.000	.518	

Appendix B

PART A - Additional Data

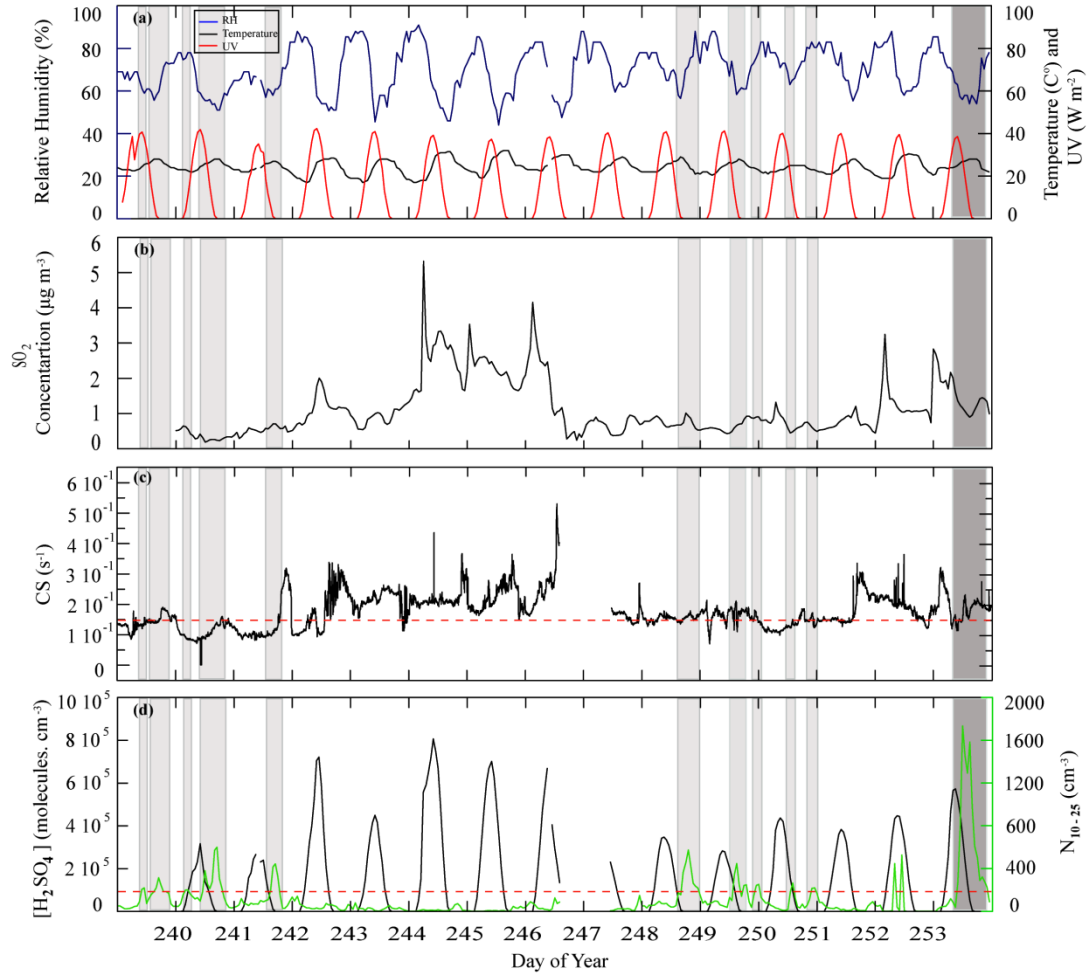


Figure B1: Time series of hourly-averaged ambient temperature (black line), relative humidity (blue line), and ultraviolet radiation (red line) (a), hourly-averaged sulfur dioxide concentration (b), condensation sink (c), sulfuric acid concentration (black line) and nucleation-mode particle number concentration (green line) (d) observed on Lemnos from 27 August to 10 September 2011. The red dashed line shown in subplot c and d indicates the threshold values of condensation sink and sulfuric acid for PT episodes. Light shaded areas indicate transportation episodes that are characterized as moderate (239, 240, 241, 248, 249, and 250 DOY), while the dark shaded indicates the day with a strong PT episode (253 DOY).

PART B - Calculation of [H₂SO₄]

The [H₂SO₄] was estimated by the empirical model described by Mikkonen et al. (2011) as:

$$[H_2SO_4] = 8.21 \times 10^{-3} \cdot k \cdot [UV] \cdot [SO_2]^{0.62} \cdot (CS \cdot RH)^{-0.13} \quad (B1)$$

where UV is the ultraviolet radiation ($\text{W}\cdot\text{m}^{-2}$), SO_2 are the sulfur dioxide concentrations, RH (%) is the relative humidity while CS (s^{-1}) and k ($\text{cm}^3\cdot\text{molecules}^{-1}\cdot\text{s}^{-1}$) are the condensation sink and the reaction rate constant, respectively. The condensation sink is given by (Dal Maso et al., 2005; Salma et al., 2011):

$$CS = 2 \cdot \pi \cdot D \cdot \int_0^\infty d \cdot \beta_m(d) \cdot N(d) dd = 2 \cdot \pi \cdot D \sum_i d_i \cdot \beta_i \cdot N_i \quad (\text{B2})$$

where d_i and N_i are the diameter and the number concentration of an *ith* particle size range obtained from the SMPS measurements, D is the diffusion coefficient of the condensing vapor, while $\beta_m(d)$ is the correction factor of the condensation mass flux from Fuchs and Sutugin (1970).

The value of k is given by (DeMore et al., 1997; Sander et al., 2002):

$$k = \frac{A \cdot k_3}{A + k_3} \exp \left[k_5 \left(1 + \log_{10} \left(\frac{A}{k_3} \right)^2 \right)^{-1} \right] \quad (\text{B3})$$

where $A = k_1 \cdot [M] \cdot (300/T)^{k_2}$, T (K) is the temperature, $[M] = 0.101 \times (1.381 \times 10^{-23} T)^{-1}$ is the air density ($\text{molecules}^{-1}\cdot\text{cm}^3$), $k_1 = 4 \times 10^{-31}$, $k_2 = 3.3$, $k_{31} = 2 \times 10^{-12}$, $k_5 = -0.8$.

References

1. Dal Maso, M., Kulmala, M., Riipinen, I., Wagner, R., Hussein, T., Aalto, P. P., and Lehtinen, K. E. J., 2005. Formation and growth of fresh atmospheric aerosols: eight years of aerosol size distribution data from SMEAR II, Hyytiälä, Finland. *Boreal Environ. Res.*, 10, 323–336.
2. DeMore, W., Sander, S., Golden, D., Hampson, R., Kurylo, M., Howard, C., Ravishankara, A., Kolb, C., and Molina, M., 1997. Chemical kinetics and photochemical data for use in stratospheric modeling, Evaluation 12. JPL Publ, 97-4, 266.
3. Fuchs N.A. & Sutugin A.G., 1970. Highly dispersed aerosols. Ann Arbor Science Publishers, Ann Arbor, London.
4. Mikkonen, S., Romakkaniemi, S., Smith, J.N., Korhonen, H., Petäjä, T., Plass-Duelmer, C., Boy, M., McMurry, P.H., Lehtinen, K.E.J., Joutsensaari, J., Hamed, A., Mauldin III, R.L., Birmili, W., Spindler, G., Arnold, F., Kulmala, M., Laaksonen, A., 2011. A statistical proxy for sulphuric acid concentration. *Atmos. Chem. Phys.*, 11, 11319–11334.
5. Sander, S. P., Friedl, R. R., Golden, D. M., Kurylo, M. J., Huie, R.E., Orkin, V. L., Ravishankara, A. R., Kolb, C. E., and Molina, M. J., 2002. Chemical kinetics and photochemical data for use in stratospheric modeling, in: evaluation 14. JPL Publ. 02-25, Jet Propul. Lab., Pasadena, Calif..
6. Salma, I., Borsós, T., Weidinger, T., Aalto, P., Hussein, T., Dal Maso, M., Kulmala, M., 2011. Production, growth and properties of ultrafine atmospheric aerosol particles in an urban environment. *Atmos. Chem. Phys.*, 11, 1339–1353.

Appendix C

Additional Data

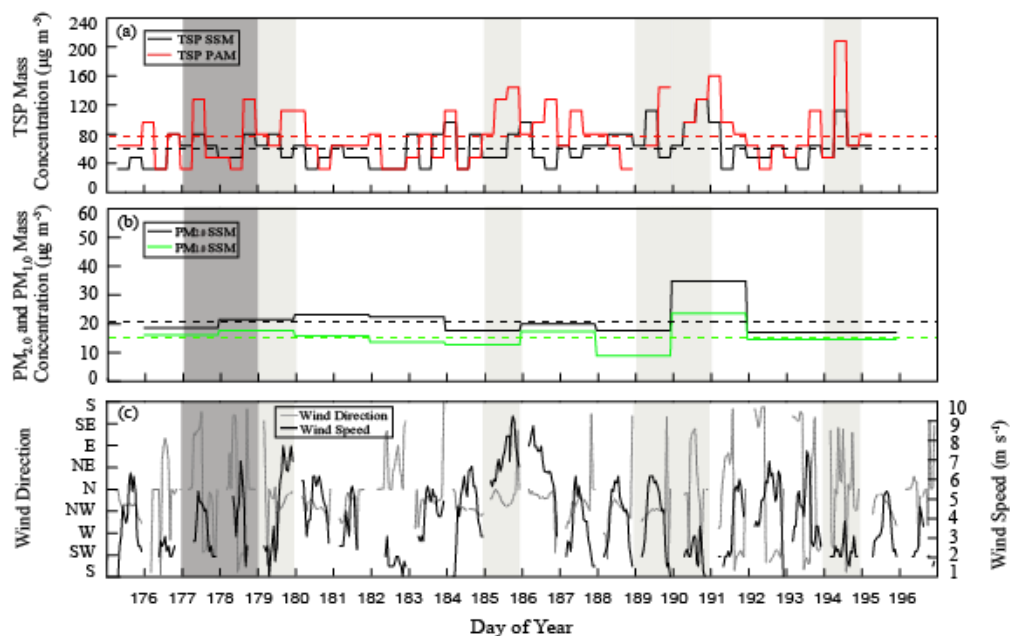


Figure C1: The time series of concentrations of TSP on an 8h basis (a), $\text{PM}_{2.0}$ and $\text{PM}_{1.0}$ on a 48h basis (b), as well as average 1h values of wind direction and wind speed (c) in Mytilene during summer period. The dashed lines in 3a and 3b show the average TSP concentrations at SSM and PAM (black and red lines, respectively) and the average $\text{PM}_{2.0}$ and $\text{PM}_{1.0}$ concentrations at SSM (black and green lines, respectively). The light and dark grey shaded areas refer to the days when pollution was transported to Mytilene from distant and desert dust sources, respectively.

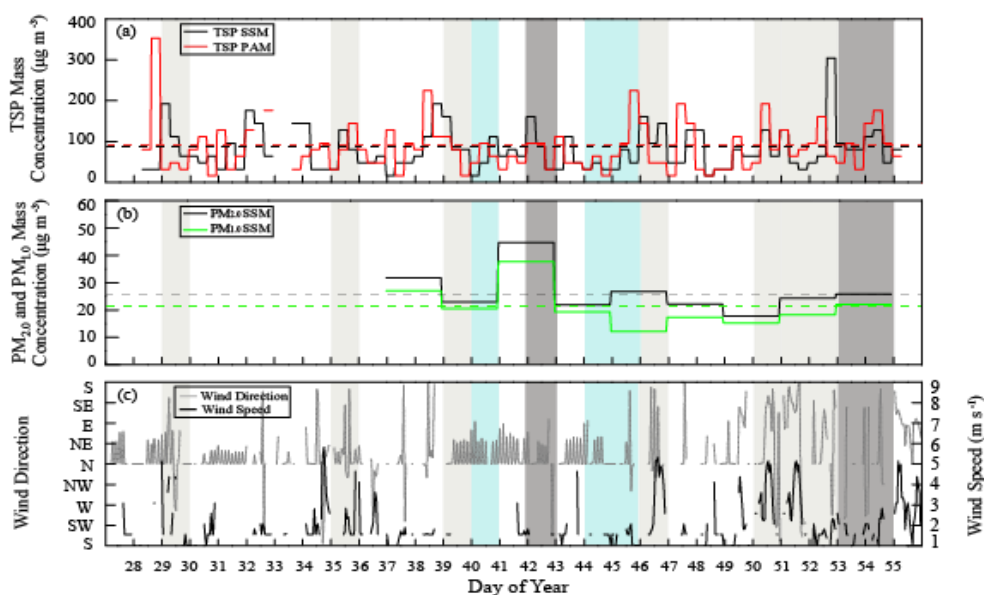


Figure C2: The time series of concentrations of TSP on an 8h basis (a), $PM_{2.0}$ and $PM_{1.0}$ on a 48h basis (b), as well as average 1h values of wind direction and wind speed (c) in Mytilene during winter period. The dashed lines in 1a and 1b show the average TSP concentrations at SSM and PAM (black and red lines, respectively) and the average $PM_{2.0}$ and $PM_{1.0}$ concentrations at SSM (black and green lines, respectively). The light and dark grey shaded areas refer to the days when pollution was transported to Mytilene from distant and desert dust sources, respectively. Light blue shaded areas show the days with precipitation.

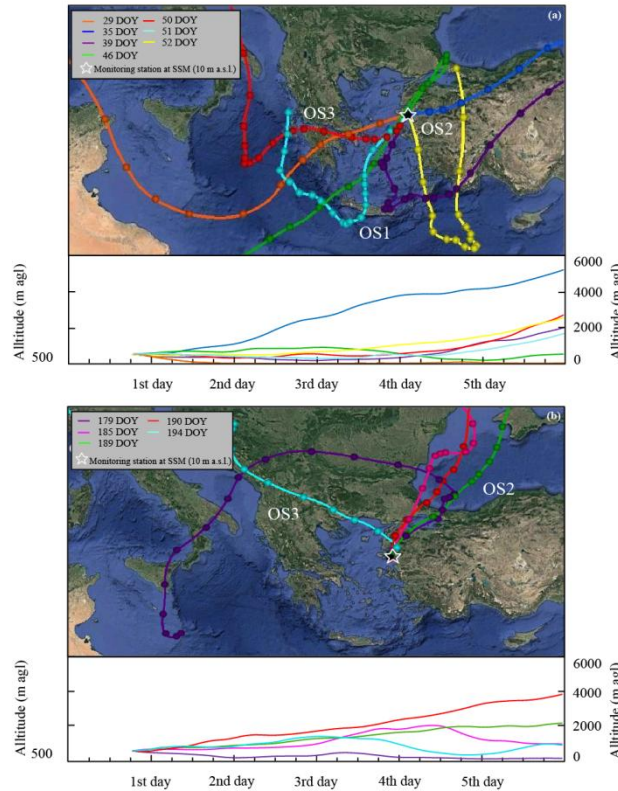


Figure C3: Map and the figure show the horizontal (top) and vertical (bottom) motion of the 5-day back-trajectory calculations arriving at SSM in Mytilene during the winter (a) and summer (b). All the trajectories on 29 (29 DOY) January, and on 4 (35 DOY), 8 (39 DOY), 15 (46 DOY), 19 (50 DOY), 20 (51 DOY) and 21 (52 DOY) February (orange, blue, magenta, green, red, turquoise and yellow lines, respectively), as well as on 28 (179 DOY) June and on 4 (185 DOY), 8 (189 DOY), 9 (190 DOY) and 13 (194 DOY) July (magenta, pink, green, red and turquoise lines, respectively) start at 12 UTC. The dots on each trajectory indicate the position of air parcels at the end of each 6-h interval before reaching the monitoring station. The main origin sectors of air masses during the sampling periods were: OS1-western air masses transported from the region of Crete, OS2-northeastern and southeastern air masses coming from the Turkey and OS3-northwestern and southwestern from the region of Thessaloniki and Athens, respectively.

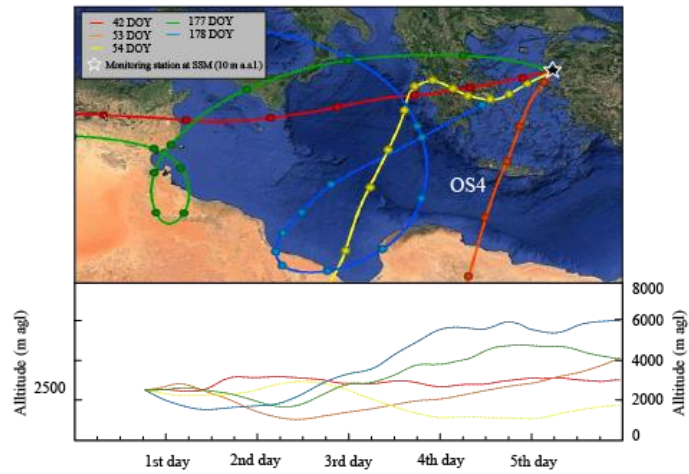


Figure C4: Map and the figure show the horizontal (top) and vertical (bottom) motion of the 5-day back-trajectory calculations arriving at the monitoring site in Mytilene when air masses transported from North Africa (OS4) during winter and summer period. All the trajectories on 11 (42 DOY), 22 (53 DOY) and 23 (54 DOY) February, and on 26 (177 DOY) and 27 (178 DOY) June (red, orange, yellow, green and blue lines, respectively) start at 12 UTC. The dots on each trajectory indicate the position of air parcels at the end of each 6-h interval before reaching the monitoring station.

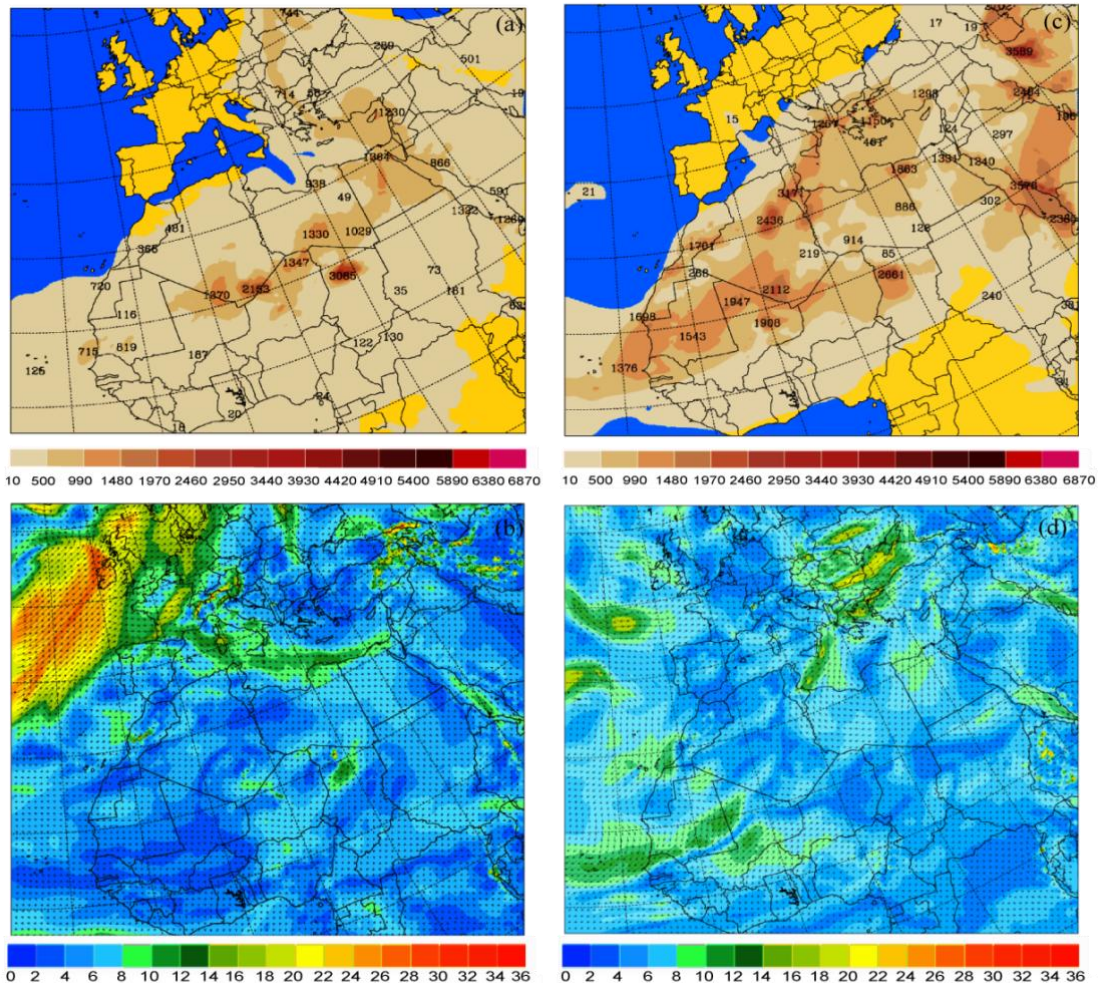


Figure C5: Maps of dust aerosol concentrations ($\mu\text{g m}^{-3}$) by SKIRON model and the motion of wind speed (m s^{-1}) at 12 UTC when air masses transported from North Africa on 23 (53 DOY) February (a and b, respectively) and on 26 (177 DOY) June (c and d, respectively).

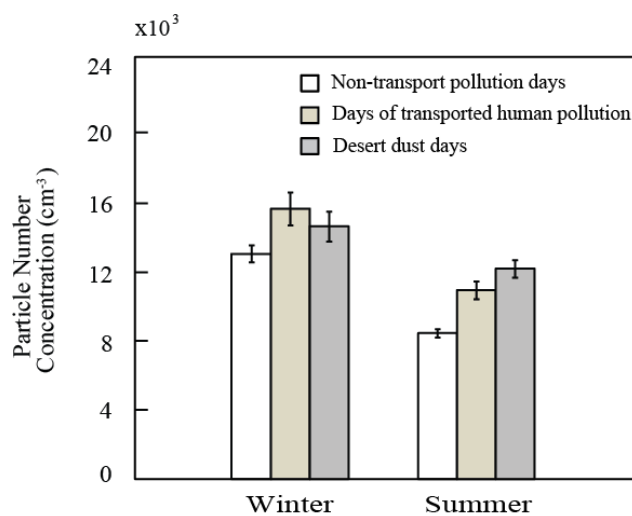


Figure C6: Average number concentrations having sizes in the range 10-500 nm during the days without transported air pollution, with transport of anthropogenic air pollution and with desert dust sources measured at SSM of Mytilene during winter and summer.